A STUDY OF BLIND CHANNEL ESTIMATION TECHNIQUES

A DISSERTATION

Submitted in partial fulfillment of the requirements for the award of the degree of

MASTER OF TECHNOLOGY

in

ELECTRONICS AND COMMUNICATION ENGINEERING

(With Specialization in Communication Systems)

By

SAMEERA BHARADWAJA H

DEPARTMENT OF ELECTRONICS AND COMPUTER ENGINEERING
INDIAN INSTITUTE OF TECHNOLOGY ROORKEE
ROORKEE -247 667 (INDIA)

JUNE, 2011

CANDIDATE'S DECLARATION

I hereby declare that the work, which is presented in this dissertation report entitled, **"A STUDY OF BLIND CHANNEL ESTIMATION TECHNIQUES"** towards the partial fulfilment of the requirement for the award of the degree of **Master of Technology** with specialization in **Communication Systems**, submitted in the **Department of Electronics and Computer Engineering, Indian Institute of Technology Roorkee, Roorkee (UK, India)** is an authentic record of my own work carried out during the period from July, 2010 to June, 2011, under the guidance of **Dr. D. K. Mehra, Professor, Department of Electronics and Computer Engineering, Indian Institute of Technology Roorkee**.

I have not submitted the matter embodied in this dissertation for the award of any other degree or diploma.

Date: 29-06-2011

Place: Roorkee

SAMEERA BHARADWAJA H.

CERTIFICATE

This is to certify that the above statement made by the candidate is correct to the best of my knowledge and belief.

Date: 30.06.11

Place: Roorkee

Dmehra

D. K. MEHRA

Professor, E&CE department

IIT Roorkee, Roorkee – 247 667

Uttarakhand, India

ACKNOWLEDGEMENT

I would like to extend by heartfelt gratitude to my guide, D. K. Mehra for his able guidance, valuable suggestions and constant attention. It is his constant encouragement that has inspired me throughout my dissertation work. I consider myself fortunate to have my dissertation done under him.

Thanks are due to the staff of Signal Processing Lab, Department of Electronics and Computer Engineering, IIT Roorkee, Roorkee for providing necessary facilities. I would like to thank Central Library, IIT Roorkee for providing me with the study materials necessary for my dissertation work. I am indebted to my family for their constant support and ample moral support throughout the year.

Finally, I would like to extend my gratitude to all those who have directly or indirectly contributed towards this work.

SAMEERA BHARADWAJA H

ABSTRACT

Channel estimation plays a crucial role in wireless communication receivers with coherent detection. In contrast to training-based methods, the blind (self-recovering) approach to channel estimation in which the estimate is done purely based on the knowledge of channel output is addressed in this work. Currently in practice, most of the wireless standards employ training-based methods or pilot subcarriers for estimation of CIR. Blind techniques are being researched on from past three decades. The advantage of adopting blind techniques is the conservation of signal bandwidth through the elimination of training/ pilot symbols. This transforms into higher spectral efficiency and thus higher information rates can be achieved at given channel bandwidth.

Recently, orthogonal frequency division multiplexing (OFDM) has become an attractive choice in wireless standards. Further, use of multiple antennas at both ends of a wireless link: multiple-input multiple-output (MIMO) technology has been demonstrated to have the potential of achieving extraordinary data rates. The use of MIMO technology in combination with OFDM, i.e., MIMO-OFDM, therefore seems to be an attractive solution for future broadband wireless systems.

Blind channel estimation using second-order statistics in SISO-OFDM and MIMO-OFDM systems are addressed. To be more specific, the two most sought out approaches namely: subspace decomposition method and precoder-induced-correlation averaging method are described and compared in terms of their performance and practical applicability. Finally, the techniques to resolve the constant complex scalar estimation ambiguity fundamental to all second-order statistics based methods are addressed. A novel completely/ totally blind channel estimation technique via source constellation-splitting and modified phase-directed algorithm for SISO-OFDM systems is proposed and evaluated.

CONTENTS

Chapter 1

INTRODUCTION

In a digital communication link, prior to coherent detection, the incoming information symbol needs to be removed of the distortion caused due to imperfect channel variations in order to prevent erroneous decisions. This is termed as channel equalization [1-2]. In the case of non-coherent detection, equalization is not compulsory, but use of non-coherent detection causes SNR loss of around 3 dB. The channel equalization can be achieved in two ways: either directly or indirectly. In the former case, a filter tuned to function as inverse-channel is designed to work as an equalizer. The channel impulse response (CIR) knowledge is utilized implicitly. In the latter scenario, it is achieved in two steps; first the channel is estimated explicitly and then the incoming signal is recovered by de-convolution. Given any arbitrary channel, direct equalization is more challenging since modelling the inverse function is not always practically feasible (e.g. non-minimum phase and/ or singular channel, ill-conditioned channel function). As far as second approach is concerned, the channel estimation can be achieved in two ways: via training or in blind manner. The former involves transmitting a known set of data through the channel. At the receiver, the channel response is estimated simply by solving the channel input-output relation. In blind (self-recovering) techniques, the channel response is estimated purely based on the knowledge of the channel output as illustrated in *fig. 1.1.*

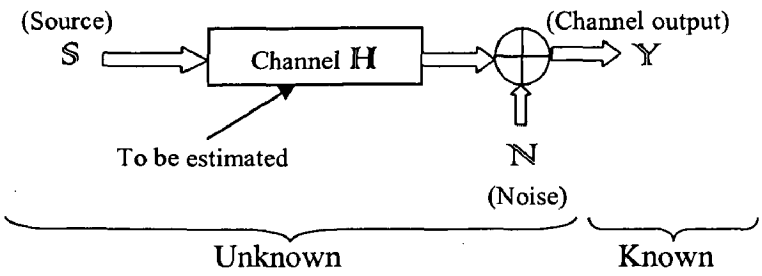

Figure 1.1: Illustration of blind channel estimation problem

Currently, most of the wireless standards employ training based methods for estimation of CIR. For example, GSM (Global Systems for Mobile or Groupe Spécial Mobile) standard dedicates almost a 50% of the total bandwidth for training on an average. In 3GPP-LTE (Long term evolution), in OFDM frames, known symbols called pilots are inserted at specific

locations in the time-frequency grid in order to facilitate channel estimation (The pilot spacing in frequency direction equals 6 subcarriers, while in time direction there are 2 OFDM symbols per slot containing pilots, at a distance of 4 and 3 OFDM symbols from one another). Around 33% of total subcarriers per frame are reserved for pilots/ reference symbols. The advantage of adopting blind techniques is the conservation of signal bandwidth through the elimination of training/ pilot symbols. This transforms into higher spectral efficiency and thus higher information rates can be achieved for given channel bandwidth. The essence of blind techniques rests on the exploitation of structures of the channel and certain statistical properties of the input.

1.1. LITERATURE SURVEY

Blind techniques are being researched for past three decades. Several blind algorithms have been proposed, each significantly different from the other. Most of the blind channel estimation approaches irrespective of the communication platform can be classified under one or more of the groups [3-5] as depicted in *fig. 1.2.*

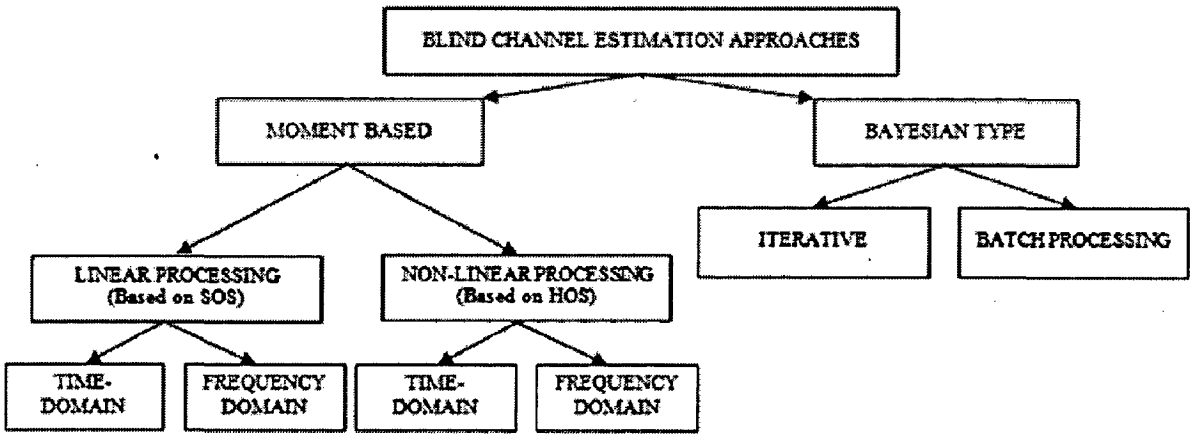

Figure 1.2: The classification tree for blind channel estimation techniques

As depicted by the classification tree, most of the blind techniques mainly fall into either Bayesian or moment-based methods. Bayesian techniques (ML/ MAP) are non-linear in nature and use higher-order statistics of the channel output. Bayesian techniques in turn can be classified as recursive or batch-processing approaches. Recursive techniques are not feasible in busty or asynchronous transmission systems. Bayesian batch-processing techniques normally exhibit fast-convergence but demand high computational complexity. Moment-based approaches on the other hand are batch-processing techniques, which rely on

the estimate of channel output signal statistics obtained by time-averaging. Moment-based approaches can be classified as linear or non-linear depending upon whether they rely on SOS or HOS respectively. HOS-based methods are computationally complex and exhibit low convergence. Each of these can further be divided into frequency-domain or time-domain approaches depending upon the domain in which the processing is done for channel estimation. In the following, we give a brief introduction to some prominent moment-based (especially SOS-based) blind channel estimation algorithms.

1.1.1. SINGLE CARRIER SYSTEMS

For a single-carrier SISO communication link, wherein the channel transfer function is non-minimum phase, the unique relationship does not exist between the amplitude and phase responses of the channel. Hence, one of the solutions for these systems is to estimate both amplitude and phase response which is possible by utilizing the HOS contained in the channel output. The earliest works on blind channel estimation includes the works of Godard [6], Sato [7], Bellini (Bussgang algorithm) [8]. They are a form of blind stochastic gradient channel equalization algorithms which consists of minimizing a non-convex cost function. They can be extended to work as blind channel estimators under the assumption that the channel is linear and has zero initial condition. Unlike above methods, HOS can be explicitly employed in channel estimation as proposed in [9-12]. As far as these approaches are concerned, HOS are represented in time-domain by higher-than-second-order cumulants and moments. Their frequency domain counterparts obtained by multidimensional Fourier transforms are called poly-spectra and moment spectra. In general, HOS are useful in situations where-in non-linearity and coloured noise is to be accounted for. Extracting information from HOS means large variance and non-linear processing. Thus, they require large number of data samples and have low convergence rate. This is unacceptable in applications where the channel is fast time-varying (mobile channels); data rates are high or sent in short bursts (TDMA). Further, HOS provides only an incomplete probabilistic characterization of the signal and suffer from local convergence.

These problems were partially overcome by an algorithm presented by L. Tong, G. Xu and T. Kailath (TXK algorithm) [13], which use linear processing via second order statistics (SOS) and oversampling in time-domain. This algorithm is better than those using HOS in a sense that they require less number of computations and data samples for estimation. Over-sampling the channel output (virtual SIMO systems) at the receiver makes it cyclo-stationary. The cyclo-stationarity can also be induced by employing physical SIMO systems, MISO/

multi-rate transmission systems and periodic modulation [14-16]. This second-order cyclo-stationarity (SOCS) property is utilized for channel estimation. By utilizing SOCS, the SISO channel can be estimated irrespective of the location of channel zeros, noise characteristics (colour), and channel order over-estimation errors [13]. Apart from cyclo-stationary based methods, many SOS-based algorithms have been proposed. They normally utilize the channel structure for estimation purpose.

Sub-channel matching (correlation matching) method by H. Liu, G. Xu, and L. Tong [17] was presented as deterministic approach (i.e., the channel noise is assumed to be negligible) and later as statistical approach to include the effect of noise. A sub-space (decomposition) method was proposed by E. Moulines et al. [18]. This approach is a direct descendent of the TXK approach. The algorithm is based on the channel structure introduced due to oversampling at the receiver and the orthogonality property of the signal and the noise subspaces. Owing to SIMO structure of the channel, a linear parameterization of the noise subspace in terms of the channel parameters is possible. This yields a cost function that can be minimized in least-squares sense to obtain the channel estimate. Subspace methods can be divided into deterministic subspace methods and statistical subspace methods. Deterministic methods do not assume that the input source has a specific statistical structure. In statistical subspace methods, a stochastic source with known SOS is assumed. All practical channel impulse responses are IIR in nature. But, owing to receiver sensitivity issues, for non-sparse channels, most of the energy is concentrated in first few samples allowing the FIR approximation to be feasible. The length of the approximate FIR model is known as "effective length". This corresponds to significant part of the channel impulse response and provides a good approximation to the true channel response. The estimation of effective length is crucial and the analysis of performance degradation of the blind estimation algorithm due to errors in channel length estimation is important. Although, subspace based approaches have significant advantage of being simple in structure, they suffer from estimation errors when the order of the channel is unknown. The subspace algorithm can be made robust to channel order over-estimation by utilizing the specular structure of the channel as mentioned in [19]. This leads to parametric formulation of subspace approach. An extension to the original approach which is robust to both over-estimation and lack of channel disparity (e.g. the sub-channels have common zeros) was proposed by Hoteit [20]. When the channel roots are close to unit circle or in SIMO case when the common zeros of the sub-channels are close to unit circle, the FIR equivalent filter length required to model the inverse

filter becomes exceedingly large and hence is practically not feasible. To overcome this problem, sufficient-order equalizers wherein equalization structure that is based upon two IIR filters and an FIR filter together with two block-based time reversers have been proposed by Lamotharan [21]. A sub-space fitting approach for channel-order estimation for non-minimum phase channels by utilizing distance between subspace matrices was proposed by G. Panci et al [22]. As far as subspace approaches are concerned, either linear or quadratic parameterizations (constraints) of signal subspace or noise subspace can be used for estimation purpose [23-25]. The noise subspace methods are deterministic subspace methods. The variation of subspace approach that uses parametric noise subspace is also known as weighted-subspace method. In practice, the impulse response of communication channel will normally be time-varying and can assume an arbitrary impulse response at any instant of time.

Linear predictor error based methods (linear prediction approach: LPA) by K. Abed Meraim et al. [26] and Yifeng Zhou et al [27] utilize only partial SOS information of channel output. The basic idea behind the linear prediction approach is to recognize that the channel input-output relation; which is a moving-average (MA) process is also a finite-order autoregressive (AR) process. Only the first few columns of channel output's auto-covariance matrix, where leading channel coefficients dominate, are utilized. Hence, the estimation error can be very large if the channel has a weak precursor impulse response [28]. The Outer-product decomposition approach (OPDA) proposed by Zhi Ding [29] unlike LPA is more robust to channel noise. This approach utilizes the block Hankel structure of channel matrix for channel estimation. The above mentioned algorithms (LPA and OPDA) assume that the channel input is temporally white. This can be relaxed if linear smoothing (in contrast to prediction) is used. The formulation of L-S smoothing leads to joint order and channel estimation, as well as robust lattice implementation as proposed by L. Tong and Q. Zhoa [30 and 31]. The main drawbacks of SOS-based time domain methods are that most of them require a good estimate of channel order/ length. This can be overcome by frequency response sampling and second order cyclostationarity (see Gardner, 1991 [32] and L. Tong et al. [33]). These approaches are based on the fact that the magnitude response of the channel can be estimated by PSD and the phase response of a band-limited channel (true for most of the practical communication channels) can be estimated up to a constant phase ambiguity [28] by making use of the relationship between Spectral Correlation Density (SCD) and the channel response $H(j\omega)$ with cycle frequency $\alpha = k/T$ with $k = 1$ (has the largest support).

As signal processing tools became more powerful with VLSI technologies, Kalman and Particle filters [34] have begun to occupy researcher's interest, which in addition to estimation are capable of tracking the time variation in the channel. These approaches use HOS implicity and unlike block estimation techniques, exhibit fast convergence but are not suitable for communication links with busty transmission (TDMA). Blind estimation of sparse channels (hilly-terrain communication link, under-water acoustic communication systems) has been proposed in [35].

Most of the blind estimation algorithms assume that the source covariance matrix is diagonal with known variance. This is not true for practical communication links wherein channel coding is employed to combat AWGN and residual ISI after equalization. Blind channel estimation algorithms applicable for channel-coded systems are reported in literature [36-37]. These algorithms use relaxed/ modified input conditions and/or utilize the coded input structure for channel estimation. Coding introduces input/ transmitter diversity that can be used at the receiver end for channel estimation. Apart from SOS and HOS, the derivatives of generalized characteristic function of the channel output evaluated at arbitrary non-zero points can be used for channel estimation by formulating LS equations [38]. This type of approach can be viewed as a compromise between SOS- and HOS-based methods and are known as "fixed-order statistics (FOS)" approaches.

1.1.2. MULTI-CARRIER SYSTEMS

During past few years, the digital transmission system structure has been altered owing to advances in signal processing and VLSI technologies. Multi-carrier transmission has been adopted in most of the wireless standards owing to higher-data rates that can be achieved due to reduction in ISI. Among them, orthogonal frequency division multiplexing (OFDM) also called as Discrete Matrix Multi-Tone (DMMT) is the most commonly used [39]. OFDM has been adopted as a standard in DAB, DVB (HDTV), Wireless LAN (IEEE 802.11), WiMAX (IEEE 802.16), 3 GPP Long-Term Evolution (LTE) etc. The classical approaches are being extended and generalized so as to be compatible with the technological advances. The performance and applicability of symbol detection and channel estimation algorithms have improved drastically compared to their classical counterparts. This sub-section provides a brief survey of blind channel estimation approaches available in the literature for single and multiple antenna OFDM systems.

Amongst the various blind estimation techniques, subspace decomposition based methods have been proposed owing to their structural simplicity. By employing OFDM modulation schemes, the shortcomings of subspace methods can be overcome by making the algorithm robust to channel nulls (singularity). In OFDM systems, the channel estimation can be achieved either in time-domain or in frequency-domain. In time-domain, the redundancy introduced due to virtual carriers (VC) and/ or cyclic prefix (CP) is utilized in formulating the subspace structure at the receiver end. This can be used to decompose the channel output auto-covariance matrix into two orthogonal subspaces viz. channel or signal subspace and the noise subspace. The orthogonality condition is used for blind estimation of FIR channels subject to channel disparity conditions (conditions to be satisfied for channel identifiability) [40]. In literature, many types of subspace-based approaches are available of which, techniques that utilize the redundancy information induced by employing CP [41] and using VC [42] to estimate the channel dominate. The virtual carriers are used in commercial systems for signal shaping purpose. The cyclic prefix converts the linear time-domain convolution between the channel and the input into cyclic convolution. After DFT operation at the receiver end, this transforms into complex multiplicative factor on each sub channel in the frequency domain. This facilitates use of computationally efficient single-tap complex equalizer in frequency-domain at the receiver [39]. The CP is also known to introduce cyclo-stationarity at the transmitter. This can be used to formulate a time-domain channel estimation algorithm at the receiver [43]. The cyclic prefix can be viewed as redundant time-domain precoding technique. The redundancy introduced at the transmitter can be utilized to form a time-domain subspace-based algorithm at the receiver for channel estimation [41].

The minimum requirement on the length of CP and/ or VC is that it should be greater than the channel support. The VC-based subspace approach can perform even under in-sufficient CP or no-CP conditions. The same analogy holds for the CP-based approach. From the applications of CP and VC respectively, it is clear that employing CP makes way for a computationally efficient channel equalizer in frequency-domain which is more attractive. Whereas VC is used for signal shaping, which is also important; but the VC length can be kept minimal. Using too much virtual carriers causes reduction in spectral efficiency and worst of all, tends to increase peak-to-average-power ratio (PAPR) of the OFDM frame. High PAPR can cause power amplifiers to saturate unless they are operated with sufficiently high back-off. This can cause inter-modulation interference and adjacent channel interference (ACI). With proper signal shaping ACI can be kept minimal, but even then spectral efficiency

would be low without any other advantage. Thus between subspace approaches that adopt either CP or VC, CP-based approaches (with minimal VC) are more attractive.

Further, analogous to subspace approach in single-carrier modulation system, wherein SIMO channel model is employed as an aid for channel estimation, the same can be utilized to formulate subspace based channel estimation algorithm in case of OFDM systems [44]. This type of channel formulation utilizes receiver diversity (in contrast to precoding where transmitter diversity is used) and leads to time-domain algorithms that can function without CP. Other than CP, any redundant precoding at the transmitter can be used to create low-rank correlation matrix at the receiver via which subspace based channel estimation can be performed [45]. It has been found that, it is simpler in terms of system complexity if cyclostationary is induced at the transmitter [15]. Insufficient or no-CP systems can at most estimate the channel up to complex scalar (amplitude plus phase) ambiguity.

The magnitude/ amplitude ambiguity can be resolved in frequency-domain using precoding techniques. Lately, arbitrary precoding has been adopted in blind channel estimation for OFDM based transmission systems [46-51]. These methods are similar except for slight changes in precoder design and structure. The method of [46] uses a linear precoder to induce partial correlation structure on one of the subcarriers per OFDM frame. The approaches given by [49 and 51] are generalized version of [46] i.e., the correlation is induced on every sub-carrier of the OFDM frame. The channel estimation is done via row-column correlation averaging of output auto-covariance matrix in frequency-domain. Due to higher-order of correlation introduced in the latter method, the estimation accuracy is improved. The approach given in [50] uses SVD based algorithm at receiver for channel estimation.

1.1.3. MULTIPLE-INPUT MULTIPLE-OUTPUT (MIMO) OFDM SYSTEMS

The use of multiple antennas at both ends of a wireless link: multiple-input multiple-output (MIMO) technology has been demonstrated to have the potential of achieving extraordinary data rates [52]. The main performance improvements using MIMO systems are antenna gain, diversity gain (both of which increase coverage and QoS), multiplexing gain (increases spectral efficiency) and co-channel interference reduction (increases cellular capacity). MIMO is an important part of modern wireless communication standards such as IEEE 802.11n (Wifi), 3GPP Long Term Evolution, WiMAX and HSPA+. The use of MIMO

technology in combination with OFDM, i.e., MIMO-OFDM, seems to be an attractive solution for future broadband wireless systems [53].

Blind channel estimation techniques have been generalized so as to be applicable for MIMO-OFDM systems. Of them, as far as SOS-based approaches are concerned, subspace-based approach and non-redundant frequency-domain linear precoding approaches mentioned above have occupied a special place. The extension of subspace-based approach in both the scenarios viz. number of transmit antenna greater than or equal to number of receiver antenna and vice-versa are presented in [54]. The proposed method of [54] is a unification of sub-space approach via CP and VC for SISO-OFDM and hence is a generalized version of their SISO-OFDM counterpart. For the case when the number of transmit antenna is greater than the number of receive antenna, the channel output is oversampled at suitable rate such that the total number of virtual output channels/ antenna are greater than transmit antenna; thereby rendering the channel matrix tall-thin low (column) rank. This structure is used along with redundancy introduced due to CP and/ or VC for subspace decomposition and eventually the channel estimation. The performance analysis and identifiability issues of subspace based algorithm are given in [55]. A reformulation of subspace-based approach via reduced-time averaging is proposed in [56] for fast time-varying FIR channels. This approach employs frequency-grouping induced via space-time-frequency (STF) to reduce the effective dimensions of data blocks used to estimate channel output's auto-covariance matrix and sub-space decomposition.

In contrast to SISO-OFDM systems, wherein subspace based approaches could at most estimate the channel vector up to a complex scalar constant ambiguity; in MIMO-OFDM, the estimate suffers from a constant complex matrix ambiguity. The channel estimate can be obtained with just a scalar ambiguity per transmit antenna by adopting precoding as described in [57]. The linear non-redundant precoding of [51] has been extended for MIMO-OFDM systems. The precoder is used to induce correlation among transmitted OFDM frames which can be used at the receiver for channel estimation via row-column averaging. Unlike the case of SISO-OFDM, wherein the precoding matrix is time-invariant; this MIMO-OFDM channel estimation algorithm demands use of periodic block-time-variant precoding matrix.

1.2. PROBLEM STATEMENT

This work mainly concentrates on SOS-based approaches. The scope of this work is as follows:

1) Study of SOS-based subspace decomposition method and TXK algorithm for blind channel estimation in single-carrier systems using SIMO channel model.
2) Study of subspace decomposition method for SISO-OFDM and MIMO-OFDM systems.
3) Study of precoding techniques for blind channel estimation in SISO-OFDM and MIMO-OFDM systems..
4) A comparison of two approaches: time-domain subspace decomposition based method and blind channel estimation using linear non-redundant frequency-domain generalized arbitrary precoding induced correlation-averaging in terms of performance analysis for SISO-OFDM and MIMO-OFDM systems.
5) A study of techniques available to resolve the inherent estimation ambiguity in blind channel estimation approaches using SOS for SISO-OFDM systems and design.

1.3. REPORT ORGANIZATION

The report is organized into five chapters (including *Chapter 1*) as follows:

Chapter 1 provides a literature survey of various blind channel estimation techniques and problem statement.

Chapter 2 presents a blind channel estimation technique using subspace decomposition approach for both single-carrier and multi-carrier (OFDM) systems in both SISO and MIMO antenna scenarios. TXK approach which is the basis for all the SOS-based approach is also described for single-carrier systems. The performance evaluation of subspace method via MATLAB simulations for single-carrier systems is also presented.

Chapter 3 presents a brief overview on use of precoding technique for blind channel estimation. Blind channel estimation via linear non-redundant frequency-domain arbitrary precoding-induced-correlation-averaging approach is described for SISO-OFDM and MIMO-OFDM systems.

Chapter 4 provides the MSE performance analysis of above mentioned approaches; a comparison is provided using MATLAB simulations on practical applicability of the same in both SISO-OFDM and MIMO-OFDM systems.

Chapter 5 provides a brief overview of completely/ totally blind channel estimation techniques for SISO-OFDM systems. Completely blind channel estimation techniques for SISO-OFDM systems using constellation-splitting and modified phase-directed algorithm are proposed. The performance analysis of the same via MATLAB simulation is also presented.

Chapter 6 concludes the report.

The following notations are used in this report: The vectors and matrices are represented by bold ($\boldsymbol{a}$) and bold-uppercase ($\boldsymbol{A}$) alphabets respectively. The transpose, complex conjugate, Hermitian, inverse and Moore-Penrose pseudo-inverse of the matrix $\mathbf{A}$ are denoted by $\mathbf{A}^T$, $\mathbf{A}^*$, $\mathbf{A}^H$, $\mathbf{A}^{-1}$ and $\mathbf{A}^\dagger$, respectively; $\mathbf{a}_R$ and $\mathbf{a}_I$ represent the real and imaginary parts of a vector $\boldsymbol{a}$ (similar notations are used in case of matrix); tr($\mathbf{A}$) stands for the trace operation; diag$(\boldsymbol{a})$ denotes the diagonal matrix with the diagonal element constructed from $\mathbf{a}$; $\otimes$ and $\odot$ stand for the Kronecker and Hadamard products respectively; vec($\mathbf{A}$) represents the vectorization operation of $\mathbf{A}$; $\boldsymbol{I}_p$ is $p \times p$ identity matrix; $\boldsymbol{0}_m$ and $\boldsymbol{0}_{mn}$ represents $m \times m$ and $m \times n$ zero matrices respectively; $\|\mathbf{A}\|_2$ represents the Forbinius norm of a matrix and $E\{\cdot\}$ denotes the statistical expectation. MATLAB notations are used. For example, $\mathbf{A}(m, q)$ and $\mathbf{A}(:, q)$ represent the (m, q)-th entry and the q-th column of matrix $\mathbf{A}$ respectively; "./ " represents element-wise division of two matrices or vectors of same size. The following words are used interchangeably:

1. OFDM vector, OFDM frame and OFDM block.
2. Channel support, channel order and channel length.

They have the same meaning unless otherwise mentioned.

Chapter 2

SUBSPACE BASED BLIND CHANNEL ESTIMATION

As far as SOS-based blind channel estimation techniques are concerned, the subspace decomposition based technique has been mainly considered in the literature owing to its structural simplicity. In this chapter, we discuss subspace based approach for single-carrier and multi-carrier systems.

2.1. BLIND CHANNEL ESTIMATION FOR SINGLE-CARRIER SYSTEMS

The subspace decomposition approach proposed in [18] and the TXK algorithm [13] for single-carrier system is described in this section. The channel model and the algorithm formulation are presented. The performance analysis through MATLAB simulation for subspace approach for single-carrier systems is also presented.

2.1.1. CHANNEL MODEL

This sub-section provides a description of channel model adopted by SOS-based algorithms [18]. Consider a SISO baseband equivalent digital communication link as shown in the *fig. 2.1.*

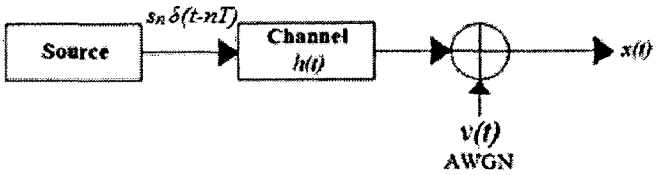

Figure 2.1: SISO baseband equivalent digital communication link

The received signal $x(t)$ is represented as,

$$x(t) = \sum_{n=-\infty}^{\infty} s_n h(t - nT) + v(t) \quad \ldots (2.1)$$

where, s_n's are the transmitted symbols with symbol duration T; $h(t-nT)$ represents the shifted versions of channel impulse response $h(t)$ by times nT and $v(t)$ is additive wide-sense stationary circular complex Gaussian channel noise with zero mean and variance σ^2. The channel impulse response $h(t)$ is assumed to be of finite order/ support and is assumed to

encompass the effects of transmitter filter, receiver filter and modulator/ demodulator which are assumed to be linear. Most of the SOS-based algorithms depend upon the channel matrix structure or cyclostationarity introduced due to single-input multiple-output (SIMO) like structure of the communication link. The SIMO like structure can be introduced either by taking several measurements of incoming channel output signal during the interval T or by adopting multi-rate transmission. Further, several measurements of the channel output at the receiver can be taken in the following two ways [18]:

A. Oversampling approach for SISO system (Virtual SIMO system)

B. Using multiple receiving antenna (Physical SIMO system)

Both the techniques result in similar channel model. For the present discussion, virtual SIMO model is described.

A. Oversampling approach for SISO system (Virtual SIMO system) -

The received signal, $x(t)$ is assumed to be oversampled at rate Δ in order to construct $P = T/\Delta$ sequences corresponding to P virtual channels according to $x_n^{(i)} = x(t_0 + i\Delta + nT)$ for $0 \leq i \leq P-1$. Each sequence $x_n^{(i)}$ is sampled with period T, with a sampling epoch $t_0+i\Delta$ depending on the sequence. Assuming that the channel order is L, we get,

$$x_n^{(i)} = \sum_{k=0}^{L} s_{n-k} h(t_0 + i\Delta + kT) + v_n^{(i)} \quad \ldots (2.2)$$

where, $v_n^{(i)} = v(t_0 + i\Delta + nT)$ are the samples of $v(t)$. The SIMO model with P virtual channels is shown in *fig. 2.2.*

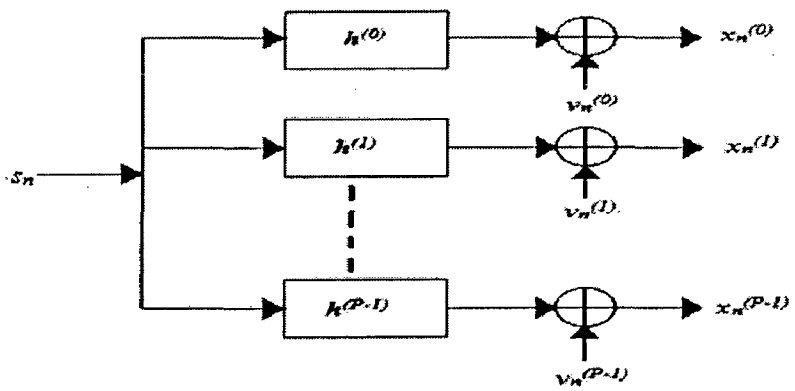

Figure 2.2: Representation of an oversampled SISO (virtual SIMO) channel model

Each sequence $x_n^{(i)}$ depends upon a discrete-time impulse response characterized by i^{th} channel given by:

$$\boldsymbol{h}^{(i)} = \left[h_0^{(i)} \quad \cdots \quad h_L^{(i)}\right]^T = \left[h(t_0 + i\Delta) \quad \cdots \quad h(t_0 + i\Delta + LT)\right]^T \tag{2.3}$$

Let N be the number of received sequence samples collected to form a block. The virtual SIMO channel model can be written as:

$$\boldsymbol{x}_n^{(i)} = \boldsymbol{H}_N^{(i)}\boldsymbol{s}_n + \boldsymbol{v}_n^{(i)} \qquad for\ 0 \le i \le P-1 \tag{2.4}$$

where, $\boldsymbol{x}_n^{(i)} = \left[x_n^{(i)} \quad \cdots \quad x_{n-N+1}^{(i)}\right]^T$, $\boldsymbol{v}_n^{(i)} = \left[v_n^{(i)} \quad \cdots \quad v_{n-N+1}^{(i)}\right]^T$ and $\boldsymbol{s}_n = [s_n \quad \cdots \quad s_{n-N-L+1}]^T$ represents the output, noise and input sequences respectively; $\boldsymbol{H}_N^{(i)}$ is the $N\times(N+L)$ channel convolutional matrix given by,

$$\boldsymbol{H}_N^{(i)} = \begin{bmatrix} h_0^{(i)} & h_1^{(i)} & \cdots & h_L^{(i)} & 0 & \cdots & 0 \\ 0 & h_0^{(i)} & \cdots & h_{L-1}^{(i)} & h_L^{(i)} & \cdots & 0 \\ \vdots & \vdots & \vdots & \vdots & \vdots & \vdots & \vdots \\ 0 & 0 & \cdots & h_0^{(i)} & h_1^{(i)} & \cdots & h_L^{(i)} \end{bmatrix}_{N\times(L+N)} \tag{2.5}$$

The final channel model is given by,

$$\begin{pmatrix} \boldsymbol{x}_n^{(0)} \\ \vdots \\ \boldsymbol{x}_n^{(P-1)} \end{pmatrix} = \begin{pmatrix} \boldsymbol{H}_N^{(0)} \\ \vdots \\ \boldsymbol{H}_N^{(P-1)} \end{pmatrix} \boldsymbol{s}_n + \begin{pmatrix} \boldsymbol{v}_n^{(0)} \\ \vdots \\ \boldsymbol{v}_n^{(P-1)} \end{pmatrix} \tag{2.6}$$

The above equation can be represented in a compact form by a linear system of dimension $PN \times (L+N)$ given by:

$$\boldsymbol{X}_n = \mathbf{H}_N\boldsymbol{s}_n + \boldsymbol{V}_n \tag{2.7}$$

where, $\boldsymbol{X}_n = \begin{pmatrix} \boldsymbol{x}_n^{(0)} \\ \vdots \\ \boldsymbol{x}_n^{(P-1)} \end{pmatrix}$, $\mathbf{H}_N = \begin{pmatrix} \boldsymbol{H}_N^{(0)} \\ \vdots \\ \boldsymbol{H}_N^{(P-1)} \end{pmatrix}$ and $\boldsymbol{V}_n = \begin{pmatrix} \boldsymbol{v}_n^{(0)} \\ \vdots \\ \boldsymbol{v}_n^{(P-1)} \end{pmatrix}$

Note:

1. The channel matrix $\mathbf{H}_N$ given in *eqn. 2.7* can be reformulated and represented instead as $PN \times (L+N)$ block-Toeplitz (or Sylvester resultant) matrix by grouping the P virtual channel coefficients having same delay index together [2].

2. Instead of introducing receiver diversity as mentioned above by oversampling, transmitter diversity can be introduced by employing multi-rate transmission [28]. This technique yields the channel model similar to the one given by *eqn. 2.7.*
3. In contrast to virtual SIMO channel model obtained by employing oversampling at the receiver (or equivalently up-sampling at the transmitter) described above; physical SIMO channel can be realized using multiple-receiving antennas [2].
4. The multi-rate transmission (up-sampling by Δ_t) and over-sampling the channel output at the receiver (by factor Δ_r-> Δ_t) can be combined to form a virtual multiple-input multiple-output (MIMO) systems on which the subspace decomposition method can be applied.

2.1.2. ALGORITHMS FOR BLIND CHANNEL ESTIMATION

A SOS-based method for blind channel estimation known as time-domain TXK algorithm was proposed by Tong, Xu, and Kailath [13]. This approach forms the basis for rest of the SOS-based approaches that followed, including the famous subspace-decomposition method for single-carrier systems. This sub-section describes the TXK approach followed by the subspace approach.

A. TXK algorithm

As mentioned earlier, oversampling the channel output induces cyclostationarity. This cyclostationarity can be utilized in channel estimation. This is the basis for the working of TXK algorithm. The main features of this algorithm are [13]:

i. Since the signal sub-space and over-sampling is employed, the algorithm is immune to noise, timing recovery errors, interference and frequency-selective fading.
ii. The algorithm relies on only SOS making it more computationally efficient and faster.
iii. If the correlation function of the received signal is known exactly (or can be estimated), the algorithm can be applied to possibly non-minimum phase systems asymptotically.
iv. There is no restriction imposed on the probability distribution of the source symbols. The random source may be real or complex, continuous or discrete.

It is assumed that the received signal $x(t)$ is wide-sense cyclostationary i.e. $E[x(t_1)x^*(t_2)] = E[x(t_1+T)x^*(t_2+T)]$. The sampled signal $x(nT)$ may or may not be cyclostationary depending on whether the sampling was done at baud rate or at rate higher than baud rate

respectively. If sampling is done at baud rate, then the signal is only wide-sense stationary and does not contain any phase information. On the other hand, if the sampling rate is higher than the baud rate, the resulting output sequence is wide sense cyclostationary. The SOS of the over-sampled observation contains the phase information of the channel. Thus, virtual SIMO channel structure described in previous sub-section is utilized. Using *eqn. 2.7*, the correlation function of $\boldsymbol{X}_n$ can be written as,

$$\boldsymbol{R}_x(k) = E\{\boldsymbol{X}_n \boldsymbol{X}_{n-k}^H\} = \mathbf{H}_N \boldsymbol{R}_s(k) \mathbf{H}_N^H + \boldsymbol{R}_v(k) \tag{2.8}$$

where, $\boldsymbol{R}_v(k)$ is noise correlation matrix of order $PN \times PN$. Assume that the input signal $\boldsymbol{s}_n$ (*eqn. 2.7*) is white with zero mean and unit variance such that its correlation matrix is:

$$\boldsymbol{R}_s(k) = E\{\boldsymbol{s}_n \boldsymbol{s}_{n-k}^H\} = \begin{cases} \boldsymbol{J}^k & , \ k \geq 0 \\ \left(\boldsymbol{J}^{|k|}\right)^H & , \ k < 0 \end{cases}$$

where, $\boldsymbol{J}$ is the forward shifting matrix defined as,

$$\boldsymbol{J} = \begin{bmatrix} 0 & 0 & \cdots & 0 & 0 \\ 1 & 0 & \cdots & 0 & 0 \\ \vdots & \vdots & \ddots & \vdots & \vdots \\ 0 & 0 & \cdots & 1 & 0 \end{bmatrix}_{(N+L)\times(N+L)}$$

The channel coefficient vector $\boldsymbol{h} = [\boldsymbol{h}^{(0)T} \ \cdots \ \boldsymbol{h}^{(P-1)T}]^T_{P(L+1)\times 1}$ is to be estimated. Note that, for noiseless scenario: $\boldsymbol{R}_x(0) = \mathbf{H}_N \mathbf{H}_N^H$ and $\boldsymbol{R}_x(1) = \mathbf{H}_N \boldsymbol{J} \mathbf{H}_N^H$. Denote the SVD of $\boldsymbol{R}_x(0)$ as

$$\boldsymbol{U}^H \boldsymbol{R}_x(0) \boldsymbol{U} = \begin{bmatrix} \sigma_1^2 & & & & \\ & \ddots & & & \\ & & \sigma_d^2 & & \\ & & & 0 & \\ & & & & \ddots \\ & & & & 0 \end{bmatrix}_{PN\times PN} \tag{2.9}$$

where, $d = N+L$. Let $\boldsymbol{u}_i$ be the i^{th} column of $\boldsymbol{U}$ and construct,

$$\boldsymbol{U}_s = [\boldsymbol{u}_1 \ \cdots \ \boldsymbol{u}_d] \ and \ \boldsymbol{\Sigma}_s = \begin{bmatrix} \sigma_1^2 & & \\ & \ddots & \\ & & \sigma_d^2 \end{bmatrix} \tag{2.10}$$

Form a whitening matrix, $\boldsymbol{F} = \sum_s^{-1} \boldsymbol{U}_s^H$. Since channel input is uncorrelated, using the expression: $\boldsymbol{R}_x(0) = \mathbf{H}_N \mathbf{H}_N^H$ in *eqn. 2.9*, we get [13]:

$$\boldsymbol{H}_N = \boldsymbol{U}_s \boldsymbol{\Sigma}_s \boldsymbol{V}_s \tag{2.11}$$

where V_s is an unknown unitary $d \times d$ matrix yet to be identified from $R_x(1)$. *Eqn. 2.11* implies that the signal subspace is spanned by the columns of channel matrix. This renders the linear parameterization of noise subspace in terms of channel coefficients (elaborated in next sub-section) and thus forms the basis for subspace approach. Thus, we have:

$$\boldsymbol{F}\mathbf{H}_N = \boldsymbol{\Sigma}_s^{-1}\boldsymbol{U}_s^H\boldsymbol{U}_s\boldsymbol{\Sigma}_s\boldsymbol{V}_s = \boldsymbol{V}_s$$

Construct a new matrix:

$$\boldsymbol{D} = \boldsymbol{F}\boldsymbol{R}_x(1)\boldsymbol{F}^H = \boldsymbol{F}\mathbf{H}_N\boldsymbol{J}\mathbf{H}_N^H\boldsymbol{F}^H = \boldsymbol{V}_s\boldsymbol{J}\boldsymbol{V}_s^H \tag{2.12}$$

This relationship allows the identification of the unknown unitary matrix V_s. More specifically, there are two ways of obtaining V_s [13]: the first one is based on the fact that since V_s is unitary, right side of above equation is Jordan decomposition of D (which is computationally tedious comparatively) and the second one is based on the fact that v_d (d^{th} column of V_s) is the right singular vector of D. Let the SVD of D be:

$$[\boldsymbol{y}_1 \quad \cdots \quad \boldsymbol{y}_d]^H\boldsymbol{D}[\boldsymbol{z}_1 \quad \cdots \quad \boldsymbol{z}_d] = diag(\gamma_1^2, \cdots, \gamma_d^2) \tag{2.13}$$

Also,

$$\boldsymbol{D}^H\boldsymbol{D} = \boldsymbol{V}diag(1, \cdots, 1, 0)\boldsymbol{V}^H$$

Thus, there exists a φ such that,

$$\boldsymbol{v}_d = \boldsymbol{z}_d e^{j\varphi}$$

From the Jordan chain, we have,

$$\begin{aligned} \boldsymbol{D}\boldsymbol{v}_k &= \boldsymbol{v}_{k+1}, \quad k = 1, \cdots, d-1 \\ \boldsymbol{D}\boldsymbol{v}_d &= 0 \end{aligned}$$

Thus, we have:

$$\boldsymbol{v}_i = \left(\boldsymbol{D}^{\dagger}\right)^{d-i}\boldsymbol{v}_d$$

Thus,

$$\boldsymbol{V} = [\boldsymbol{v}_1 \quad \cdots \quad \boldsymbol{v}_d] = \left[\left(\boldsymbol{D}^{\dagger}\right)^{d-1}\boldsymbol{v}_d \quad \left(\boldsymbol{D}^{\dagger}\right)^{d-2}\boldsymbol{v}_d \quad \cdots \quad \boldsymbol{v}_d\right]$$

Then channel matrix estimate can be found through:

$$\hat{\mathbf{H}}_N = \boldsymbol{U}_s\boldsymbol{\Sigma}_s\left[\left(\boldsymbol{D}^{\dagger}\right)^{d-1}\boldsymbol{v}_d \quad \left(\boldsymbol{D}^{\dagger}\right)^{d-2}\boldsymbol{v}_d \quad \cdots \quad \boldsymbol{v}_d\right] = \boldsymbol{U}_s\boldsymbol{\Sigma}_s\left[\left(\boldsymbol{D}^{\dagger}\right)^{d-1}\boldsymbol{z}_d \quad \left(\boldsymbol{D}^{\dagger}\right)^{d-2}\boldsymbol{z}_d \quad \cdots \quad \boldsymbol{z}_d\right]e^{j\varphi}$$

...(2.14)

The term φ is the phase ambiguity inherent to the problem.

Note: For noisy case, the noise part is eliminated from the auto-covariance matrices at *lag-0* and *lag-1* respectively to obtain:

$$\boldsymbol{R}_x[0] = \boldsymbol{R}_x(0) - \sigma_n^2 \boldsymbol{I} \text{ and } \boldsymbol{R}_x[1] = \boldsymbol{R}_x(1) - \boldsymbol{R}_n(1) = \boldsymbol{R}_x(1) - \sigma_n^2 \boldsymbol{J}^{T_s \Delta}$$

where, T_s is the symbol rate and Δ is the oversampling rate. Modified auto-covariance matrices $\boldsymbol{R}_x[0]$ and $\boldsymbol{R}_x[1]$ are used with equations: *2.9* to *2.14* instead of $\boldsymbol{R}_x(0)$ and $\boldsymbol{R}_x(1)$ to obtain the channel estimates.

The TXK algorithm utilizes only channel output's SOS to obtain the channel estimate in blind manner. This approach forms the basis of existing SOS-based blind channel estimation techniques. The drawback is that, assuming that the channel order is known at the receiver, TXK algorithm uses two Eigen-value decompositions (eqn. *2.9* and *2.13*), which is computationally costly. Further, compared to subspace based technique described in the next sub-section, TXK algorithm has slower convergence rate [18].

B. Subspace decomposition based algorithm

From the previous discussions it is clear that the auto-covariance matrix can be decomposed into two subspaces, the signal subspace and the noise subspace. The channel identification is based on this property of autocorrelation matrix $\boldsymbol{R}_x$ of the channel output $\boldsymbol{X}_n$ estimated via time-averaging [18]. Using *eqn. 2.7* and *eqn. 2.8*, $\boldsymbol{R}_x$ can be written as:

$$\boldsymbol{R}_x = E\{\boldsymbol{X}_n \boldsymbol{X}_n^H\} = \mathbf{H}_N \boldsymbol{R}_s \mathbf{H}_N^H + \sigma_n^2 \boldsymbol{I}_{PN} \qquad (2.15)$$

Note: $\boldsymbol{R}_x(0) = \boldsymbol{R}_x$ and $\boldsymbol{R}_s(0) = \boldsymbol{R}_s$

Let the PN number of Eigen-values obtained from Eigen-value/ singular-value decomposition (SVD) of $\boldsymbol{R}_x$ be denoted as $\lambda_0, \lambda_1, \ldots, \lambda_{PN-1}$. Assuming that the Eigen-values are arranged in non-increasing order and that $\boldsymbol{R}_s$ is full rank, the signal part of the covariance matrix $\boldsymbol{R}_x$ has rank $L+N$, hence:

$$\lambda_i > \sigma_n^2, \quad for\ i = 0, \cdots, L+N-1$$
$$\lambda_i = \sigma_n^2, \quad for\ i = L+N, \cdots, PN-1$$

Denoting the unit-norm Eigen-vectors associated with the Eige -values $\lambda_0, \ldots, \lambda_{L+N-1}$ as $\boldsymbol{u}_0, \ldots, \boldsymbol{u}_{L+N-1}$; and those unit-norm Eigen-vectors associated with the Eigen-values $\lambda_{L+N}, \ldots, \lambda_{PN-1}$

as g_0, ..., $g_{PN-L-N-1}$, we can define: $U_s = [u_0 \cdots u_{L+N-1}]_{PN\times(L+N)}$ and $G = [g_0 \cdots g_{PN-L-N-1}]_{PN\times(PN-L-N)}$. Thus the covariance matrix can be represented as:

$$R_x = U_s diag(\lambda_0, \cdots, \lambda_{L+N-1}) U_s^H + \sigma_n^2 G G^H \qquad (2.16)$$

The columns of matrix U_s span the signal subspace, while the columns of G span its orthogonal complement, the noise subspace. From *eqn. 2.11* it is clear that the signal subspace is a linear space spanned by the columns of channel filtering matrix $\mathbf{H}_N$. By orthogonality between noise and signal subspaces, the columns of $\mathbf{H}_N$ are orthogonal to any vector in the noise subspace. This leads to linear parameterization of noise subspace bases in terms of channel coefficients. The orthogonality condition can be written as:

$$g_i^H \mathbf{H}_N = 0, \qquad for\ 0 \le i \le PN - N - L \qquad (2.17)$$

The noise subspace can uniquely determine the channel up to a constant multiplicative factor (inherent to the problem) provided the following theorem is satisfied [18]:

Theorem: Assume that

i) $N \geq L$

ii) Matrix $\mathbf{H}_{N-1}$ is full rank i.e., $rank(\mathbf{H}_{N-1}) = L+N-1$.

Let $\mathbf{H}_N''$ be a non-zero filtering matrix with the same dimensions as $\mathbf{H}_N$. The range of $\mathbf{H}_N''$ is included in the range of $\mathbf{H}_N$ if and only if the corresponding vectors H and H'' (H is defined in *eqn. 2.19*) are proportional.

In practice, the covariance matrix is estimated via time-averaging. Thus, only estimates of noise Eigen-vectors $\hat{g}_i$ are available and the orthogonality condition can only be satisfied in least-squares sense. This leads to minimization of following quadratic problem:

$$q(H) = \sum_{i=0}^{PN-L-N-1} \left| \hat{g}_i^H \mathbf{H}_N \right|^2 \qquad \text{... (2.18)}$$

By exploiting the block Toeplitz structure of $\mathbf{H}_N$, the above equation can be put in terms of H. To be more precise, it can be shown that [58]:

$$g_i^H \mathbf{H}_N = H^H G_i$$

where, $\boldsymbol{G}_i = \begin{bmatrix} \boldsymbol{G}_i^{(0)} \\ \vdots \\ \boldsymbol{G}_i^{(P-1)} \end{bmatrix}_{P(L+1)\times(L+N)}$; $\mathbf{H}_N = \begin{bmatrix} \boldsymbol{H}_N^{(0)} \\ \vdots \\ \boldsymbol{H}_N^{(P-1)} \end{bmatrix}_{PN\times(L+N)}$; $\boldsymbol{H} = \begin{bmatrix} \boldsymbol{H}^{(0)} \\ \vdots \\ \boldsymbol{H}^{(P-1)} \end{bmatrix}_{P(L+1)\times 1}$

$$\text{and } \boldsymbol{G}_i^{(l)} = \begin{bmatrix} g_{i,0}^{(l)} & \cdots & g_{i,0}^{(l)} & 0 & \cdots & \cdots & 0 \\ 0 & g_{i,0}^{(l)} & \cdots & g_{i,0}^{(l)} & 0 & \cdots & 0 \\ \vdots & \vdots & \vdots & \ddots & \vdots & \vdots & \vdots \\ 0 & \cdots & \cdots & 0 & g_{i,0}^{(l)} & \cdots & g_{i,0}^{(l)} \end{bmatrix}_{(L+1)\times(L+N)} \tag{2.19}$$

Proof: Partition $\boldsymbol{g}_i$ as

$$\boldsymbol{g}_i = \begin{bmatrix} \boldsymbol{g}_i^{(0)} \\ \vdots \\ \boldsymbol{g}_i^{(P-1)} \end{bmatrix} \quad where \ \boldsymbol{g}_i^{(j)} = \begin{bmatrix} g_{i,0}^{(j)} \\ \vdots \\ g_{i,N-1}^{(j)} \end{bmatrix}$$

Now,

$$\boldsymbol{g}_i^H \mathbf{H}_N = \sum_{l=0}^{P-1} \left(\boldsymbol{g}_i^{(l)}\right)^H \mathbf{H}_N^{(l)}$$

Expanding, each term in above equation yields:

$$\left(\boldsymbol{g}_i^{(l)}\right)^H \mathbf{H}_N^{(l)} = \begin{bmatrix} g_{i,0}^{(l)} & \cdots & g_{i,N-1}^{(l)} \end{bmatrix} \begin{bmatrix} h_0^{(l)} & h_1^{(l)} & \cdots & h_L^{(l)} & 0 & \cdots & 0 \\ 0 & h_0^{(l)} & \cdots & h_{L-1}^{(l)} & h_L^{(l)} & \cdots & 0 \\ \vdots & \vdots & \vdots & \vdots & \vdots & \vdots & \vdots \\ 0 & 0 & \cdots & h_0^{(l)} & h_1^{(l)} & \cdots & h_L^{(l)} \end{bmatrix}$$

It is clear from the structure of above equation that the operation corresponds to convolution of two vectors and since convolution satisfies the commutative law, the above equation can be re-written as:

$$\left(\boldsymbol{g}_i^{(l)}\right)^H \mathbf{H}_N^{(l)} = \begin{bmatrix} h_0^{(l)} & \cdots & h_L^{(l)} \end{bmatrix} \begin{bmatrix} g_{i,0}^{(l)} & g_{i,1}^{(l)} & \cdots & g_{i,N-1}^{(l)} & 0 & \cdots & 0 \\ 0 & g_{i,0}^{(l)} & \cdots & g_{i,N-2}^{(l)} & g_{i,N-1}^{(l)} & \cdots & 0 \\ \vdots & \vdots & \vdots & \vdots & \vdots & \vdots & \vdots \\ 0 & 0 & \cdots & g_{i,0}^{(l)} & g_{i,N-2}^{(l)} & \cdots & g_{i,N-1}^{(l)} \end{bmatrix} = \left[\boldsymbol{H}^{(l)}\right]^H \boldsymbol{G}_i^{(l)}$$

Thus,

$$\boldsymbol{g}_i^H \mathbf{H}_N = \sum_{l=0}^{P-1} \left(\boldsymbol{g}_i^{(l)}\right)^H \mathbf{H}_N^{(l)} = \sum_{l=0}^{P-1} \left(\boldsymbol{H}^{(l)}\right)^H \mathbf{G}_i^{(l)} = \boldsymbol{H}^H \boldsymbol{G}_i$$

Thus, the cost function can be written as:

$$q(\boldsymbol{H}) = \sum_{i=0}^{PN-L-N-1} \left|\widehat{\boldsymbol{g}}_i^H \mathbf{H}_N\right|^2 = \sum_{i=0}^{PN-L-N-1} \left|\boldsymbol{H}^H \widehat{\boldsymbol{G}}_i\right|^2 = \boldsymbol{H}^H \boldsymbol{Q} \boldsymbol{H}, \quad where \;\; \boldsymbol{Q} = \sum_{i=0}^{PN-L-N-1} \widehat{\boldsymbol{G}}_i \widehat{\boldsymbol{G}}_i^H$$

... (2.20)

The *eqn. 2.20* can be minimized subjected to quadratic criterion $||\boldsymbol{H}|| = 1$ to obtain the estimate of the channel. The solution of above minimization problem is the unit-norm Eigen-vector associated with the smallest Eigen-value of matrix $\boldsymbol{Q}$ [58]:

Proof: Assume that $||\boldsymbol{H}|| = \boldsymbol{H}^H\boldsymbol{H} = 1$

The minimization of *eqn. 2.20* can be done using Lagrange's multipliers. Let,

$$J = q(\boldsymbol{H}) + \lambda(1-\boldsymbol{H}^H\boldsymbol{H}) = \boldsymbol{H}^H\boldsymbol{Q}\boldsymbol{H} + \lambda(1-\boldsymbol{H}^H\boldsymbol{H})$$

Differentiating the above equation with respect to $\boldsymbol{H}^H$ and equating the result to zero:

$$\frac{\partial J}{\partial \boldsymbol{H}^H} = \boldsymbol{Q}\boldsymbol{H} - \lambda\boldsymbol{H} = 0$$

Thus, $\boldsymbol{Q}\boldsymbol{H} = \lambda\boldsymbol{H}$. Substituting this result in *eqn. 2.20*:

$$q(\boldsymbol{H}) = \boldsymbol{H}^H\boldsymbol{Q}\boldsymbol{H} = \boldsymbol{H}^H\lambda\boldsymbol{H} = \lambda\boldsymbol{H}^H\boldsymbol{H} = \lambda$$

Since the estimate of $\boldsymbol{H}$ can be obtained by minimizing $q(\boldsymbol{H})$, $\boldsymbol{H}$ corresponds to Eigen-vector corresponding to smallest Eigen-value (λ) of $\boldsymbol{Q}$.

Q.E.D

From the above discussion, it is clear that the subspace based technique for blind channel estimation depends upon the intrinsic SIMO like structure of the oversampled channel and is based on the fact that for a SIMO channel, a linear parameterization of the noise subspace in terms of the channel parameters is possible. A quadratic cost function is formed, which can be minimized to obtain the channel estimate up to a constant complex scalar ambiguity factor. The ambiguity term can be resolved by employing periodic reference symbols [18].

2.1.3. PERFORMANCE ANALYSIS OF SUBSPACE TECHNIQUE

The performance analysis of subspace decomposition approach [18] supported by MATLAB simulations is presented in this subsection.

A. Simulation Parameters

The simulation parameters are given as follows:

- The discrete baseband equivalent channel is assumed to be complex FIR with support length (L) = 2.
- Number of virtual channels assumed (P) = 3.
- The channel power-delay-profile is assumed to be uniform.
- Smoothing factor i.e., the length of data samples per block (N) = 5.
- The total length of data blocks used unless otherwise mentioned (M) = *1000*.
- SNR (unless otherwise mentioned) = 25 dB.
- Baseband modulation/ mapping: 16-QAM
- Reference symbol value = $\sqrt{10}$
- The results are averaged over 100 Monte-Carlo simulation runs.

It is assumed (pre-checked) that the channel response satisfies the necessary identifiability conditions mentioned in [18] for unique determination of channel estimate. The flowchart depicting the procedure to obtain channel estimates using subspace based technique is shown in *fig. 2.3.* The channel estimate which is the Eigen-vector corresponding to the smallest Eigen-value of $\boldsymbol{Q}$ (as mentioned earlier) is obtained as follows. The SVD of matrix $\boldsymbol{Q}$ in MATLAB yields three matrices, the left singular vector matrix ($\boldsymbol{U}$), diagonal singular value matrix ($\boldsymbol{D}$) and right singular vector matrix ($\boldsymbol{V}$). The Eigen-values are arranged in non-increasing order in matrix $\boldsymbol{D}$. The corresponding left Eigen-vectors are arranged column-wise in the matrix $\boldsymbol{U}$. Thus, the last column of $\boldsymbol{U}$ corresponds to the Eigen-vector corresponding to the smallest Eigen-value of $\boldsymbol{Q}$. The complex scalar ambiguity inherent to the approach is resolved by using reference symbols inserted at a period of 25 data symbols.

B. Simulation results and conclusion

The plot of MSE versus varying length of channel output (data) blocks (M) at 25 dB SNR is shown in *fig. 2.4.* It can be seen that the performance improves exponentially as the length of data blocks is increased. From the figure it can be seen that, when the length of data blocks is *100*, the MSE is 1.86×10^{-3}. It can be seen that the MSE reduces by a factor of *12* when

the data block length is increased by a factor of *10* (i.e., the MSE value is 1.55×10^{-4} when the length of data blocks is *1000*). Similarly, the reduction in value of MSE by a factor of *2* can be observed when the data block length is increased from *1000* to *2500* (*2.5* times increase).

The plot of MSE versus varying SNR (dB) values assuming that the length of data blocks (*M*) equal to *1000* is shown in *fig. 2.5*. It can be seen that the MSE curve is almost linear and falls at a steady rate. At *0* dB SNR, the MSE achieved is *2.112* (of the order of 10^0). As SNR is increased, in the range from *0* dB to *15* dB, the MSE reduces by a factor of *1000*. Further increase in SNR does not reflect much reduction in MSE comparably, but yet the improvement is signification. Around *5* times reduction in MSE on an average; per *5* dB increase in SNR can be observed. At *25* dB, the MSE value is 1.8×10^{-4}.

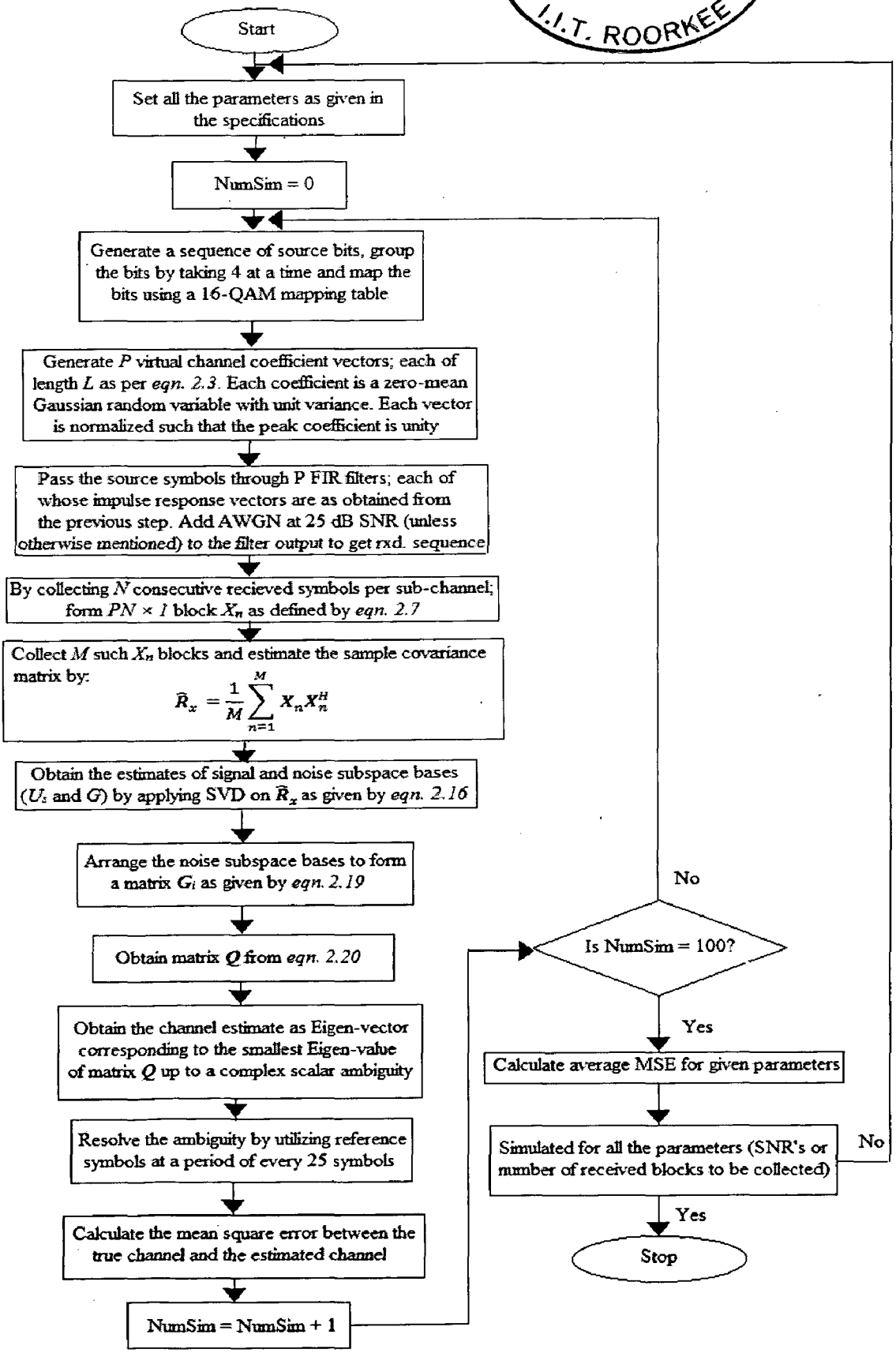

Figure 2.3: Blind channel estimation using subspace decomposition technique (flowchart for generation of plots given in fig. 2.4 and fig. 2.5)

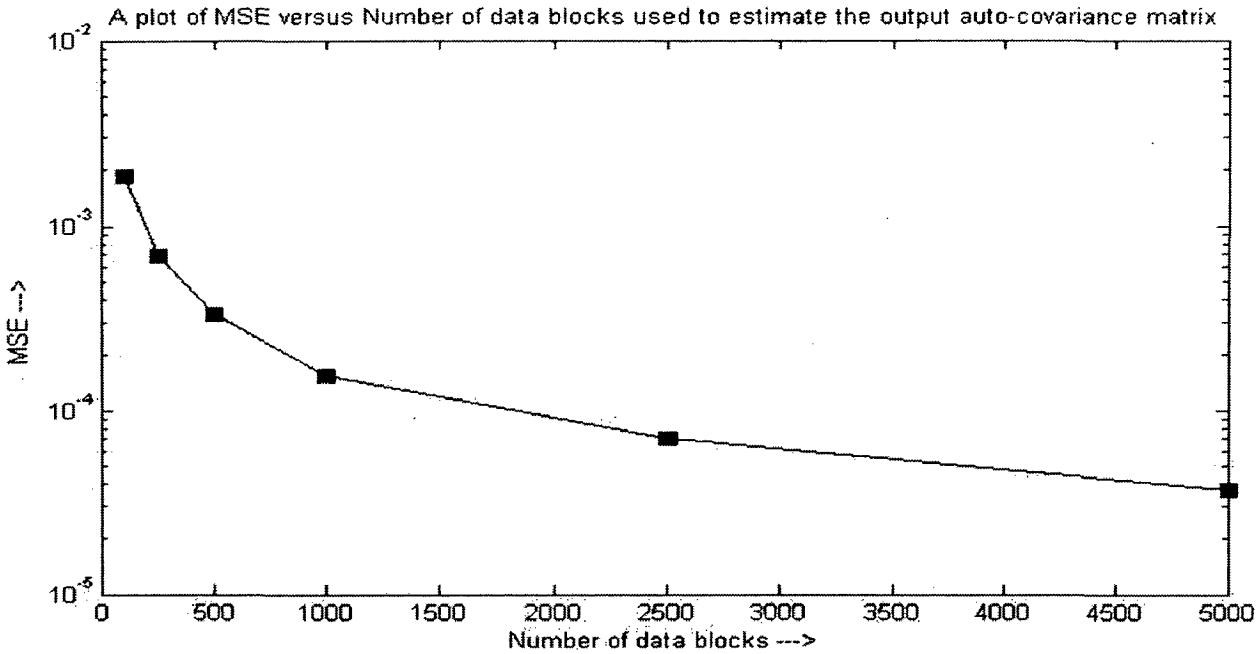

Figure 2.4: The plot of MSE versus length of data blocks at SNR = 25 dB.

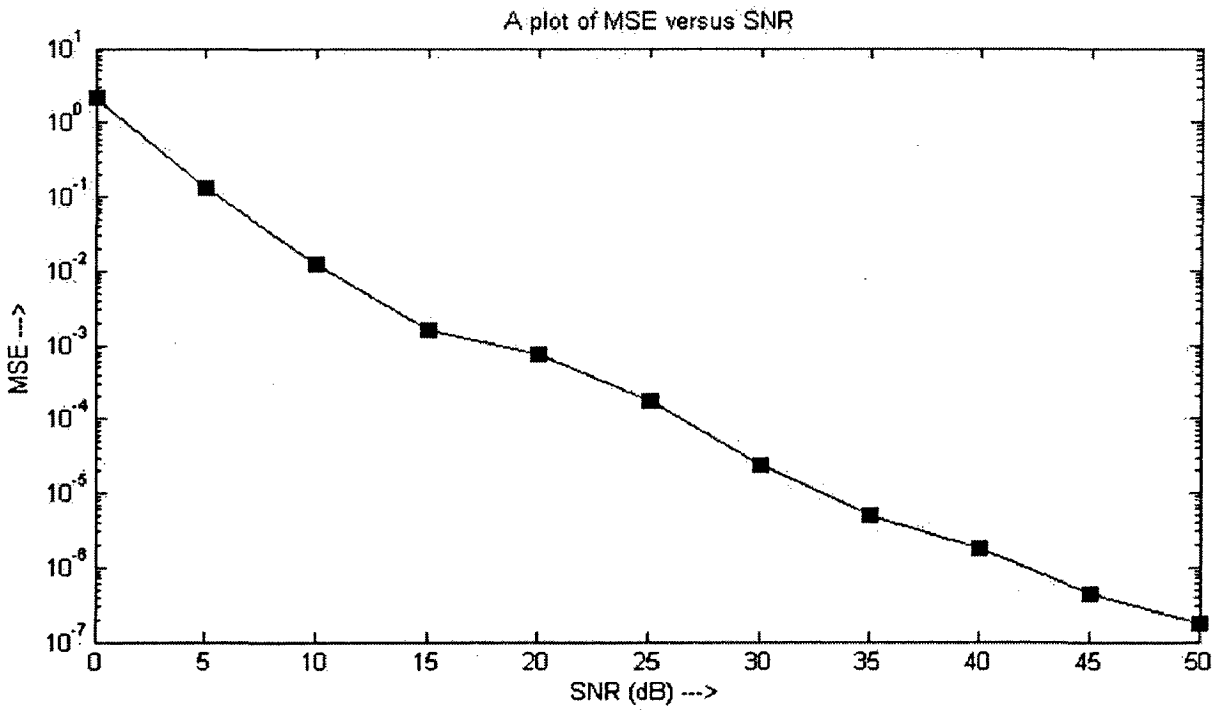

Figure 2.5: The plot of MSE versus SNR (dB) with 1000 data blocks collected for covariance matrix estimation

2.2. BLIND CHANNEL ESTIMATION FOR MULTI-CARRIER SYSTEMS

2.2.1. SISO-OFDM SYSTEMS

The subspace decomposition approach proposed in [41] for SISO-OFDM system is described in this section.

A. SISO-OFDM channel model

The time-domain channel model for SISO-OFDM communication link as applicable to subspace decomposition approach given in [41] is described in this sub-section. Consider, a baseband equivalent SISO-OFDM channel model shown in *fig. 2.6.*

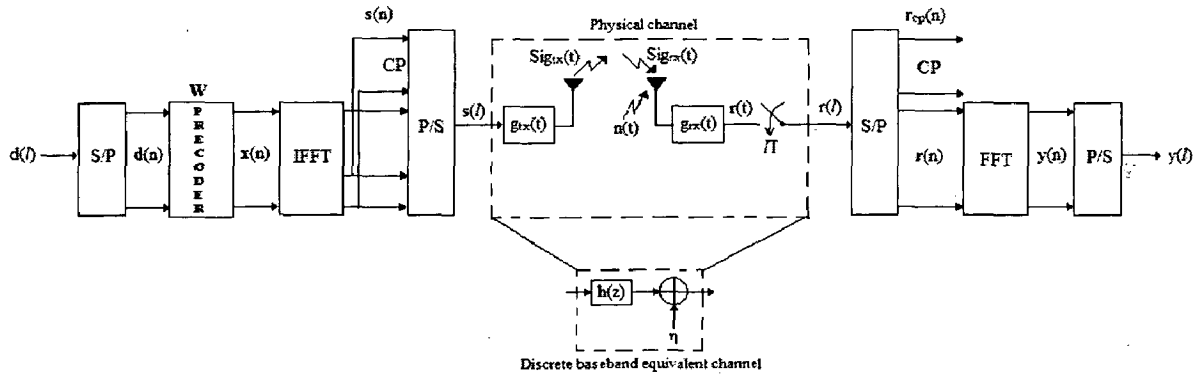

Figure 2.6: Discrete baseband equivalent SISO-OFDM system

The channel model is presented as a special case ($M_t = M_r = 1$) of that given in [54] for MIMO-OFDM systems for the sake of uniformity. A precoder block is included to make the model compatible with the blind channel estimation via precoding-induced correlation-averaging (*Chapter 3*). Addition of the precoder block does not alter the channel model and the algorithm formulation.

Assume N subcarriers per OFDM frames, and let the subcarriers numbered k_0 to $(k_0 + D - 1)$ represent the information data. Let the n^{th} block of the frequency-domain information symbols be written as, $\boldsymbol{d}(n) = [d(n, k_0), d(n, k_0 + 1), \ldots, d(n, k_0 + D - 1)]^T$. Each symbol $d(n,k)$ is taken from a baseband frequency-domain signal constellation (map). The precoder block multiplies the incoming OFDM frame by a predefined matrix $\boldsymbol{W}$ to yield $\boldsymbol{x}(n)$. The precoding matrix $\boldsymbol{W}$ is assumed to be an identity matrix ($\boldsymbol{I}_N$) as far this section is concerned. Hence, $\boldsymbol{d}(n) = \boldsymbol{x}(n)$. The function of precoder block in the context of blind channel estimation is taken up in detail in *Chapter 3*. Assuming that the length of the CP is P, the OFDM modulator adds $N - D$ zeros for virtual carriers to the data block in above equation, applies

an N-point inverse fast Fourier transform (IFFT) to this block, and inserts the CP in front of the IFFT output vector, which is a copy of the last P samples of the IFFT output. This results in the time-domain sample vector of the n^{th} OFDM symbol written as $s(n) = [s(n, N-P), \ldots, s(n, N-1), s(n, 0), \ldots, s(n, N-1)]^T$. To generate the continuous-time signal to be sent on the channel, each element in the vector $s(n)$ is pulse-shaped by a transmit filter $g_{tx}(t)$,

$$Sig_{tx}(t) = \sum_{n=-\infty}^{\infty} \sum_{k=0}^{N+P-1} s(n, \langle N-P+k \rangle_N) g_{tx}[t-(k+n(N+P))T] = \sum_{a=-\infty}^{\infty} s(aT) g_{tx}[t-aT]$$

... (2.21)

During the transmission, the transmitted signal $Sig_{tx}(t)$ passes through a dispersive channel with an impulse response $c(t)$, it gets corrupted by an uncorrelated additive white Gaussian noise $n(t)$, and it finally enters the front-end receive filter $g_{rx}(t)$. Let the composite impulse response be $h(t) = g_{tx}(t) * c(t) * g_{rx}(t)$ which is assumed to be of finite support $[0,(L+N)T]$ with $L \leq P$, with the filtered noise at the receive antenna as $\eta(t) = n(t) * g_{rx}(t)$, the received signal $r(t)$ can be expressed as,

$$r(t) = \sum_{a=-\infty}^{\infty} s(aT) h[t-aT] + \eta(t)$$

... (2.22)

As mentioned in *Chapter 1*, the redundancy introduced by VCs and/or CP can be utilized in channel estimation. This work deals with the system with no virtual carriers i.e., $k_0 = 0$ and $D = N$ and the CP length equal to the channel support i.e., $P = L$. The signal $r(t)$ is sampled at baud rate i.e., $t = lT$. Assuming perfect time-synchronization at the receiver, the sampled sequence $r(l)$ can be written as:

$$r(l) = \sum_{a=-\infty}^{\infty} s(a) h[l-a] + \eta(l) = \sum_{a=-\infty}^{\infty} s(a) h_{l-a} + \eta(l)$$

... (2.23)

The redundancy introduced by CP in time-domain is used along with subspace decomposition for channel estimation purpose [41]. The authors in [41] consider channel estimation based on subspace decomposition for $N = 4L$ (which is not always true for any practical system). The channel model is provided for its generalization to any N and L in

Appendix A of [41]. In this work, we present a formulation of subspace decomposition approach based on this generalized channel model. The generalized model is presented next.

The received sequence, *r(l)* is grouped into *(N+L)×1* dimension vectors to form received time-domain OFDM frames $r_{cp}(n)$ where *n* indicates the block number. Assuming that the channel impulse response vector length *L* is smaller than the number of subcarriers *N* per OFDM frames, the present OFDM block suffers from IBI (inter-block interference) due to previous OFDM block only. Let, $\mathbf{H}_0$ be a *(N+L)* × *(N+L)* lower triangular Toeplitz matrix with first column $[h_0 \quad \cdots \quad h_L \quad 0 \quad \cdots \quad 0]^T$ and first row $[h_0 \quad 0 \quad \cdots \quad 0]^T$. Let $\mathbf{H}_1$ be a *(N+L)* × *(N+L)* upper triangular Toeplitz matrix with first column $[0 \quad \cdots \quad 0]^T$ and first row $[0 \quad \cdots \quad 0 \quad h_L \quad \cdots \quad h_1]^T$. The relationship between the n^{th} time-domain transmitted block *s(n)* and the time-domain received block $r_{cp}(n)$ before CP is discarded is given by [41]:

$$\boldsymbol{r}_{cp}(n) = \mathbf{H}_0\boldsymbol{s}(n) + \mathbf{H}_1\boldsymbol{s}(n-1) + \boldsymbol{\eta}(n) \tag{2.24a}$$

where, $\boldsymbol{\eta}(n)$ represents the *(N+L)* × *1* noise vector corrupting the n^{th} OFDM block. The above equation is the vector-matrix representation of the convolution operation between the source symbols and the channel impulse response coefficients given in *eqn. 2.23*. The vector *s(n)* can be partitioned into three sub-vectors of size *L, N-L, L,* respectively represented by $\boldsymbol{s}(n) = [\boldsymbol{s}_0(n)^T \quad \boldsymbol{s}_1(n)^T \quad \boldsymbol{s}_2(n)^T]^T$ with $s_0(n) = s_2(n)$. Similarly, both the $r_{cp}(n)$ and $\boldsymbol{\eta}(n)$ can be written as: $\boldsymbol{r}_{cp}(n) = [\boldsymbol{r}_0(n)^T \quad \boldsymbol{r}_1(n)^T \quad \boldsymbol{r}_2(n)^T]^T$ and $\boldsymbol{\eta}(n) = [\boldsymbol{n}_0(n)^T \quad \boldsymbol{n}_1(n)^T \quad \boldsymbol{n}_2(n)^T]^T$ respectively. The components of $r_{cp}(n)$ and $\boldsymbol{\eta}(n)$ are defined below.

Let, $\mathbf{C}_0$ be a *L*×*L* Toeplitz matrix with first column $[h_0 \quad \cdots \quad h_{L-1}]^T$ and first row $[h_0 \quad 0 \quad \cdots \quad 0]^T$ and $\mathbf{C}_1$ be *L*×*L* Toeplitz matrix with first column $[h_L \quad 0 \quad \cdots \quad 0]^T$ and first row $[h_L \quad \cdots \quad h_1]^T$. Thus, *eqn. 2.24a* can be rewritten as:

$$\boldsymbol{r}_{cp}(n) = \begin{bmatrix}\boldsymbol{r}_0(n)\\ \boldsymbol{r}_1(n)\\ \boldsymbol{r}_2(n)\end{bmatrix} = \begin{bmatrix}\mathbf{C}_0 & 0 & 0\\ \mathbf{C}_1' & \mathbf{C}_0' & 0\\ 0 & \mathbf{C}_1'' & \mathbf{C}_0\end{bmatrix}\begin{bmatrix}\boldsymbol{s}_2(n)\\ \boldsymbol{s}_1(n)\\ \boldsymbol{s}_2(n)\end{bmatrix} + \begin{bmatrix}0 & 0 & \mathbf{C}_1\\ 0 & 0 & 0\\ 0 & 0 & 0\end{bmatrix}\begin{bmatrix}\boldsymbol{s}_2(n-1)\\ \boldsymbol{s}_1(n-1)\\ \boldsymbol{s}_2(n-1)\end{bmatrix} + \begin{bmatrix}\boldsymbol{n}_0(n)\\ \boldsymbol{n}_1(n)\\ \boldsymbol{n}_2(n)\end{bmatrix} \tag{2.24b}$$

where, $\mathbf{C}_0'$ is a (N-*L*)×*(N-L)* Toeplitz matrix with first column $[h_0 \quad \cdots \quad h_L \quad 0 \quad \cdots \quad 0]^T$ and first row $[h_0 \quad 0 \quad \cdots \quad 0]^T$; $\mathbf{C}_1' = [\mathbf{C}_1^T \quad \mathbf{0}_{L\times(N-2L)}]^T$ and $\mathbf{C}_1'' = [\mathbf{0}_{L\times(N-2L)} \quad \mathbf{C}_1]$. By, collecting two consecutive received OFDM symbols, the following input-output relation can be formed which is used for subspace decomposition [41],

$$\bar{\boldsymbol{r}}(n) = \begin{bmatrix} r_1(n-1) \\ r_2(n-1) \\ r_0(n) \\ r_1(n) \\ rr_2(n) \end{bmatrix} = \begin{bmatrix} \mathbf{C}_0' & \mathbf{C}_1' & 0 & 0 \\ \mathbf{C}_1'' & \mathbf{C}_0 & 0 & 0 \\ 0 & \mathbf{C}_1 & 0 & \mathbf{C}_0 \\ 0 & 0 & \mathbf{C}_0' & \mathbf{C}_1' \\ 0 & 0 & \mathbf{C}_1'' & \mathbf{C}_0 \end{bmatrix} \begin{bmatrix} s_1(n-1) \\ s_2(n-1) \\ s_1(n) \\ s_2(n) \end{bmatrix} + \begin{bmatrix} n_1(n-1) \\ n_2(n-1) \\ n_0(n) \\ n_1(n) \\ n_2(n) \end{bmatrix} = \mathbf{H}(h)\bar{\boldsymbol{s}}(n) + \bar{\boldsymbol{n}}(n)$$

... (2.25)

B. Generalized subspace-based algorithm

Using *eqn. 2.25,* the auto-covariance matrix $\boldsymbol{R}_{\bar{r}\bar{r}}$ of $\bar{\boldsymbol{r}}(n)$ is evaluated by time-averaging and can be written as:

$$\boldsymbol{R}_{\bar{r}\bar{r}} = E\{\bar{\boldsymbol{r}}(n)\bar{\boldsymbol{r}}(n)^H\} = \mathbf{H}(h)\boldsymbol{R}_{\bar{s}\bar{s}}\mathbf{H}(h)^H + \sigma_n^2\boldsymbol{I}_{2N+L} \qquad (2.26)$$

where, the source covariance matrix is given by: $\boldsymbol{R}_{\bar{s}\bar{s}} = E\{\bar{\boldsymbol{s}}(n)\bar{\boldsymbol{s}}(n)^H\}$ with $\bar{\boldsymbol{s}}(n)$ as defined in *eqn. 2.25.* If $\boldsymbol{R}_{\bar{s}\bar{s}}$ is full rank, the matrix $\mathbf{H}(h)\boldsymbol{R}_{\bar{s}\bar{s}}\mathbf{H}(h)^H$ has rank *8L*. Therefore the null-space has dimension *L* and is spanned by a basis of *L* vectors $\boldsymbol{g}_0, \ldots, \boldsymbol{g}_{L-1}$ [41]. This subspace is referred to as noise subspace and it is orthogonal to the channel/ signal subspace. Further, as mentioned earlier, noise subspace bases can be found by applying SVD on $\boldsymbol{R}_{\bar{r}\bar{r}}$.

The generalized subspace algorithm for the channel model with $N \geq 2L$ is presented. Analogous to single-carrier case, the left null-space of $\boldsymbol{R}_{\bar{r}\bar{r}}$ of dimension *(2N+L)* × *L* can be represented by:

$$\boldsymbol{g}_i = \left(\begin{bmatrix} \boldsymbol{g}_i^{1T} & \boldsymbol{g}_i^{2T} & \boldsymbol{g}_i^{3T} & \boldsymbol{g}_i^{4T} & \boldsymbol{g}_i^{5T} \end{bmatrix}^T\right)_{(2N+L)\times 1} \quad for \quad 0 \leq i \leq L-1 \qquad (2.27)$$

where,

$$\boldsymbol{g}_i^1 = ([g_i(1) \quad \cdots \quad g_i(N-L)]^T)_{(N-L)\times 1} = ([g_i^1(1) \quad \cdots \quad g_i^1(N-L)]^T)_{(N-L)\times 1}$$

$$\boldsymbol{g}_i^2 = ([g_i(N-L+1) \quad \cdots \quad g_i(N)]^T)_{L\times 1} = ([g_i^2(1) \quad \cdots \quad g_i^2(L)]^T)_{L\times 1}$$

$$\boldsymbol{g}_i^3 = ([g_i(N+1) \quad \cdots \quad g_i(N+L)]^T)_{L\times 1} = ([g_i^3(1) \quad \cdots \quad g_i^3(L)]^T)_{L\times 1}$$

$$\boldsymbol{g}_i^4 = ([g_i(N+L+1) \quad \cdots \quad g_i(2N)]^T)_{(N-L)\times 1} = ([g_i^4(1) \quad \cdots \quad g_i^4(N-L)]^T)_{(N-L)\times 1}$$

$$\boldsymbol{g}_i^5 = ([g_i(2N+1) \quad \cdots \quad g_i(2N+L)]^T)_{L\times 1} = ([g_i^5(1) \quad \cdots \quad g_i^5(L)]^T)_{L\times 1}$$

The orthogonality between signal/ channel and noise subspace can be mathematically put as,

$$\boldsymbol{g}_i^H\mathbf{H}(h) = 0, \qquad for\ 0 \leq i \leq L-1 \qquad (2.28)$$

Eqn. 2.28 gives the linear parameterization of the noise subspace in terms of the channel parameters. As mentioned earlier, since the covariance matrix is calculated by time-averaging, in practice, above condition can be minimized in least-squares sense to obtain the channel coefficients. Looking at the structure of unknown channel matrix in *eqn. 2.28*, solving for channel coefficients using *eqn. 2.28* is difficult. A dual form of *eqn. 2.28*, whose minimization is simpler and more straight-forward, must be formed. The details of derivation of dual form of the *eqn. 2.28* by mathematical induction are described in *Appendix A* of the dissertation report. The result of the derivation is summarized here. The dual form can be defined by the following set of equations:

1) For $j = 1, 4$; define the following matrices-

$$\boldsymbol{A}_i^j = \begin{bmatrix} g_i^j(N-2L+1) & \cdots & g_i^j(N-L) \\ \vdots & \iddots & \vdots \\ g_i^j(N-L) & \cdots & 0 \\ 0 & \cdots & 0 \end{bmatrix}_{(L+1)\times L} \quad and \quad \boldsymbol{B}_i^j = \begin{bmatrix} 0 & \cdots & 0 \\ 0 & \cdots & g_i^j(1) \\ \vdots & \iddots & \vdots \\ g_i^j(1) & \cdots & g_i^j(L) \end{bmatrix}_{(L+1)\times L}$$

2) For $j = 2, 3$ *and* 5; define the following matrices-

$$\boldsymbol{A}_i^j = \begin{bmatrix} g_i^j(1) & \cdots & g_i^j(L) \\ \vdots & \iddots & \vdots \\ g_i^j(L) & \cdots & 0 \\ 0 & \cdots & 0 \end{bmatrix}_{(L+1)\times L} \quad and \quad \boldsymbol{B}_i^j = \begin{bmatrix} 0 & \cdots & 0 \\ 0 & \cdots & g_i^j(1) \\ \vdots & \iddots & \vdots \\ g_i^j(1) & \cdots & g_i^j(L) \end{bmatrix}_{(L+1)\times L}$$

Now, the components of noise subspace bases matrices can be written as:

$$\boldsymbol{G}_i^1 = \begin{bmatrix} g_i^1(1) & g_i^1(2) & \cdots & g_i^1(N-2L) \\ \vdots & \vdots & \ddots & \vdots \\ g_i^1(L+1) & g_i^1(L+2) & \cdots & g_i^1(N-L) \end{bmatrix}_{(L+1)\times(N-2L)}$$

$$\boldsymbol{G}_i^2 = \boldsymbol{A}_i^1 + \boldsymbol{B}_i^2$$

$$\boldsymbol{G}_i^3 = \boldsymbol{A}_i^2 + \boldsymbol{B}_i^3 + \boldsymbol{B}_i^1$$

$$\boldsymbol{G}_i^4 = \begin{bmatrix} g_i^4(1) & g_i^4(2) & \cdots & g_i^4(N-2L) \\ \vdots & \vdots & \ddots & \vdots \\ g_i^4(L+1) & g_i^4(L+2) & \cdots & g_i^4(N-L) \end{bmatrix}_{(L+1)\times(N-2L)}$$

$$\boldsymbol{G}_i^5 = \boldsymbol{A}_i^4 + \boldsymbol{B}_i^5$$

$$\boldsymbol{G}_i^6 = \boldsymbol{A}_i^5 + \boldsymbol{B}_i^6 + \boldsymbol{A}_i^3$$

Combining these sub-matrices, the dual noise-subspace matrix can be formed as:

$$\boldsymbol{G}_i = [\boldsymbol{G}_i^1 \quad \boldsymbol{G}_i^2 \quad \boldsymbol{G}_i^3 \quad \boldsymbol{G}_i^4 \quad \boldsymbol{G}_i^5 \quad \boldsymbol{G}_i^6]_{(L+1)\times 2N} \tag{2.29}$$

Thus, the dual orthogonality condition can be written as:

$$\boldsymbol{h}^H \boldsymbol{G}_i = \mathbf{0}_{1\times 2N} \quad for\ 0 \le i \le L-1 \tag{2.30}$$

where, $\boldsymbol{h} = [h_0\ h_1 \ldots\ h_L]^T$ is the channel impulse response vector. *Eqn. 2.30* can be minimized in least-squares sense to obtain the channel estimate in time-domain up to complex scalar ambiguity factor. The quadratic cost function given by:

$$q(\boldsymbol{H}) = \boldsymbol{h}^H \boldsymbol{Q} \boldsymbol{h}, \quad where\ \ \boldsymbol{Q} = \sum_{i=0}^{L-1} \widehat{\boldsymbol{G}}_i \widehat{\boldsymbol{G}}_i^H \tag{2.31}$$

is solved subjected to condition $||\boldsymbol{h}|| = 1$ to obtain an estimate of $\boldsymbol{h}$. It is a well known fact that the channel impulse response estimate $\widehat{\boldsymbol{h}}$ is the unit-norm Eigen-vector associated with the smallest Eigen-value of $\boldsymbol{Q}$.

Note: The persistence of excitation assumption (p.o.e) [41] states that the minimum number of OFDM blocks that should be used for estimation of covariance matrix should be greater than or equal to *2N*.

2.2.2. MIMO-OFDM SYSTEMS

We next present a generalization of the subspace based approach of [41] proposed in [54] for MIMO-OFDM systems.

A. MIMO-OFDM channel model

In continuation with the channel model presented in the previous sub-section, we provide a brief description of generalization of the same for MIMO-OFDM systems. Consider the discrete baseband equivalent channel model of MIMO-OFDM system with M_t transmitting antenna and M_r receiving antenna as shown in the *fig. 2.7.*

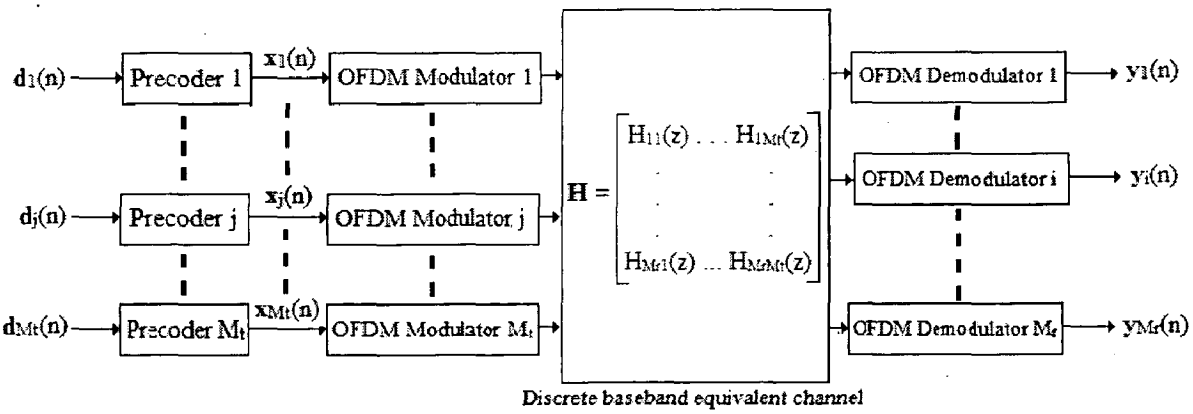

Figure 2.7: Discrete baseband equivalent MIMO-OFDM system model

Analogous to the SISO model, assuming zero VC and N subcarriers per OFDM frame, the frequency-domain transmitted OFDM frame from the j^{th} transmitter antenna is given by $\boldsymbol{d_j(n)} = [d_j(n, 0), d_j(n, k_0 + 1), \ldots, d_j(n, N)]^T$. Each symbol $d_j(n,k)$ is taken from a baseband frequency-domain signal constellation (map). As in SISO case, the precoding matrices are assumed to be identity matrices ($\boldsymbol{I_N}$) as far this section is concerned. Hence, $\boldsymbol{d_j(n)} = \boldsymbol{x_j(n)}$. The time-domain sample vector of the n^{th} OFDM symbol can be written as $\boldsymbol{s_j(n)} = [s_j(n, N - P), \ldots, s_j(n, N-1), s_j(n, 0), \ldots, s_j(n, N - 1)]^T$. To generate the continuous-time signal to be sent on the channel, each element in the vector $\boldsymbol{s_j(n)}$ is pulse-shaped according to *eqn. 2.21*. Denoting the composite impulse response between the j^{th} transmitter antenna and i^{th} receiving antenna by $h_{ij}(t)$ (assumed to be of finite support $[0,(L+N)T]$ with $L \leq P$ as previously stated), the received signal at i^{th} receiving antenna $r_i(t)$ can be expressed as,

$$r_i(t) = \sum_{j=1}^{M_t} \sum_{a=-\infty}^{\infty} s_j(aT) h_{ij}[t - aT] + \eta_i(t)$$

where, $\eta_i(t)$ is the filtered noise at i^{th} receiving antenna. The signal $r_i(t)$ is sampled at baud rate as mentioned in previous sub-section to obtain sampled time-domain sequence. Depending on the values of M_t and M_r, the analysis can be carried out for two cases, $M_t > M_r$ and $M_t \leq M_r$ [54]. In this work, the second case is taken up in detail. The alterations to make the model compatible with the first case are described in the footnote. Construct a composite frequency-domain signal vector,

$$\boldsymbol{d}(n,k) = [d_1(n,k) \quad \cdots \quad d_{M_t}(n,k)]^T$$

and (2.32a)

$$\boldsymbol{d_n} = [\boldsymbol{d}(n,0)^T \quad \cdots \quad \boldsymbol{d}(n,N)^T]^T$$

where, $d_j(n, k)$ is an information symbol loaded on the k^{th} subcarrier in the n^{th} OFDM block to be transmitted from the j^{th} transmitter antenna. By collecting J consecutive OFDM frames from M_t transmitting antennas, the information symbol vector $\boldsymbol{d}(n)$ is constructed as:

$$\boldsymbol{d}(n) = \left[\boldsymbol{d}_n^T \quad \cdots \quad \boldsymbol{d}_{n-J+1}^T\right]^T \tag{2.32b}$$

Define the IFFT matrices as:

$$\begin{gathered}\boldsymbol{W}(i) = \frac{1}{\sqrt{N}}[1 \quad w_N^i \quad \cdots \quad w_N^N] \\ \boldsymbol{W_N} = [\boldsymbol{W}(N-1)^T \quad \cdots \quad \boldsymbol{W}(0)^T \quad \boldsymbol{W}(N-1)^T \quad \cdots \quad \boldsymbol{W}(N-P)^T]^T \\ \mathbf{W} = \boldsymbol{I}_J \otimes \boldsymbol{W_N} \otimes \boldsymbol{I}_{M_t}\end{gathered} \tag{2.33}$$

Further, construct a similar composite time-domain OFDM frame as:

$$\begin{gathered}\boldsymbol{s}(n,k) = [s_1(n,k) \quad \cdots \quad s_{M_t}(n,k)]^T \\ \boldsymbol{s_n} = [\boldsymbol{s}(n,N-1)^T \quad \cdots \quad \boldsymbol{s}(n,0)^T \quad \boldsymbol{s}(n,N-1)^T \quad \cdots \quad \boldsymbol{s}(n,N-P)^T]^T \\ \boldsymbol{s}(n) = \left[\boldsymbol{s}_n^T \quad \cdots \quad \boldsymbol{s}_{n-J+1}^T\right]^T\end{gathered} \tag{2.34}$$

Combining *eqn. 2.32, 2.33 and 2.34*, we can obtain a composite relationship representing the function of both IFFT block and CP insertion operations as:

$$\boldsymbol{s}(n) = \mathbf{W}\boldsymbol{d}(n) \tag{2.35}$$

As mentioned earlier, assuming that the length of channel impulse response vector between each of i^{th} receiving antenna and j^{th} transmitting antenna is upper-bounded by L, the $M_r \times M_t$ channel matrix $\boldsymbol{H(l)}$ between all pairs of transmitting and receiving antennas at lag-l can be constructed as:

$$\boldsymbol{H}(l) = \begin{bmatrix} h_{11}(l) & \cdots & h_{1M_t}(l) \\ \vdots & \ddots & \vdots \\ h_{M_r1}(l) & \cdots & h_{M_rM_t}(l) \end{bmatrix} \tag{2.36}$$

The sampled received signal from *eqn. 2.23* is similarly stacked to form a composite time-domain vector as given by:

$$\begin{gathered}\boldsymbol{r}(n,k) = [r_1(n,k) \quad \cdots \quad r_{M_r}(n,k)]^T \\ \boldsymbol{r_n} = [\boldsymbol{r}(n,Q-1)^T \quad \cdots \quad \boldsymbol{r}(n,0)^T]^T \\ \boldsymbol{r}(n) = \left[\boldsymbol{r}_n^T \quad \cdots \quad \boldsymbol{r}_{n-J+1}^T[1:(Q-L)M_r]\right]^T\end{gathered} \tag{2.37}$$

where, $Q = N+P = N+L$ and the term $[1:(Q-L)M_r]$ denotes that the dimension of each $\boldsymbol{r}_{n-p}$ (for all $p = 0$ to $J-1$) is $(Q-L)M_r \times 1$. The composite noise vector $\boldsymbol{\eta}(n)$ can similarly be formed. Define the $(JQ-L)M_r \times JQM_t$ channel matrix as:

$$\mathbf{H} = \begin{bmatrix} \boldsymbol{H}(0) & \cdots & \boldsymbol{H}(L) & \mathbf{0} & \cdots & \mathbf{0} \\ \mathbf{0} & \boldsymbol{H}(0) & \cdots & \boldsymbol{H}(L) & \cdots & \mathbf{0} \\ \vdots & \cdots & \cdots & \cdots & \cdots & \vdots \\ \mathbf{0} & \cdots & \mathbf{0} & \boldsymbol{H}(0) & \cdots & \boldsymbol{H}(L) \end{bmatrix}_{(JQ-L)M_r \times JQM_t} \tag{2.38}$$

The channel input-output relationship can be expressed in terms of composite transmit-receive vector and channel matrix as:

$$\boldsymbol{r}(n) = \boldsymbol{H}\boldsymbol{s}(n) + \boldsymbol{\eta}(n) = \mathbf{H}\mathbf{W}\boldsymbol{d}(n) + \boldsymbol{\eta}(n) = \mathbf{A}\boldsymbol{d}(n) + \boldsymbol{\eta}(n) \tag{2.39}$$

Note: For a MIMO-OFDM system with $M_t > M_r$, the sampling rate at the receiver is set to q/T with $q \geq M_t/M_r$ [54] such that the number of effective (virtual) receiving antennas after oversampling is greater than or equal to the number of physical transmitting antenna. The relevant alterations for the channel model are described as follows:

The channel sub-matrix of *eqn. 2.36* can be re-framed as:

$$\tilde{\boldsymbol{H}}(l) = \begin{bmatrix} h_{11}^{(0)}(l) & \cdots & h_{1M_t}^{(0)}(l) \\ \vdots & \ddots & \vdots \\ h_{11}^{(q-1)}(l) & \cdots & h_{1M_t}^{(q-1)}(l) \\ \vdots & \ddots & \vdots \\ h_{M_r1}^{(0)}(l) & \cdots & h_{M_rM_t}^{(0)}(l) \\ \vdots & \ddots & \vdots \\ h_{M_r1}^{(q-1)}(l) & \cdots & h_{M_rM_t}^{(q-1)}(l) \end{bmatrix}$$

Hence, the channel matrix can be written as:

$$\tilde{\mathbf{H}} = \begin{bmatrix} \tilde{\boldsymbol{H}}(0) & \cdots & \tilde{\boldsymbol{H}}(L) & \mathbf{0} & \cdots & \mathbf{0} \\ \mathbf{0} & \tilde{\boldsymbol{H}}(0) & \cdots & \tilde{\boldsymbol{H}}(L) & \cdots & \mathbf{0} \\ \vdots & \cdots & \cdots & \cdots & \cdots & \vdots \\ \mathbf{0} & \cdots & \mathbf{0} & \tilde{\boldsymbol{H}}(0) & \cdots & \tilde{\boldsymbol{H}}(L) \end{bmatrix}_{(JQ-L)qM_r \times JQM_t}$$

Analogous to *eqn. 2.37*, representing the oversampled received signal vector as:

$$\tilde{\boldsymbol{r}}(n,k) = \left[r_1^{(0)}(n,k) \quad \cdots \quad r_1^{(q-1)}(n,k) \quad \cdots \quad r_{M_r}^{(0)}(n,k) \quad \cdots \quad r_{M_r}^{(q-1)}(n,k)\right]^T$$

$$\tilde{\boldsymbol{r}}_n = \left[\tilde{\boldsymbol{r}}(n,Q-1)^T \quad \cdots \quad \tilde{\boldsymbol{r}}(n,0)^T\right]^T$$

$$\tilde{\boldsymbol{r}}(n) = \left[\tilde{\boldsymbol{r}}_n^T \quad \cdots \quad \tilde{\boldsymbol{r}}_{n-J+1}^T[1:(Q-L)qM_r]\right]^T$$

The channel model is given by:

$$\tilde{\boldsymbol{r}}(n) = \tilde{\boldsymbol{H}}\boldsymbol{s}(n) + \tilde{\boldsymbol{\eta}}(n) = \tilde{\mathbf{H}}\mathbf{W}\boldsymbol{d}(n) + \tilde{\boldsymbol{\eta}}(n) = \tilde{\mathbf{A}}\boldsymbol{d}(n) + \tilde{\boldsymbol{\eta}}(n) \tag{2.40}$$

Similar subspace algorithm formulation can be obtained for channel estimation [54].

B. Subspace based algorithm

Analogous to the subspace decomposition method for SISO-OFDM, the composite channel output auto-covariance matrix estimated via time-averaging is used for channel estimation. Assuming that the source covariance matrix is diagonal with known variance, from *eqn. 2.39*, the composite channel output auto-covariance matrix can be written as:

$$\boldsymbol{R}_{rr} = E\{\boldsymbol{r}(n)\boldsymbol{r}(n)^H\} = \sigma_d^2\mathbf{A}\mathbf{A}^H + \sigma_n^2\boldsymbol{I}_{(JQ-L)M_r} \tag{2.41}$$

Singular-value decomposition (SVD) of the output auto-covariance matrix yields two subspaces namely, signal subspace spanned by columns of the channel matrix **A** and an orthogonal null-space referred to as noise subspace. For the MIMO-OFDM channel to be identified by the noise subspace method, the matrix **A** in *eqn. 2.39* (or matrix $\tilde{\boldsymbol{A}}$ in *eqn. 2.40*) should have a full column rank. *Theorem 1* gives a necessary and sufficient condition for the full column rank requirement [54]:

Theorem 1: In the case of $M_t \leq M_r$ and $L \leq (Q - N)$, the matrix **A** has a full column rank, if and only if $rank\left(\mathbf{H}\left(w_N^i\right)\right) = M_t \;\forall\; i \in \{k\}_{k=0}^{N-1}$ where, **H**(z) is given by:

$$\mathbf{H}(z) = \sum_{l=0}^{L} \boldsymbol{h}(l)z^{-l}$$

Note: The above theorem can be re-phrased for $M_t > M_r$ [54] by replacing $\boldsymbol{A}$ by $\tilde{\boldsymbol{A}}$; $\boldsymbol{h}(l)$ by $\tilde{\boldsymbol{h}}(l)$ and hence $\mathbf{H}(z)$ by $\tilde{\mathbf{H}}(z)$ where:

$$\tilde{\mathbf{H}}(z) = \sum_{l=0}^{L} \tilde{\boldsymbol{h}}(l)z^{-l}$$

The condition to be satisfied for full rank requirement remains the same as given above. The diagonalization of auto-covariance matrix yields Eigen-values and corresponding Eigen-vectors $\boldsymbol{U}$ which can be partitioned into two subspaces viz. signal subspace $\boldsymbol{U}_s$ and noise subspace $\boldsymbol{U}_n$ as:

$$\boldsymbol{U} = [\boldsymbol{U}_s|\boldsymbol{U}_n] = [\boldsymbol{u}_1 \quad \cdots \quad \boldsymbol{u}_{JNM_t}|\boldsymbol{u}_{JNM_t+1} \quad \cdots \quad \boldsymbol{u}_{(JQ-L)M_r}] \tag{2.42}$$

Since span(**A**) and span($\boldsymbol{U}_s$) share the same JNM_t dimensional space and are orthogonal to span($\boldsymbol{U}_n$), the following orthogonality relationship holds and can be used in channel estimation:

$$\boldsymbol{u}_k^H \mathbf{A} = 0, \qquad \forall \ k \in \{n\}_{n=JNM_t+1}^{(JQ-L)M_r} \tag{2.43}$$

Define, $(L+1)M_r \times 1$ channel response vector associated with the channel impulse responses between the i^{th} transmit antenna and M_r receive antennas as,

$$\boldsymbol{h}_i = [\mathbf{h}(0)[:,i]^T \quad \cdots \quad \mathbf{h}(L)[:,i]^T]^T \quad for \quad 1 \le i \le M_t$$

Define the channel coefficient matrix $\mathbf{H}_c$ as:

$$\mathbf{H}_c = [\boldsymbol{h}_1, \ldots, \boldsymbol{h}_{Mt}] = [\boldsymbol{h}(0)^T, \ldots, \boldsymbol{h}(L)^T]^T$$

Under the appropriate conditions given by *Theorem 2* [54], the noise subspace can determine the channel coefficient matrix $\mathbf{H}_c$ up to an $M_t \times M_t$ multiplicative matrix ambiguity. The following notations are used in the theorem. Let $\mathbf{H}_c'$ be a matrix that has same dimension as that of $\mathbf{H}_c$. Let $\mathbf{H}'$ be a non-zero matrix constructed from $\mathbf{H}_c'$ in the same manner as the matrix $\mathbf{H}$ is constructed from $\mathbf{H}_c$. Denote $\mathbf{H}'\mathbf{W}$ as $\mathbf{A}'$ and let $\mathbf{H}'(z) = \sum_{l=0}^{L} \boldsymbol{h}'(l)z^{-l}$. *Theorem 2* can be stated as follows [54]:

Theorem 2: Assume that the matrix **A** in *eqn. 2.39* has a full column rank with $J \ge 2$, $M_r \ge M_t$ and $(Q\text{-}N) \ge L$. Then, $\mathbf{H}_c'$ is equal to $\mathbf{H}_c\boldsymbol{\Omega}$ with an $M_t \times M_t$ invertible matrix $\boldsymbol{\Omega}$, if and only if $span(\mathbf{A}')$ is equal to $span(\mathbf{A})$.

Since, the output auto-covariance matrix is estimated using time-averaging; the orthogonality condition of *eqn. 2.43* is solved in least-squares sense to obtain the channel coefficient estimates. The quadratic cost function defined by *eqn. 2.44* is minimized under the criterion that $||\boldsymbol{h}_i|| = 1$ for $1 \le i \le M_t$ to estimate the channel up to a complex matrix ambiguity (follows from *Theorem 2*) [54]:

$$\boldsymbol{C}(\mathbf{H}) = \sum_{k=JNM_t+1}^{(JQ-L)M_r} \|\hat{\boldsymbol{u}}_k^H \mathbf{A}\|_2^2 \tag{2.44}$$

The estimate of **H** can be obtained by solving the dual form of *eqn. 2.44* under the condition $||\boldsymbol{h}_i||_2 = 1$ given by:

$$\widehat{\mathbf{H}} = [\widehat{\boldsymbol{h}}_1 \quad \cdots \quad \widehat{\boldsymbol{h}}_{M_t}] = \underset{\|\boldsymbol{h}_i\|_2=1}{\arg\min} \left(\sum_{i=1}^{M_t} \boldsymbol{h}_i^H \boldsymbol{\Psi} \boldsymbol{h}_i \right)$$

... (2.45)

where,

$$\boldsymbol{\Psi} = \sum_{k=JNM_t+1}^{(JQ-L)M_r} \widehat{\boldsymbol{V}}_k (\boldsymbol{I}_J \otimes \mathbf{W}^* \mathbf{W}^T) \widehat{\boldsymbol{V}}_k^H$$

... (2.46)

and the estimate of V_k 's are constructed by partitioning the estimate of k^{th} noise subspace basis vector $\boldsymbol{u}_k$ as given below:

$$\widehat{\boldsymbol{V}}_k = \begin{bmatrix} \widehat{\boldsymbol{v}}_1^{(k)} & \cdots & \widehat{\boldsymbol{v}}_{JQ-L}^{(k)} & 0 & \cdots & 0 \\ 0 & \widehat{\boldsymbol{v}}_1^{(k)} & \cdots & \widehat{\boldsymbol{v}}_{JQ-L}^{(k)} & \cdots & 0 \\ \vdots & \vdots & \vdots & \vdots & \vdots & \vdots \\ 0 & \cdots & 0 & \widehat{\boldsymbol{v}}_1^{(k)} & \cdots & \widehat{\boldsymbol{v}}_{JQ-L}^{(k)} \end{bmatrix}_{(L+1)M_r \times JQ} \quad where \quad \widehat{\boldsymbol{u}}_k = \begin{bmatrix} \widehat{\boldsymbol{v}}_1^{(k)} \\ \vdots \\ \widehat{\boldsymbol{v}}_{JQ-L}^{(k)} \end{bmatrix}$$

... (2.47)

Note: Analogous to SISO-OFDM case, the persistence of excitation assumption (p.o.e) for MIMO-OFDM states that the minimum required number of OFDM blocks for channel estimation using subspace decomposition to be feasible is equal to JNM_t.

Note that the above treatment is valid for SISO-OFDM system, where $M_t = 1$. Further, for SISO-OFDM case, p. o. e. assumption can be stated as the minimum number of OFDM blocks required is equal to JN and when $J = 2$, (i.e., 2 consecutive OFDM blocks are taken at a time) it is equal to $2N$ which is same as mentioned before for SISO-OFDM case in the previous sub-section.

Chapter 3

PRECODING-INDUCED CORRELATION AVERAGING APPROACH

As mentioned earlier, the blind channel estimation employing subspace method uses receiver diversity, introduced by oversampling the channel output for channel estimation in single-carrier system. Subspace techniques for SISO-OFDM and MIMO-OFDM systems utilize the redundancy introduced due to CP (and oversampling for MIMO case) as described in *Chapter 2*. These techniques are capable of estimating the channel up to a constant complex scalar ambiguity for SISO-OFDM channels and up to a constant complex matrix ambiguity for MIMO-OFDM channels. By using precoding, the amplitude ambiguity in the SISO-OFDM channel estimate can be resolved and the matrix ambiguity can be reduced to complex scalar ambiguity per transmitter in MIMO-OFDM. An introduction to precoding and its applications in the context of blind channel estimation problem is described in this chapter followed by a joint estimation algorithm via precoding-induced correlation-averaging method for both SISO-OFDM [51] and MIMO-OFDM [57] systems.

3.1. PRECODING

Precoding is a transmitter end technique used to introduce certain redundancy or correlation (or both) among the subcarriers in an OFDM frame. This information can be utilized at the receiver end for the purpose of blind channel estimation. Further, precoding can be used to add resilience to impulsive noise and multiplexing (e.g. STF coding). The precoding techniques can be classified as shown in *fig. 3.1* depending upon whether the transmitter has the knowledge of the CSI or not. As far as blind channel estimation problem is concerned, the channel knowledge at the transmitter is assumed to be unknown; in which case the arbitrary precoding techniques are used. One type of precoding: CP (cyclic prefix), which was mentioned in previous chapters can be classified as redundant precoding technique, in which partial knowledge of the channel (FIR channel impulse response length in this case) is used to decide the minimum CP length. Apart from this, the details of the precoding techniques in which CSI knowledge is necessary are not considered in this work.

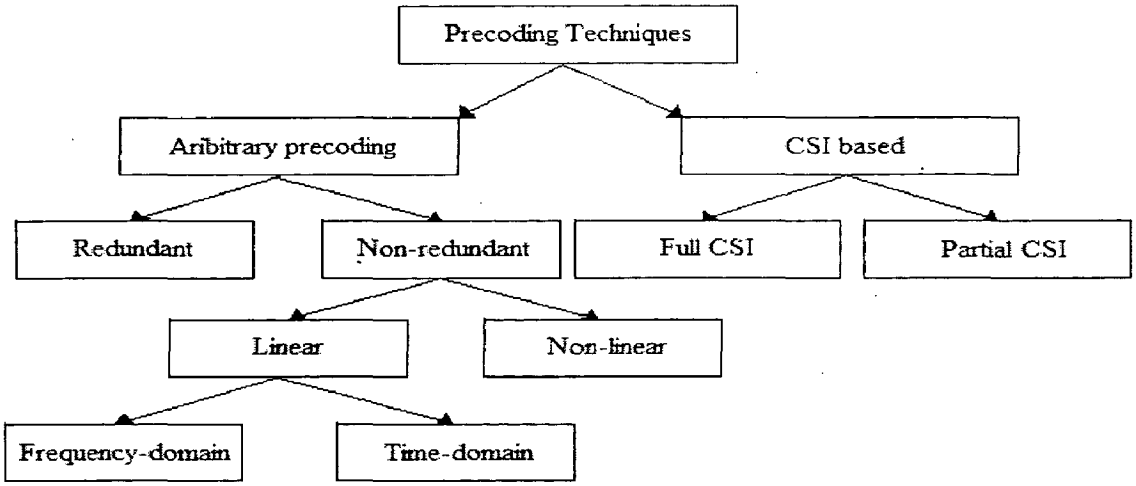

Figure 3.1: Classification tree for Precoding techniques

The precoder can either be linear or non-linear. The non-linear type precoders are generally optimum precoders; in terms of performance but are highly complex and hence rarely used. The redundant type of precoding is analogous to error-correction coding (or modulated coding: ECC over complex field) which has been used to mitigate ill-effects of AWGN (block codes) and ISI (convolutional decoders) [59]. A redundancy is introduced by appending or prefixing a part of either time-domain (e.g. CP) or frequency-domain information frame to be transmitted. Owing to the redundancy introduced at the transmitter, the blind equalization is feasible at the receiver even when there is no receiver diversity (e.g. oversampling the channel output).

Redundancy introduced does not change the time or frequency characteristics of the transmitted signal frame. The spectrum is simply spread making the algorithm insensitive to spectral nulls. The redundant precoders results in waste of bandwidth, but if the number of subcarriers of OFDM frame are chosen sufficiently large compared to the channel length, the wastage can be considered insignificant for all practical purposes. The non-redundant or block precoders are still preferred over redundant precoders. Further, as mentioned earlier, precoding can either be in time-domain (after IFFT block) or in frequency-domain (before IFFT block) in an OFDM transmitter. Some systems use both redundant and non-redundant precoding (e.g. CP-OFDM with linear block precoding [51]).

3.2. BLIND CHANNEL ESTIMATION FOR SISO-OFDM SYSTEMS

3.2.1. FREQUENCY-DOMAIN EQUIVALENT SISO-OFDM CHANNEL MODEL

In continuation with the SISO-OFDM channel model described in *fig. 2.6*, a frequency-domain equivalent model which is the basis for the blind approach given in [51] is described. In contrast to the channel model of *Chapter 2*, in which the precoding matrix $\boldsymbol{W}$ was assumed to be an identity matrix; for the present discussion, the precoding matrix $\boldsymbol{W}$ is assumed to be a linear frequency-domain non-redundant matrix of dimension $N \times N$. The equivalent parallel-carrier channel model [41] with the precoder is shown in *fig. 3.2*.

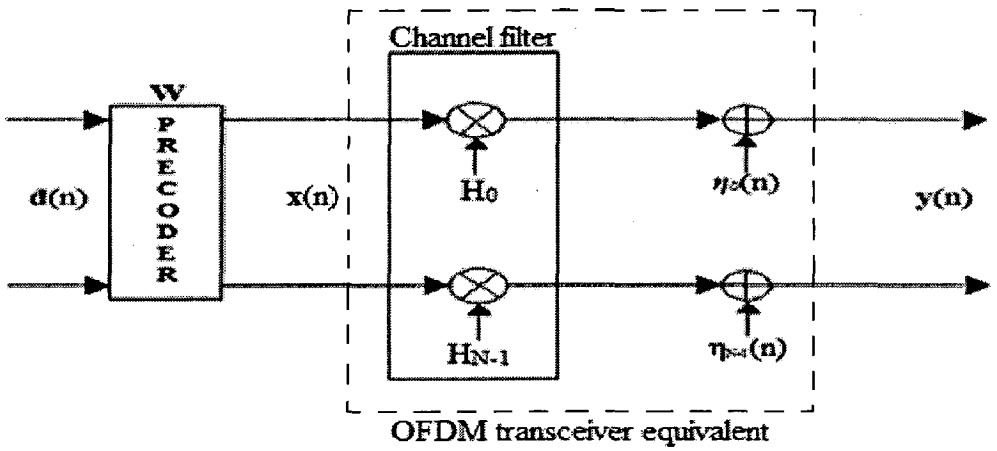

Figure 3.2: Frequency-domain parallel-carrier equivalent OFDM transceiver model

As mentioned in the previous chapter, for SISO-OFDM systems, we consider a discrete baseband equivalent FIR channel impulse response with a known length L represented by a $L \times 1$ vector as: $\boldsymbol{h} = [h_0, \ldots, h_L]^T$. Define the normalized $N \times N$ DFT matrix defined as:

$$\boldsymbol{F} = \frac{1}{\sqrt{N}} \begin{bmatrix} 1 & 1 & \cdots & 1 \\ 1 & f_N^1 & \cdots & f_N^{N-1} \\ \vdots & \vdots & \ddots & \vdots \\ 1 & f_N^{N-1} & \cdots & f_N^{(N-1)(N-1)} \end{bmatrix} \tag{3.1}$$

where, $f_N = \exp\left(-\frac{j2\pi}{N}\right)$ is the Wronskian or Kernel of DFT. The frequency response vector $\boldsymbol{H}$ can be obtained by taking N-point DFT of $\boldsymbol{h}$ as:

$$\boldsymbol{H} = [H_0 \quad \cdots \quad H_{N-1}] = DFT(\boldsymbol{h}) = \sqrt{N}F(:, 1: L+1)\boldsymbol{h} \tag{3.2}$$

Assuming that the n^{th} frequency-domain transmitted OFDM frame and received OFDM frame is given as (*fig. 2.6* and *fig. 3.2*): $\boldsymbol{x(n)} = [x(n, 0), x(n, 1), \ldots, x(n, N-1)]^T$ and $\boldsymbol{y(n)} =$

$[y(n, 0), y(n, 1), \ldots, y(n, N-1)]^T$ respectively, the frequency-domain received OFDM vector can be expressed as [51]:

$$\boldsymbol{y}(n) = \tilde{\mathbf{H}}\boldsymbol{x}(n) + \tilde{\boldsymbol{n}}(n) \tag{3.3}$$

where, $\tilde{\boldsymbol{n}}(n)$ is the post-DFT $N \times 1$ noise vector and $\tilde{\mathbf{H}}$ is a diagonal $N \times N$ channel matrix given by:

$$\tilde{\mathbf{H}} = diag\{\boldsymbol{H}\} = \begin{bmatrix} H_0 & 0 & \cdots & 0 \\ 0 & H_1 & \cdots & 0 \\ \vdots & \vdots & \ddots & \vdots \\ 0 & 0 & \cdots & H_{N-1} \end{bmatrix} \tag{3.4}$$

The precoder block multiples the incoming OFDM block with a precoding matrix $\boldsymbol{W}$ as:

$$\boldsymbol{x}(n) = \boldsymbol{W}\boldsymbol{d}(n) \tag{3.5}$$

Thus,

$$\boldsymbol{y}(n) = \tilde{\mathbf{H}}\boldsymbol{W}\boldsymbol{d}(n) + \tilde{\boldsymbol{n}}(n) \tag{3.6}$$

3.2.2. CORRELATION-AVERAGING ALGORITHMS FOR BLIND ESTIMATION

Two precoding techniques for correlation-averaging based channel estimation are considered in the following. The first method uses a simple (partial) precoder, which induces correlation on a single subcarrier [46] and forms a basis for rest of the precoding-induced correlation-averaging techniques that followed. The second approach (a generalization of first technique) uses a joint precoder, which induces correlation in entire OFDM block [51].

A. Blind channel estimation using simple precoding

Consider, a precoded OFDM system model defined by *eqn. 3.6*. The linear precoder transforms the n^{th} source block of N subcarriers denoted by: $\boldsymbol{d}(n) = [d(n, 0), d(n, 1), \ldots, d(n, N-1)]^T$ according to [46]:

$$x(n,k) = \frac{1}{\sqrt{1+|A|^2}}(d(n,k) + (-1)^k A d(i,R)), \qquad k = 0, \ldots, N-1 \tag{3.7}$$

where, the predefined precoding constants A and R are assumed to be known to the receiver. R is an integer in the range $[0, N-1]$ and A is a purely imaginary number with $|A| < 1$ [46]. The features of this precoding technique are [46]:

1) Introduces no redundancy to the transmitted data, which makes it bandwidth efficient.
2) Since the normalization factor is driven by A: an imaginary number, the approach preserves transmitted power on each subcarrier.
3) Maintains zero-mean of the signal transmitted on each subcarrier.
4) Maintains zero DC offset in each OFDM block.
5) Introduces a correlation structure in the transmitted signal that can be utilized at the receiver for channel estimation.

Referring to the OFDM transceiver model of *fig. 3.2* and *eqn. 3.6*; the n^{th} frequency-domain received OFDM symbol can be written as:

$$y(n,k) = H_k x(n,k) + \tilde{n}(n,k) = \left[\frac{1}{\sqrt{1+|A|^2}} H_k (d(n,k) + (-1)^k A d(i,R))\right] + \tilde{n}(n,k) \quad \ldots (3.8)$$

where, H_k is the frequency-domain channel coefficient on k^{th} subcarrier as defined by *eqn. 3.2*. It is assumed that the source covariance matrix is diagonal: $\sigma_d^2 \boldsymbol{I}_N$ and the channel length $L \leq N$. Consider the correlation of the signals on k^{th} and R^{th} subcarriers given by [46]:

$$Z(k,R) = E\{y(n,k)y^*(n,R)\} = \begin{cases} \dfrac{(-1)^k A + (-1)^{k+R}|A|^2}{1+|A|^2} \sigma_d^2 H_R^* H_k, & k = 0,\ldots,N-1; k \neq R \\ \sigma_d^2 H_R^* H_R + \sigma_{\tilde{n}}^2, & k = R \end{cases} \quad \ldots (3.9)$$

Observe that in practice, the expectation in *eqn. 3.9* can be realized by time-averaging over successive OFDM frames. Assuming that the source statistics is known at the receiver, the estimate of frequency-domain channel coefficient on k^{th} subcarrier H_k can be obtained by:

$$\hat{H}_k = \begin{cases} \dfrac{1+|A|^2}{(-1)^k A + (-1)^{k+R}|A|^2} \dfrac{\hat{Z}(k,R)}{\sigma_d^2}, & k = 0,\ldots,N-1; k \neq R \\ \dfrac{\hat{Z}(k,R)}{\sigma_d^2}, & k = R \end{cases} \quad \ldots (3.10)$$

The channel estimate can be further improved by performing IDFT on $\hat{\mathbf{H}}$; setting to zero the last N-L samples of IDFT output, then performing N-point DFT on the result. This procedure is known as de-noising [46]. Thus, by above procedure, the channel estimate is obtained in frequency-domain up to a constant complex scalar quantity. Assuming that the noise variance is small, observe on the R^{th} subcarrier, the estimate obtained is $\hat{H}_R \approx H_R^* H_R =$

$|H_R|^2$. Thus an estimate of magnitude of R^{th} subcarrier coefficient can be obtained. Dividing the whole estimate by this estimate, the ambiguity factor can be reduced to constant phase ambiguity. A potential problem with the estimate might arise when the R^{th} subcarrier is in deep fade, in which case $\hat{Z}(k, R)$ is close to zero for all k's. This problem can be solved by introducing correlation on more than one subcarrier, as described in [51].

B. Blind channel estimation using generalized precoding

This method uses a generalization of precoding technique that was employed in previously described technique and leads to better estimation accuracy. The channel output signal, $y(n)$'s auto-covariance matrix denoted as $\boldsymbol{R}_{yy}$ estimated via time-averaging is used for channel estimation purpose in frequency-domain [51]. Using *eqn. 3.6*, the auto-covariance matrix of $y(n)$ can be written as:

$$\boldsymbol{R}_{yy} = E\{\boldsymbol{y}(n)\boldsymbol{y}(n)^H\} = \tilde{\mathbf{H}}\boldsymbol{W}\boldsymbol{R}_d\boldsymbol{W}^H\tilde{\mathbf{H}}^H + \boldsymbol{R}_n \tag{3.11}$$

Assuming that the source symbols are iid, with variance σ_d^2 and noise samples are also iid and are distributed according to $\sim N(0, \sigma_n^2)$; we have-

$$\boldsymbol{R}_{yy} = E\{\boldsymbol{y}(n)\boldsymbol{y}(n)^H\} = \sigma_d^2\tilde{\mathbf{H}}\boldsymbol{P}\tilde{\mathbf{H}}^H + \sigma_n^2\boldsymbol{I}_N = \sigma_d^2(\boldsymbol{H}\boldsymbol{H}^H)\odot\boldsymbol{P} + \sigma_n^2\boldsymbol{I}_N \tag{3.12}$$

where, $\boldsymbol{P} = \boldsymbol{W}\boldsymbol{W}^H$. The elements of $\boldsymbol{P}$ and hence $\boldsymbol{W}$ are designed according to following criterion [51]:

1) Distortion criterion: In practice, the number of snapshots received within the channel coherence time is not infinite. Therefore, we can at best obtain a sample estimate of signal auto-covariance matrix. Each entry of $\boldsymbol{R}_{yy}$ contains the distortion due to the effect of both the noise and the lack of the number of snapshots. If one entry of $\boldsymbol{P}$ is much smaller than the other entries, the distortion in the corresponding entry of $\boldsymbol{R}_{yy}$ will be greatly enlarged after the elimination of the effect of $\boldsymbol{P}$. Hence, the entry of $\boldsymbol{R}_{yy}$ with possibly large distortion should be discarded, or the corresponding entry of $\boldsymbol{P}$ should be assigned a relatively large value. However, no prior information of the distortion can be obtained due to all unknown factors. A reasonable way is to assign equal value to all the non-diagonal entries and at the same time as large as possible.
2) Power constraint: The precoding matrix elements must be chosen such that the transmitted signal power is kept constant i.e.,

$$Power = E\{\boldsymbol{d}(n)^H\boldsymbol{W}^H\boldsymbol{W}\boldsymbol{d}(n)\} = \sigma_d^2 trace(\boldsymbol{P}) = \sigma_d^2 N$$

Thus, *trace (P) = N.*

Combining 1) and 2), we get:

$$\boldsymbol{P}(m,q) = \begin{cases} 1 & , \quad m = q \\ p \neq 0, & m \neq q \end{cases} \qquad\qquad m,q = 1,\cdots,N$$

3) Symbol Error Constraint: Due to the quadrature form of *eqn. 3.12*, $\boldsymbol{P}$ should be a positive semi-definite matrix. It can be proved that one Eigen-value of $\boldsymbol{P}$ is $(N-1)\,p + 1$, and all the other Eigen-values are $1 - p$. Hence, for channel estimation, the range of p is $-(1/N-1) < p < 1$ and $p \neq 0$.

The $\boldsymbol{P}$ matrix is designed according to these criterions. The precoding matrix $\boldsymbol{W}$ can be obtained by taking square-root of $\boldsymbol{P}$. It is reasonable to assume that the knowledge of precoding matrix $\boldsymbol{W}$ is known at the receiver end. Obtain the matrix $\boldsymbol{R}$ as:

$$\boldsymbol{R} = (\boldsymbol{R}_{yy})./\boldsymbol{P} = \begin{bmatrix} \sigma_d^2|H_0|^2 + \sigma_n^2 & \sigma_d^2 H_0 H_1^* & \cdots & \sigma_d^2 H_0 H_{N-1}^* \\ \sigma_d^2 H_1 H_0^* & \sigma_d^2|H_1|^2 + \sigma_n^2 & \cdots & \sigma_d^2 H_1 H_{N-1}^* \\ \vdots & \vdots & \ddots & \vdots \\ \sigma_d^2 H_{N-1} H_0^* & \sigma_d^2 H_{N-1} H_1^* & \cdots & \sigma_d^2|H_{N-1}|^2 + \sigma_n^2 \end{bmatrix} \tag{3.13}$$

Define,

$$\boldsymbol{r}_q = [\boldsymbol{R}(1{:}q-1,q)^T \quad \boldsymbol{R}(q+1{:}N,q)^T]^T, \qquad q = 1,\cdots,N$$

$$\boldsymbol{F}_q = [\boldsymbol{F}(1{:}q-1,1{:}L+1)^T \quad \boldsymbol{F}(q+1{:}N,1{:}L+1)^T]^T, \qquad q = 1,\cdots,N \tag{3.14}$$

Set,

$$\boldsymbol{H}_{eq} = \boldsymbol{F}(:,1{:}L+1)\boldsymbol{F}_q^{\dagger}\boldsymbol{r}_q = \sigma_d^2 H_{q-1}^* \boldsymbol{H} \tag{3.15}$$

Assuming the knowledge of source statistics at the receiver, the steps for frequency-response estimation of the channel from *eqn. 3.13* are given as follows [51]:

Step 1: Obtain the estimate of $\sigma_d^2|H_0|^2$ and hence $|H_0|$ as the first element of $\boldsymbol{H}_{eq}$ from *eqn. 3.15* with the value of q set to *1*. Assuming an arbitrary phase φ, set the estimate of H_0 as $\widehat{H}_0 = |H_0|e^{j\varphi}$.

Step 2: From $\boldsymbol{R}(2,1)$, obtain an estimate for H_1 as: $\widehat{H}_1 = \boldsymbol{R}(2,1)/\widehat{H}_0^{\,*}$.

Step 3: From ***R(3,1:2)*** solve the over-determined function using $\hat{H}_0$ and $\hat{H}_1$ to get an estimate of H_2 as $\hat{H}_2 = \begin{bmatrix} \hat{H}_0^* \\ \hat{H}_1^* \end{bmatrix}^{\dagger} \boldsymbol{R}(3,1:2)^T$.

Step 4: Calculate all the estimates of H_{q-1} from ***R(q,1:q-1)*** until all the elements of $\boldsymbol{H}$ are estimated.

Step 5: De-noising the whole estimate vector $\hat{\boldsymbol{H}} = [\hat{H}_0 \quad \cdots \quad \hat{H}_{N-1}]$, obtain the final estimate of the channel vector in frequency-domain as $\hat{\boldsymbol{H}} = \boldsymbol{F}(:,1:L+1)\boldsymbol{F}(:,1:L+1)^H\hat{\boldsymbol{H}}$.

This algorithm estimates the channel in frequency-domain as against subspace approach of *Chapter 2* that estimated the channel in time-domain. The time-domain impulse response estimate of the channel up to a constant phase ambiguity factor (unlike subspace method which estimates channel up to constant scalar ambiguity) can be obtained by taking inverse Fourier transform of the frequency-domain estimate.

3.2.3. CRAMER-RAO BOUND FOR BLIND PRECODING-BASED ESTIMATOR

The Cramér–Rao bound (CRB) states that the variance of any unbiased estimator is at least as high as the inverse of the Fisher information matrix. An unbiased estimator which achieves this lower bound is said to be efficient. This sub-section discusses the derivation of CRB for blind precoder-induced-correlation-averaging technique-based channel estimator. There are two different types of system models:

1. Conditional model (CM) - Assumes that the input signal is non-random (i.e., same in all realizations)
2. Unconditional model (UM) - Assumes that the input signal is random.

The CRBs can accordingly be classified as Conditional/ deterministic CRB and unconditional/ stochastic CRB. For the problem underhand, it is assumed that the input signal is random whose covariance matrix is multiple of identity matrix and hence, derivation of stochastic CRB is discussed. The covariance matrix of frequency-domain received blocks i.e., *y(n)* cannot be used since only *L+1* elements of frequency-domain channel vector $\boldsymbol{H}$ are linearly independent. Instead, the signal covariance matrix of time-domain received vector *r(n)* (refer *fig. 2.6*) is considered. From *eqn. 2.24a* after discarding CP (i.e., deleting first L rows from $\mathbf{H}_0$ and $\mathbf{H}_1$ and flipping and adding first L columns to last L columns of $\mathbf{H}_0$ and $\mathbf{H}_1$), the IBI term is rejected; we get [51]:

$$\boldsymbol{r}(n) = \bar{\mathbf{H}}\boldsymbol{F}^H\boldsymbol{x}(n) + \bar{\boldsymbol{\eta}}(n) = \bar{\mathbf{H}}\boldsymbol{F}^H\boldsymbol{W}\boldsymbol{d}(n) + \bar{\boldsymbol{\eta}}(n) \tag{3.16}$$

where, $\bar{\boldsymbol{\eta}}(n)$ is the $N \times 1$ noise vector before the DFT block at the receiver after the CP part (first L samples) are discarded from $\boldsymbol{\eta}(n)$ in *eqn. 2.24a* and $\bar{\mathbf{H}}$ is the $N \times N$ circulant channel matrix defined by:

$$\bar{\mathbf{H}} = \begin{bmatrix} h_0 & 0 & \cdots & h_1 \\ h_1 & h_0 & \cdots & h_2 \\ \vdots & \vdots & \ddots & \vdots \\ h_L & h_{L-1} & \cdots & 0 \\ 0 & h_L & \cdots & 0 \\ \vdots & \vdots & \ddots & \vdots \\ 0 & 0 & \cdots & h_0 \end{bmatrix}_{N\times N} \tag{3.17}$$

The signal covariance matrix is thus given by,

$$\boldsymbol{R}_{rr} = E\{\boldsymbol{r}(n)\boldsymbol{r}(n)^H\} = \sigma_d^2\bar{\mathbf{H}}\boldsymbol{F}^H\boldsymbol{P}\boldsymbol{F}\bar{\mathbf{H}}^H + \sigma_n^2\boldsymbol{I}_N \tag{3.18}$$

The noise statistics is not altered by DFT operations [51]. In general, for a circular complex zero-mean Gaussian random variable: $\mathbf{r} = \boldsymbol{r}_R + j\mathbf{r}_I$ with signal covariance matrix defined as $\boldsymbol{R}_{rr} = E\{\mathbf{r}\mathbf{r}^H\}$ parameterized by a real vector $\boldsymbol{\theta} = [\theta_1 \quad \cdots \quad \theta_K]^T$, the Fisher information matrix (FIM) is given by [60, 51]:

$$\boldsymbol{FIM}(m,q) = M\,trace\left(\frac{d\boldsymbol{R}_{rr}}{d\theta_m}\boldsymbol{R}_{rr}^{-1}\frac{d\boldsymbol{R}_{rr}}{d\theta_q}\boldsymbol{R}_{rr}^{-1}\right) \quad for\ m,q = 1,\cdots,K \tag{3.19}$$

where, M is the number of available snapshots for sample-covariance matrix estimation. The CRB is obtained by taking inverse of FIM (see *eqn. 3.24*). For this case, the signal covariance matrix is assumed to be parameterized by the $(2L + 4) \times 1$ vector: $\boldsymbol{\theta} = [\boldsymbol{h}_R^T \quad \boldsymbol{h}_I^T \quad \sigma_d^2 \quad \sigma_n^2]^T$.

The following mathematical properties are used in derivation of CRB [51]:

$$trace(\boldsymbol{XY}) = vec(\boldsymbol{X}^H)^H vec(\boldsymbol{Y})$$

$$vec(\boldsymbol{XYZ}) = (\boldsymbol{Z}^T \otimes \boldsymbol{X})vec(\boldsymbol{Y})$$

$$(\boldsymbol{X} \otimes \boldsymbol{Y})(\boldsymbol{Z} \otimes \boldsymbol{W}) = (\boldsymbol{XZ}) \otimes (\boldsymbol{YW})$$

which holds for any matrices $\boldsymbol{X}$, $\boldsymbol{Y}$, $\boldsymbol{Z}$ and $\boldsymbol{W}$. Using these properties we can write *eqn. 3.19* as:

$$\frac{1}{M}\boldsymbol{FIM}(m,q) = vec\left(\frac{d\boldsymbol{R}_{rr}}{d\theta_m}\right)^H vec\left(\boldsymbol{R}_{rr}^{-1}\frac{d\boldsymbol{R}_{rr}}{d\theta_q}\boldsymbol{R}_{rr}^{-1}\right)$$
$$= vec\left(\frac{d\boldsymbol{R}_{rr}}{d\theta_m}\right)^H (\boldsymbol{R}_{rr}^{-T}\otimes\boldsymbol{R}_{rr}^{-1})vec\left(\frac{d\boldsymbol{R}_{rr}}{d\theta_q}\right)$$

... (3.20)

Define:

$$\boldsymbol{r}_{rr} = vec(\boldsymbol{R}_{rr}) = \sigma_d^2(\bar{\mathbf{H}}^*\otimes\bar{\mathbf{H}})vec(\boldsymbol{F}^H\boldsymbol{P}\boldsymbol{F}) + \sigma_n^2 vec(\boldsymbol{I}_N) \quad (3.21)$$

Thus,

$$\frac{1}{M}\boldsymbol{FIM} = \left(\frac{d\boldsymbol{r}_{rr}}{d\boldsymbol{\theta}^T}\right)^H (\boldsymbol{R}_{rr}^{-T}\otimes\boldsymbol{R}_{rr}^{-1})\left(\frac{d\boldsymbol{r}_{rr}}{d\boldsymbol{\theta}^T}\right)$$

... (3.22)

The *eqn. 3.22* can be partitioned as [51]:

$$\frac{1}{M}\boldsymbol{FIM} = \begin{bmatrix}\boldsymbol{G}^H\\ \boldsymbol{\Delta}^H\end{bmatrix}[\boldsymbol{G} \quad \boldsymbol{\Delta}]$$

... (3.23)

where,

$$[\boldsymbol{G} \mid \boldsymbol{\Delta}] = \left(\boldsymbol{R}_{rr}^{-\frac{T}{2}}\otimes\boldsymbol{R}_{rr}^{-\frac{1}{2}}\right)\left(\frac{d\boldsymbol{r}_{rr}}{d\boldsymbol{\theta}^T}\right) = (\boldsymbol{R}_{rr}^{-T/2}\otimes\boldsymbol{R}_{rr}^{-1/2})\left(\frac{d\boldsymbol{r}_{rr}}{d\boldsymbol{h}_R^T}\frac{d\boldsymbol{r}_{rr}}{d\boldsymbol{h}_I^T}\middle|\frac{d\boldsymbol{r}_{rr}}{d\sigma_d^2}\frac{d\boldsymbol{r}_{rr}}{d\sigma_n^2}\right)$$

Since, FIM is a singular matrix [51]; certain constraints have to be put on FIM to obtain CRB as its inverse. Defining [51]:

$$\boldsymbol{CRB} = \boldsymbol{FIM}^{\dagger} \quad (3.24)$$

We have the following theorem using which CRB can be analytically calculated (see [51] and references therein):

Theorem: Suppose the FIM for $\boldsymbol{\theta} = [\boldsymbol{\theta}_1 \quad \boldsymbol{\theta}_2]^T$ is given by,

$$\boldsymbol{FIM} = \begin{bmatrix}\boldsymbol{J}_{\boldsymbol{\theta}_1\boldsymbol{\theta}_1} & \boldsymbol{J}_{\boldsymbol{\theta}_1\boldsymbol{\theta}_2}\\ \boldsymbol{J}_{\boldsymbol{\theta}_2\boldsymbol{\theta}_1} & \boldsymbol{J}_{\boldsymbol{\theta}_2\boldsymbol{\theta}_2}\end{bmatrix}$$

Assuming that FIM is singular but $\boldsymbol{J}_{\boldsymbol{\theta}_2\boldsymbol{\theta}_2}$ is non-singular; CRB can be obtained as,

$$\boldsymbol{CRB} = [\boldsymbol{J}_{\boldsymbol{\theta}_1\boldsymbol{\theta}_1} - \boldsymbol{J}_{\boldsymbol{\theta}_1\boldsymbol{\theta}_2}\boldsymbol{J}_{\boldsymbol{\theta}_2\boldsymbol{\theta}_2}^{-1}\boldsymbol{J}_{\boldsymbol{\theta}_2\boldsymbol{\theta}_1}]^{\dagger}$$

Define an $N \times N$ matrix $\mathbf{H}_l$ with (m, q)-th entry as:

$$\mathbf{H}_l(m,q) = \begin{cases} 1, & ((m-q) mod\ N) = l-1 \\ 0, & otherwise \end{cases} \qquad l = 1, \ldots, L+1$$

For this case, $\boldsymbol{\theta}_1 = [\boldsymbol{h}_R^T \quad \boldsymbol{h}_I^T]^T$ and $\boldsymbol{\theta}_2 = [\sigma_d^2 \quad \sigma_n^2]^T$; hence from *eqn. 3.23* the expression for CRB can be written as:

$$\boldsymbol{CRB} = \frac{1}{M}[\boldsymbol{G}^H\boldsymbol{G} - \boldsymbol{G}^H\boldsymbol{\Delta}(\boldsymbol{\Delta}^H\boldsymbol{\Delta})^{-1}\boldsymbol{\Delta}^H\boldsymbol{G}]^{\dagger} \tag{3.25}$$

The values of $\boldsymbol{G}$ and $\boldsymbol{\Delta}$ are calculated as follows [51]:

$$[\boldsymbol{G} \mid \boldsymbol{\Delta}] = [\boldsymbol{G}_1 \mid \boldsymbol{G}_2 \mid \mathbf{v} \mid \mathbf{u}] = (\boldsymbol{R}_{rr}^{-T/2} \otimes \boldsymbol{R}_{rr}^{-1/2})\left(\frac{d\boldsymbol{r}_{rr}}{d\boldsymbol{h}_R^T}\middle|\frac{d\boldsymbol{r}_{rr}}{d\boldsymbol{h}_I^T}\middle|\frac{d\boldsymbol{r}_{rr}}{d\sigma_d^2}\middle|\frac{d\boldsymbol{r}_{rr}}{d\sigma_n^2}\right)$$

where,

$$\boldsymbol{A}_l = \sigma_d^2 \boldsymbol{R}_{rr}^{-\frac{1}{2}} \mathbf{H}_l \boldsymbol{F}^H \boldsymbol{P} \boldsymbol{F} \mathbf{H}_l^H \boldsymbol{R}_{rr}^{-\frac{1}{2}}$$

$$\boldsymbol{G}_1(:,l) = \left(\boldsymbol{R}_{rr}^{-\frac{T}{2}} \otimes \boldsymbol{R}_{rr}^{-\frac{1}{2}}\right) vec\left(\frac{d\boldsymbol{R}_{rr}}{dh_{R,l}}\right) = vec\left(\boldsymbol{R}_{rr}^{-\frac{1}{2}} \frac{d\boldsymbol{R}_{rr}}{dh_{R,l}} \boldsymbol{R}_{rr}^{-\frac{1}{2}}\right) = vec(\boldsymbol{A}_l + \boldsymbol{A}_l^H)$$

$$\boldsymbol{G}_2(:,l) = \left(\boldsymbol{R}_{rr}^{-\frac{T}{2}} \otimes \boldsymbol{R}_{rr}^{-\frac{1}{2}}\right) vec\left(\frac{d\boldsymbol{R}_{rr}}{dh_{I,l}}\right) = vec\left(\boldsymbol{R}_{rr}^{-\frac{1}{2}} \frac{d\boldsymbol{R}_{rr}}{dh_{I,l}} \boldsymbol{R}_{rr}^{-\frac{1}{2}}\right) = vec(j\boldsymbol{A}_l - j\boldsymbol{A}_l^H)$$

$$\mathbf{v} = \left(\boldsymbol{R}_{rr}^{-\frac{T}{2}} \otimes \boldsymbol{R}_{rr}^{-\frac{1}{2}}\right) vec\left(\frac{d\boldsymbol{R}_{rr}}{d\sigma_d^2}\right) = vec\left(\boldsymbol{R}_{rr}^{-\frac{1}{2}} \frac{d\boldsymbol{R}_{rr}}{d\sigma_d^2} \boldsymbol{R}_{rr}^{-\frac{1}{2}}\right) = vec(\boldsymbol{R}_{rr}^{-\frac{1}{2}} \bar{\mathbf{H}} \boldsymbol{F}^H \boldsymbol{P} \boldsymbol{F} \bar{\mathbf{H}}^H \boldsymbol{R}_{rr}^{-\frac{1}{2}})$$

and

$$\mathbf{u} = \left(\boldsymbol{R}_{rr}^{-\frac{T}{2}} \otimes \boldsymbol{R}_{rr}^{-\frac{1}{2}}\right) vec\left(\frac{d\boldsymbol{R}_{rr}}{d\sigma_n^2}\right) = vec\left(\boldsymbol{R}_{rr}^{-\frac{1}{2}} \frac{d\boldsymbol{R}_{rr}}{d\sigma_n^2} \boldsymbol{R}_{rr}^{-\frac{1}{2}}\right) = vec(\boldsymbol{R}_{rr}^{-1})$$

3.2.4. PERFORMANCE ANALYSIS OF SIMPLE-PRECODING BASED METHOD

The performance analysis of blind channel estimation using simple-precoding induced correlation-averaging [46] supported by MATLAB simulations is presented.

A. Simulation Parameters

The simulation parameters are given as follows:

- Complex discrete baseband equivalent FIR channel is assumed to be of length (L) = 2.
- The channel power-delay-profile is assumed to be exponential [51]:

$$E\{|h_l|^2\} = e^{(-\frac{l}{10})}, \qquad l = 0, \ldots, L$$

- Number of sub-carriers/ OFDM frame (N) = *64*
- Number of OFDM frames collected for estimation purpose (M) = 250
- Precoding normalization constant (A) = *0.5j*
- Precoding symbol index (R) = *1*
- Pilot symbol index (P) = *1*
- Pilot symbol value = $\sqrt{10}$
- SNR (unless otherwise mentioned) = 30 dB.
- Baseband modulation/ mapping: 16-QAM
- The results are averaged over 100 Monte-Carlo simulation runs.

The flowchart depicting the procedure to obtain the channel estimates using simple-precoding based technique is shown in *fig. 3.3.* The timing and frequency synchronization are assumed. The estimation ambiguity is resolved by using pilot carriers.

B. Simulation results and conclusion

The plot of MSE versus varying length of output OFDM blocks used at 30 dB SNR is shown in *fig. 3.4.* It can be seen that the MSE performance improves exponentially as the length of OFDM blocks is increased. From *fig. 3.4*, it can be seen that the MSE of 10^{-3} is achieved when length of OFDM blocks is *500* and an improvement in the performance by a factor of *2* can be seen as length of blocks is doubled (at a block length of *1000*, MSE is 5×10^{-4}).

The plot of MSE versus varying SNR (dB) values assuming that the length of OFDM blocks used is equal to *250* is shown in *fig. 3.5.* In contrast to subspace approach for single-carrier system described in *Chapter 2* (see *fig. 2.5*), it can be seen that the MSE curve saturates when SNR is increased beyond 15 dB at approximately 2×10^{-3}. This is because, unlike Eigen-vector based approach (subspace technique), the correlation-averaging technique is more sensitive to distortion due to non-availability of infinite number of OFDM blocks for time-averaging than AWGN. The advantage over subspace approach is that even at SNR of 0 dB, MSE is of the order of 10^{-1} which is *10* times better than that for subspace-based method.

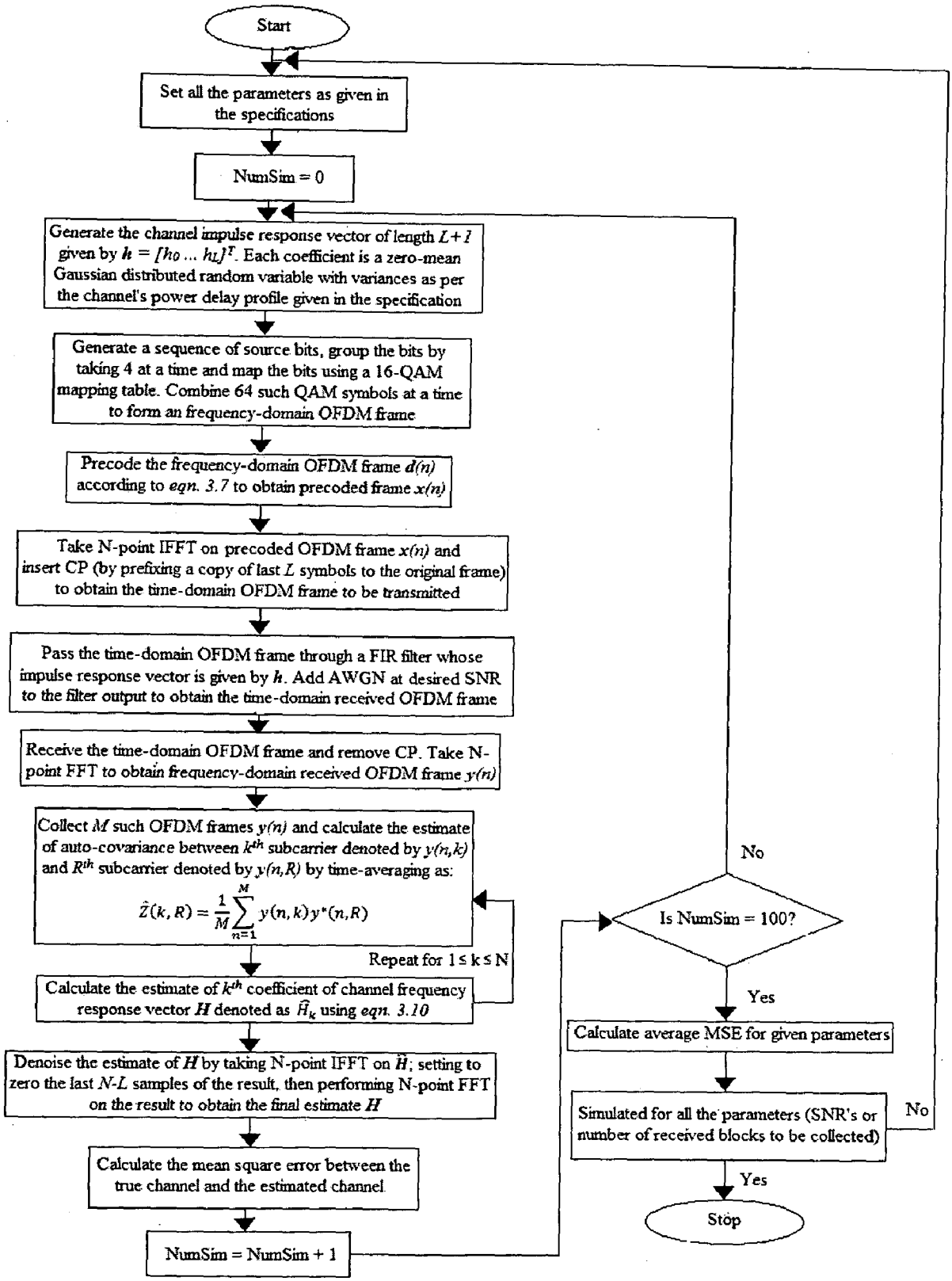

Figure 3.3: Blind channel estimation using subspace decomposition technique (flowchart for generation of plots given in fig. 3.4 and fig. 3.5)

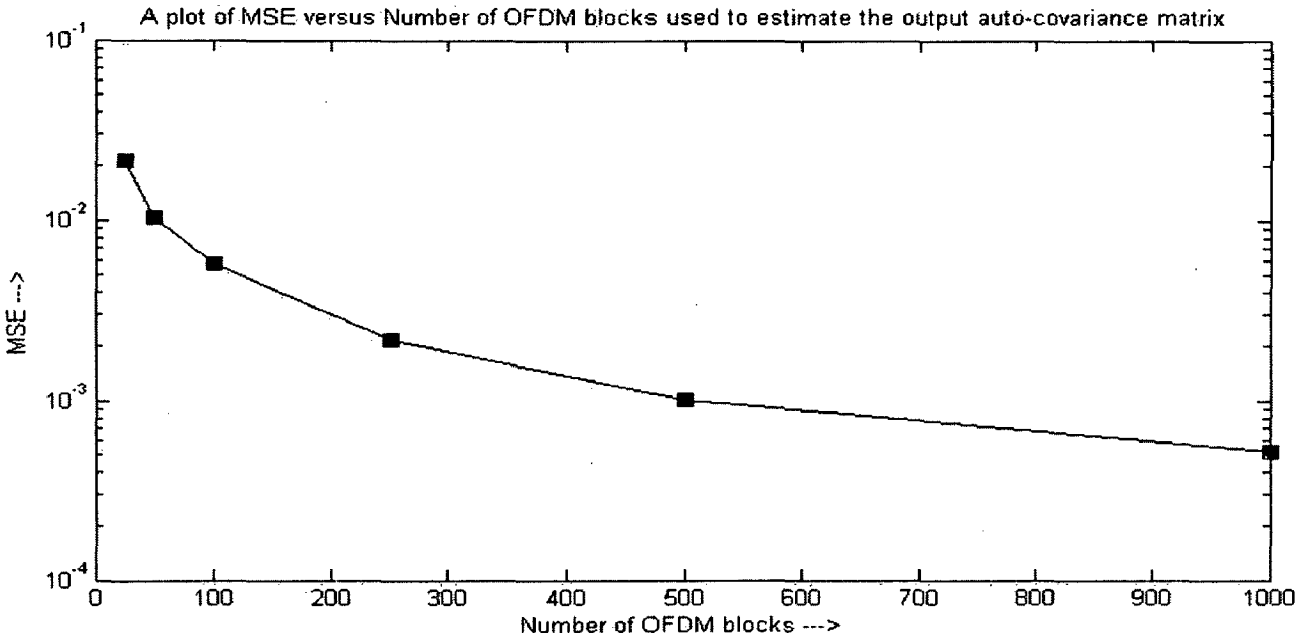

Figure 3.4: The plot of MSE versus length of OFDM blocks used at SNR = 30 dB.

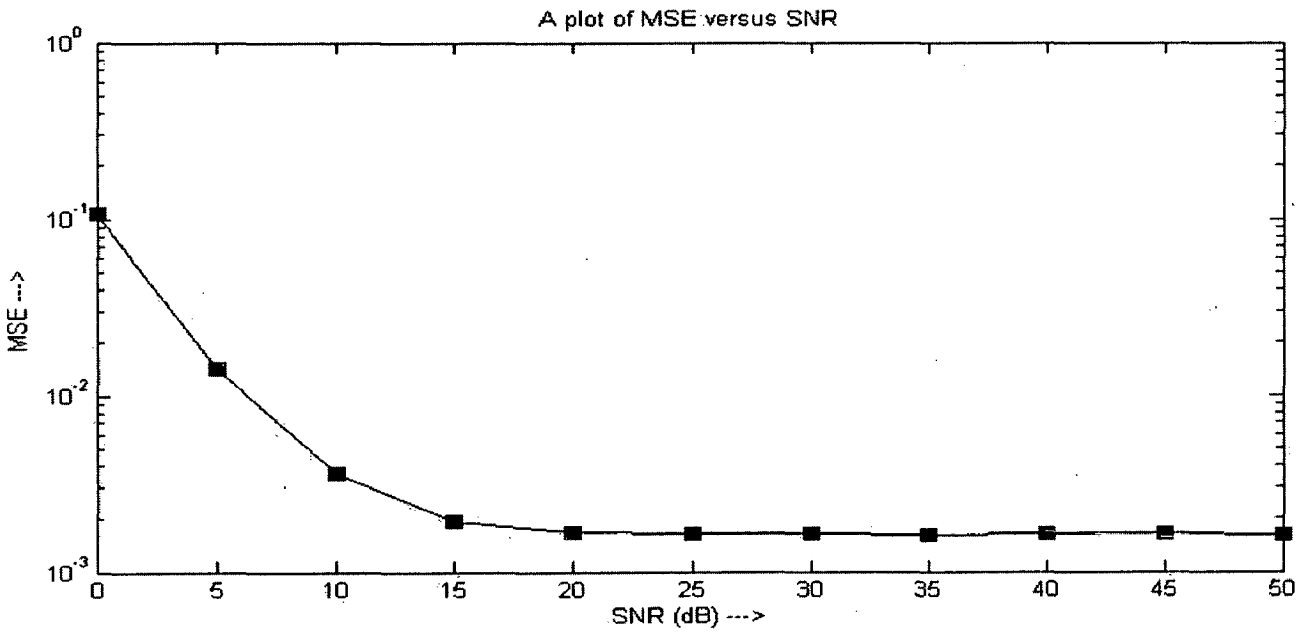

Figure 3.5: The plot of MSE versus SNR (dB) with length of OFDM blocks equal to 250

3.3. BLIND CHANNEL ESTIMATION FOR MIMO-OFDM SYSTEMS

This section presents a generalization of precoding-induced-correlation-averaging method to blind channel estimation for MIMO-OFDM systems [57]. As mentioned earlier, unlike the time-domain subspace approach of *Chapter 2* for MIMO-OFDM, this approach with a proper design of precoding block can estimate the channel in frequency-domain up to a constant scalar ambiguity factor per transmit antenna. For this purpose, in contrast to the precoding matrix for SISO-OFDM case which was time-invariant; the precoder is block-time-variant.

3.3.1. FREQUENCY-DOMAIN EQUIVALENT MIMO-OFDM CHANNEL MODEL

The block diagram of MIMO-OFDM communication link as shown in *fig. 2.7* is considered as reference for discussion. The frequency-domain model for MIMO-OFDM system [57]: an extension of the frequency-domain model for SISO-OFDM is presented in this sub-section. Consider a MIMO-OFDM transceiver with M_t transmit antenna and M_r receiving antenna. Define the impulse response vector of the channel between j^{th} transmitter antenna and i^{th} receiving antenna as $\boldsymbol{h}_{ji} = [h_{ji,0}, \ldots, h_{ii,L}]^T$ and its corresponding frequency response vector as $\boldsymbol{H}_{ji} = DFT(\boldsymbol{h}_{ji}) = [H_{ji,0}, \ldots, H_{ji,N-1}]^T$. It is assumed that, the OFDM block from the j^{th} transmitter antenna is precoded, by the $N \times N$ matrix $\boldsymbol{W}_j$ in frequency-domain. The frequency-domain received OFDM vector at i^{th} receiving antenna is given by (generalization of *eqn. 3.6*):

$$\boldsymbol{y}_i(n) = \sum_{j=1}^{M_t} \widetilde{\boldsymbol{H}}_{ji} \boldsymbol{W}_j \boldsymbol{d}_j(n) + \widetilde{\boldsymbol{n}}_i(n) \qquad \ldots (3.26)$$

where, $\widetilde{\boldsymbol{H}}_{ji} = diag\{\boldsymbol{H}_{ji}\}$ is the ji-th channel sub-matrix of dimension $N \times N$; $\boldsymbol{d}_j(n)$ is the frequency-domain transmitted OFDM frame from j^{th} transmitting antenna (see *Chapter 2*); $\widetilde{\boldsymbol{n}}_i(n)$ is the post-DFT additive white zero-mean Gaussian noise vector of dimension $N \times 1$ at i^{th} receiving antenna with variance σ_n^2. The $NM_t \times NM_r$ frequency-domain channel matrix is given by:

$$\mathbf{H}_N = \begin{bmatrix} \widetilde{\boldsymbol{H}}_{11} & \cdots & \widetilde{\boldsymbol{H}}_{M_t 1} \\ \vdots & \ddots & \vdots \\ \widetilde{\boldsymbol{H}}_{1M_r} & \cdots & \widetilde{\boldsymbol{H}}_{M_t M_r} \end{bmatrix} \qquad (3.27)$$

Define the composite frequency-domain transmitted vector as: $\boldsymbol{d}(n) = [\boldsymbol{d}_1(n)^T \quad \cdots \quad \boldsymbol{d}_{M_t}(n)^T]^T$. The composite frequency-domain received vector can be written as:

$$\boldsymbol{y}(n) = [\boldsymbol{y}_1(n)^T \quad \cdots \quad \boldsymbol{y}_{M_r}(n)^T]^T = \mathbf{H}_N \boldsymbol{W}_c \boldsymbol{d}(n) + \tilde{\boldsymbol{n}}(n) \qquad (3.28)$$

where, $\tilde{\boldsymbol{n}}(n)$ is the composite noise vector given by: $\tilde{\boldsymbol{n}}(n) = [\tilde{\boldsymbol{n}}_1(n)^T \quad \cdots \quad \tilde{\boldsymbol{n}}_{M_r}(n)^T]^T$ and $\boldsymbol{W}_c$ is the composite block-diagonal precoding matrix of dimension $NM_t \times NM_t$ given by:

$$\boldsymbol{W}_c = diag\{\boldsymbol{W}_1, \boldsymbol{W}_2, \ldots, \boldsymbol{W}_{M_t}\}$$

If block-time-variant precoding is used, *eqn. 3.28* must be reframed as:

$$\boldsymbol{y}(nM_t + \tau) = [\boldsymbol{y}_1(nM_t + \tau)^T \quad \cdots \quad \boldsymbol{y}_{M_r}(nM_t + \tau)^T]^T = \mathbf{H}_N \boldsymbol{W}_{c\tau} \boldsymbol{d}(nM_t + \tau) + \tilde{\boldsymbol{n}}(nM_t + \tau) \qquad \ldots (3.29)$$

where, $\boldsymbol{d}(nM_t + \tau) = [\boldsymbol{d}_1(nM_t + \tau)^T \quad \cdots \quad \boldsymbol{d}_{M_t}(nM_t + \tau)^T]^T$ for $\tau = 1, \ldots, M_t$; $n = 1 \ldots (M/M_t)$ (M is the total length of OFDM blocks used for time-averaging) is the composite transmit vector and the composite block-time-variant precoding matrix $\boldsymbol{W}_{c\tau}$ is defined as:

$$\boldsymbol{W}_{c\tau} = diag\{\boldsymbol{W}_{1\tau}, \boldsymbol{W}_{2\tau}, \ldots, \boldsymbol{W}_{M_t\tau}\}$$

with each of its sub-matrices as defined in next sub-section.

Note: Since the input is assumed to be stochastic; $\boldsymbol{d}(n)$ *for* $n = 1, \ldots, M$ is statistically same as $\boldsymbol{d}(nM_t + \tau)$ *for* $\tau = 1, \ldots, M_t$; $n = 1 \ldots (M/M_t)$.

3.3.2. GENERALIZED CORRELATION-AVERAGING ALGORITHM

The channel matrix is estimated via SVD and joint correlation-averaging in frequency-domain using the estimate of auto-covariance matrix of the composite receiver vector [57]. Consider, for time being a composite time-invariant block diagonal precoding matrix given by:

$$\boldsymbol{P}_c = diag\{\boldsymbol{P}_1, \boldsymbol{P}_2 \cdots \boldsymbol{P}_{M_t}\} \quad where, \ \boldsymbol{P}_j = \boldsymbol{W}_j \boldsymbol{W}_j^H$$

Let the source covariance matrix be $\boldsymbol{R}_d = E\{\boldsymbol{d}(n)\boldsymbol{d}(n)^H\} = \sigma_d^2 \boldsymbol{I}_{NM_t}$. From *eqn. 3.28*, the output signal covariance matrix can be expressed as [57]:

$$\boldsymbol{R}_y = E\{\boldsymbol{y}(n)\boldsymbol{y}(n)^H\} = \sigma_d^2 \mathbf{H}_N \boldsymbol{P}_c \mathbf{H}_N^H + \sigma_n^2 \boldsymbol{I}_{NM_r} = \begin{bmatrix} \boldsymbol{R}_{y,11} & \cdots & \boldsymbol{R}_{y,1M_r} \\ \vdots & \ddots & \vdots \\ \boldsymbol{R}_{y,M_r1} & \cdots & \boldsymbol{R}_{y,M_rM_r} \end{bmatrix} \quad (3.30)$$

with its *(b, d)*th sub-block given by,

$$\boldsymbol{R}_{y,bd} = \sigma_d^2 \sum_{j=1}^{M_t} \widetilde{\boldsymbol{H}}_{jb} \boldsymbol{P}_j \widetilde{\boldsymbol{H}}_{jd}^H + \delta(b-d)\sigma_n^2 \boldsymbol{I}_N = \sigma_d^2 \sum_{j=1}^{M_t} (\boldsymbol{H}_{jb} \boldsymbol{H}_{jd}^H) \odot \boldsymbol{P}_j + \delta(b-d)\sigma_n^2 \boldsymbol{I}_N$$

... (3.31)

By utilizing covariance matrix of *eqn. 3.30*; correlation-averaging algorithms for MIMO-OFDM systems can estimate the channel matrix up to a constant complex matrix ambiguity. For estimation of the channel matrix up to scalar ambiguity per transmitting antenna to be possible, as mentioned earlier, block-time-variant precoders must be employed [57]. Suppose at the $(nM_t + \tau)$-th time interval, $\tau = 1, \ldots, M_t$; the symbol block from the j^{th} transmitter is precoded by $\boldsymbol{W}_{j\tau}$. Then, the corresponding $\boldsymbol{P}_{j\tau}$ is represented by: $\boldsymbol{P}_{j\tau} = \boldsymbol{W}_{j\tau} \boldsymbol{W}_{j\tau}^H$ for $j, \tau = 1, \ldots, M_t$. Using *eqn. 3.29*, M_t covariance matrices can be defined as:

$$\boldsymbol{R}_y = E\{\boldsymbol{y}(nM_t + \tau)\boldsymbol{y}(nM_t + \tau)^H\}, \qquad \tau = 1, \cdots, M_t$$

The *eqn. 3.31* can thus be re-written as:

$$\boldsymbol{R}_{y\tau,bd} = \sigma_d^2 \sum_{j=1}^{M_t} \widetilde{\boldsymbol{H}}_{jb} \boldsymbol{P}_{j\tau} \widetilde{\boldsymbol{H}}_{jd}^H + \delta(b-d)\sigma_n^2 \boldsymbol{I}_N = \sigma_d^2 \sum_{j=1}^{M_t} (\boldsymbol{H}_{jb} \boldsymbol{H}_{jd}^H) \odot \boldsymbol{P}_{j\tau} + \delta(b-d)\sigma_n^2 \boldsymbol{I}_N$$

... (3.32)

Consider the following two cases [57]:

Case 1: $b \neq d$. For this case, the *(m, q)*-th entry of $\boldsymbol{R}_{y\tau,bd}$ can be expressed as:

$$[\boldsymbol{R}_{y\tau,bd}]_{mq} = \sigma_d^2 \sum_{j=1}^{M_t} [\boldsymbol{P}_{j\tau}]_{mq} H_{jb,m-1} H_{jd,q-1}^* \qquad \tau = 1, \cdots, M_t$$

... (3.33)

It can be seen that, above expression contains M_t equations and M_t unknowns. Assuming time-synchronization and the knowledge of precoding matrices at the receiver, these equations can be solved to obtain the unknown parameters as:

$$\begin{bmatrix} \sigma_d^2 H_{1b,m-1} H_{1d,q-1}^* \\ \vdots \\ \sigma_d^2 H_{M_t b,m-1} H_{M_t d,q-1}^* \end{bmatrix} = \begin{bmatrix} [\boldsymbol{P}_{11}]_{mq} & \cdots & [\boldsymbol{P}_{M_t 1}]_{mq} \\ \vdots & \ddots & \vdots \\ [\boldsymbol{P}_{1M_t}]_{mq} & \cdots & [\boldsymbol{P}_{M_t M_t}]_{mq} \end{bmatrix}^{-1} \begin{bmatrix} [\boldsymbol{R}_{y1,bd}]_{mq} \\ \vdots \\ [\boldsymbol{R}_{yM_t,bd}]_{mq} \end{bmatrix} \quad (3.34)$$

Since, the solution for above matrix equation exists if and only if the inverse of precoding matrix exists, the precoding matrices $\boldsymbol{P}_{j\tau}$ must be designed such that the matrix in *eqn. 3.34* is non-singular [57]. By considering, all pairs of *(m, q)* and organizing the terms, we can obtain:

$$\boldsymbol{Q}_{j,bd} = \sigma_d^2 \boldsymbol{H}_{jb} \boldsymbol{H}_{jd}^H \quad for\ j = 1, \cdots, M_t \quad (3.35)$$

Case 2: $b = d$. For this case, the diagonal entries of covariance matrix cannot be directly used as they are corrupted with unknown noise. Thus, we can rely upon non-diagonal ($m \neq q$) entries only. Consider,

$$[\boldsymbol{R}_{y\tau,bd}]_{mq} = \sigma_d^2 \sum_{j=1}^{M_t} [\boldsymbol{P}_{j\tau}]_{mq} H_{jb,m-1} H_{jd,q-1}^* \qquad \tau = 1, \cdots, M_t, \quad b = d, \quad m \neq q$$

... (3.36)

We can obtain the estimates of $\sigma_d^2 H_{jb,m-1} H_{jd,q-1}^*$ $for\ j = 1, \cdots, M_t$ from *eqn. 3.34*. Combining all the pairs *(m, q)* with $m \neq q$, a new vector can be formed as:

$$\boldsymbol{r}_{bd,jq} = [\sigma_d^2 H_{jb,0} H_{jd,q-1}^* \quad \cdots \quad \sigma_d^2 H_{jb,q-2} H_{jd,q-1}^* \quad \sigma_d^2 H_{jb,q} H_{jd,q-1}^* \quad \cdots \quad \sigma_d^2 H_{jb,N-1} H_{jd,q-1}^*]^T$$

for q = 1, ... , N and j = 1, ... , M_t

As long as *(M-1) ≥ (L+1)*, the estimate of $\sigma_d^2 \boldsymbol{H}_{jb} H_{jd,q-1}^*$ (analogous to *eqn. 3.15*) can be obtained as:

$$\sigma_d^2 \boldsymbol{H}_{jb} H_{jd,q-1}^* = \boldsymbol{F}(:, 1: L+1) \boldsymbol{F}_q^{\dagger} \boldsymbol{r}_{bd,jq} \quad (3.37)$$

where, $\boldsymbol{F}_q$ is as defined in *eqn. 3.14*.

Combining all $\sigma_d^2 \boldsymbol{H}_{jb} H_{jd,q-1}^*$ for $q = 1, \ldots, N$, we can obtain:

$$\boldsymbol{Q}_{j,bd} = \left[\sigma_d^2 \boldsymbol{H}_{jb} H_{jd,0}^* \quad \cdots \quad \sigma_d^2 \boldsymbol{H}_{jb} H_{jd,N-1}^*\right] = \sigma_d^2 \boldsymbol{H}_{jb} \boldsymbol{H}_{jd}^H \quad for\ j = 1, \cdots, M_t \tag{3.38}$$

Define,

$$\boldsymbol{Q}_j = \begin{bmatrix} \boldsymbol{Q}_{j,11} & \cdots & \boldsymbol{Q}_{j,1M_r} \\ \vdots & \ddots & \vdots \\ \boldsymbol{Q}_{j,M_r1} & \cdots & \boldsymbol{Q}_{j,M_rM_r} \end{bmatrix} \quad for\ j = 1, \cdots, M_t \tag{3.39}$$

and

$$\boldsymbol{U} = \begin{bmatrix} \boldsymbol{H}_{11} & \cdots & \boldsymbol{H}_{M_t1} \\ \vdots & \ddots & \vdots \\ \boldsymbol{H}_{1M_r} & \cdots & \boldsymbol{H}_{M_tM_r} \end{bmatrix} \tag{3.40}$$

It can be seen that,

$$\boldsymbol{Q}_j = \sigma_d^2 \boldsymbol{U}_j \boldsymbol{U}_j^H \tag{3.41}$$

where, $\boldsymbol{U}_j = \left[\boldsymbol{H}_{j1}{}^T \quad \cdots \quad \boldsymbol{H}_{jM_r}^T\right]^T$ represents the $NM_r \times 1$ channel response vector from the j^{th} transmitter to all the receivers i.e, the j^{th} column of $\boldsymbol{U}$.

Let $\widehat{\boldsymbol{U}}_j$ denote the Eigen-vector of $\boldsymbol{Q}_j$, corresponding to its largest Eigen-value. From subspace detection theory, $span\{\widehat{\boldsymbol{U}}_j\} = span\{\boldsymbol{U}_j\}$ when $M_t < M_rN$ [57]. Therefore $\widehat{\boldsymbol{U}}_j$ can be considered as an estimate of $\boldsymbol{U}_j$ corrupted by a constant complex scalar factor as given by,

$$\widehat{\boldsymbol{U}}_j = \alpha_j \boldsymbol{U}_j$$

Thus the estimate of $\boldsymbol{U}_j$ can be obtained from the Eigen-vector of $\boldsymbol{Q}_j$, corresponding to its largest Eigen-value obtained by singular value decomposition (SVD) up to a constant complex scalar ambiguity.

Note: Since $N > 1$ for all OFDM systems, this approach is applicable to the systems with the number of transmitting antennas greater than the number of receiving antennas (i.e., MISO-type systems) without need for oversampling at the receiver unlike subspace decomposition approach.

Chapter 4

SIMULATION RESULTS FOR BLIND TECHNIQUES

Using simulation techniques, this chapter describes the performance of blind channel estimation using subspace-based and precoding-induced correlation-averaging techniques for SISO-OFDM and MIMO-OFDM systems in terms of mean square error (MSE) over different baseband modulation (mapping) schemes and channel power delay profiles. Some common parameters used for simulation purpose are given below:

- The discrete baseband equivalent FIR channel impulse response is assumed to be static over the interval of estimation process with length/ order (L) equals to *2*. The channel coefficients are assumed to be complex zero-mean Gaussian distributed random variable with variances given according to either of the following power-delay-profiles (PDP) [61]:
  - Exponential-

$$E\{|h_l|^2\} = e^{\left(-\frac{lT}{\tau}\right)}, \qquad l = 0, \ldots, L$$

  - Uniform-

$$E\{|h_l|^2\} = 1, \qquad l = 0, \ldots, L$$

  where, T is the baud-interval and τ is the rms delay spread of the channel. For present discussion, the value of τ/T is taken to be equal to *10* [51].

- Number of subcarriers per OFDM frame (N) = *64*
- Number of OFDM block used to estimate channel output auto-covariance matrix by time-averaging unless otherwise mentioned (M) = *1000*
- SNR (unless otherwise mentioned) = 30 dB
- The estimation ambiguities are resolved using pilot carriers or reference symbols as far as this chapter is concerned.
- The time and frequency synchronization are assumed.

4.1. SISO-OFDM SYSTEMS

4.1.1. CRAMER-RAO BOUND FOR BLIND PRECODER-BASED ESTIMATOR

The stochastic CRB for blind precoding-induced-correlation averaging technique based channel estimator for SISO-OFDM system (*Chapter 3*) is calculated over varying SNR (dB) values for the following values of $p = \{0.1, 0.5, 0.9\}$ (see *eqn. 4.1*) using *eqn. 3.18* and *eqn. 3.25*. The procedure given in flowchart of *fig. 4.1* is used to estimate the channel using precoding-based technique over varying SNR (dB) values for *100* Monte-Carlo runs. The mean-square-error variances for the estimator are calculated and compared with the CRB.

A linear non-redundant frequency-domain time-invariant precoding matrix employed for channel estimation is given as:

$$\boldsymbol{W} = \boldsymbol{P}^{1/2}, \qquad where\ \boldsymbol{P} = \begin{bmatrix} 1 & p & p & \cdots & p \\ p & 1 & p & \cdots & p \\ \vdots & \vdots & \vdots & \ddots & \vdots \\ p & p & p & \cdots & 1 \end{bmatrix}_{N \times N} \tag{4.1}$$

A plot of statistical CRB and mean-square-error variance versus SNR (dB) values for blind precoder-induced-correlation-averaging based channel estimator with 16-QAM baseband mapping for $p = 0.1$ is given in *fig. 4.2* and *fig. 4.3* for exponential and uniform channel PDP respectively. Similar simulation results are obtained for $p = 0.5$ and $p = 0.9$ and are shown in *fig. 4.4 – fig. 4.7*.

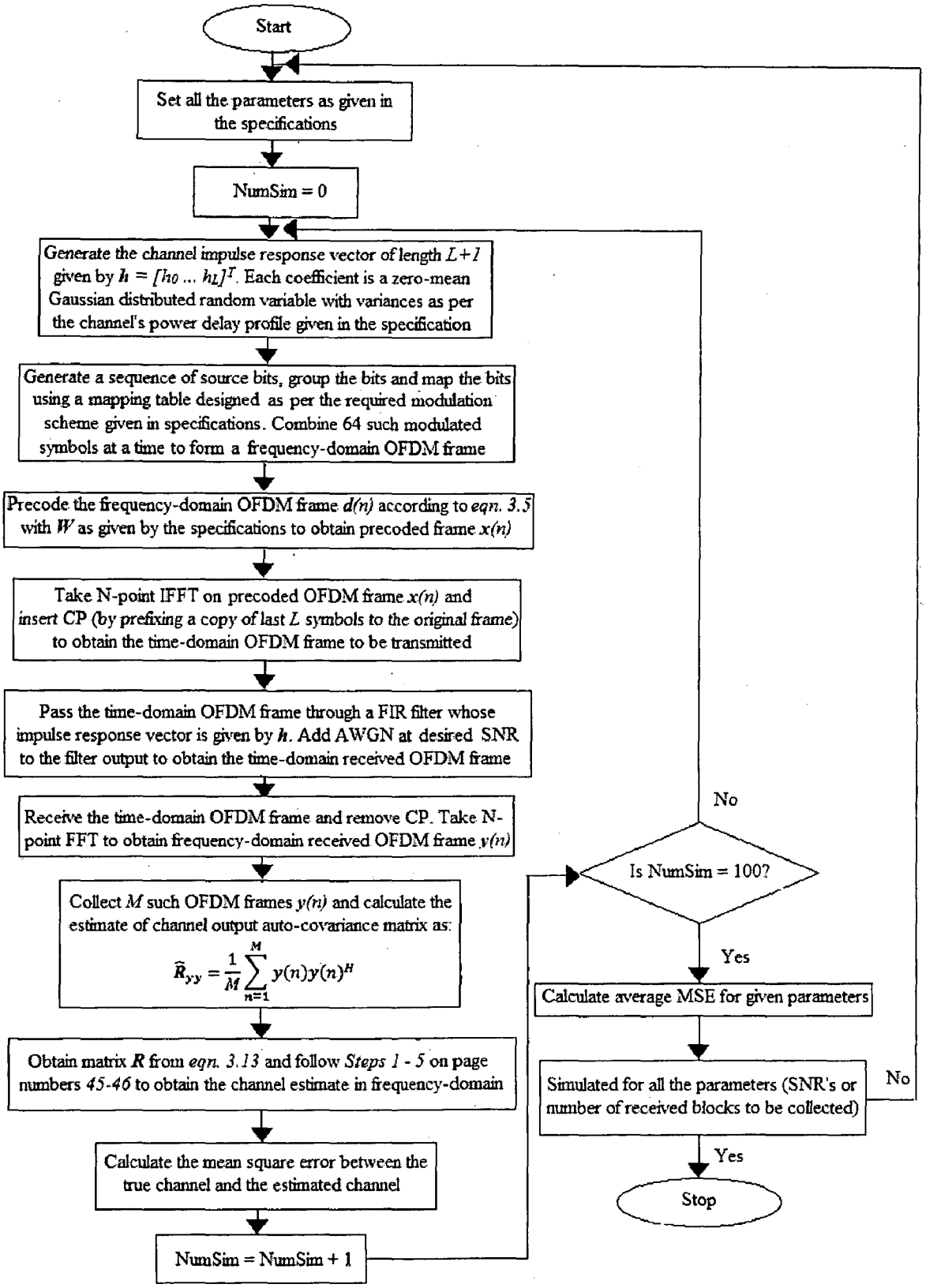

Figure 4.1: Blind channel estimation using precoding-induced correlation-averaging for SISO-OFDM systems

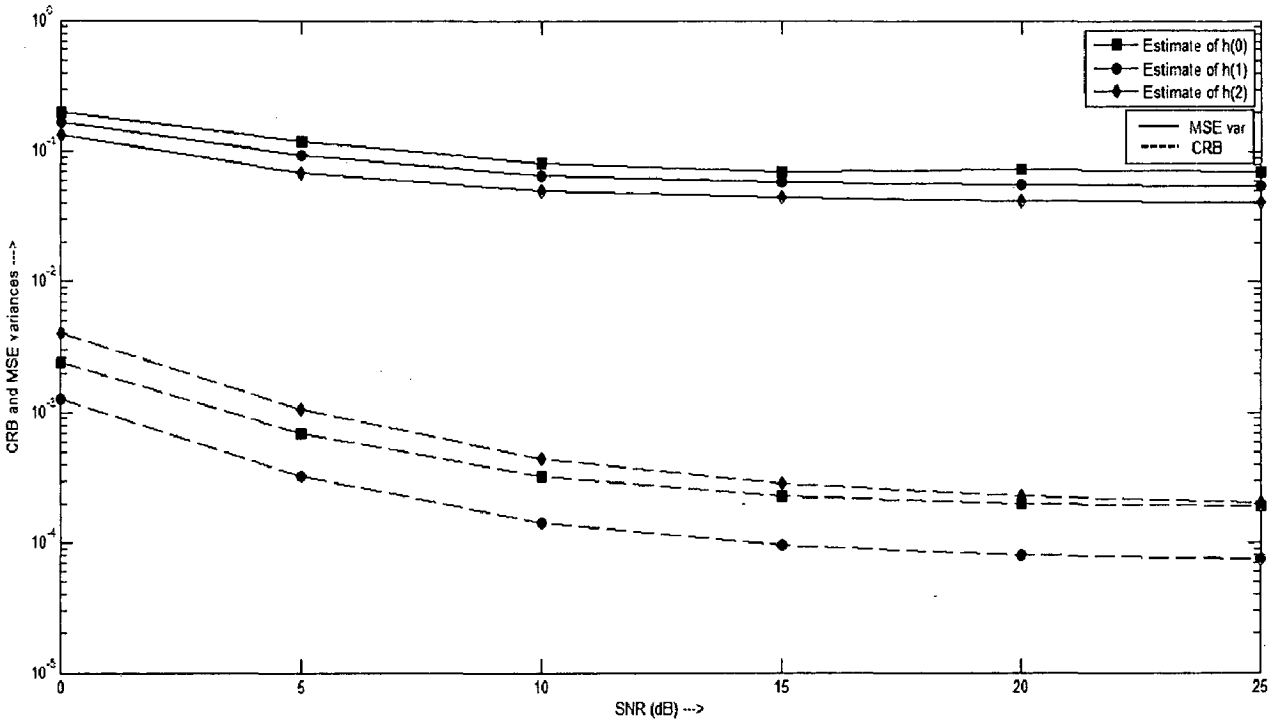

Figure 4.2: CRB and MSE variance versus varying SNR (dB) values for blind precoding-based algorithm with precoding constant (p) = 0.1 for exponential channel PDP

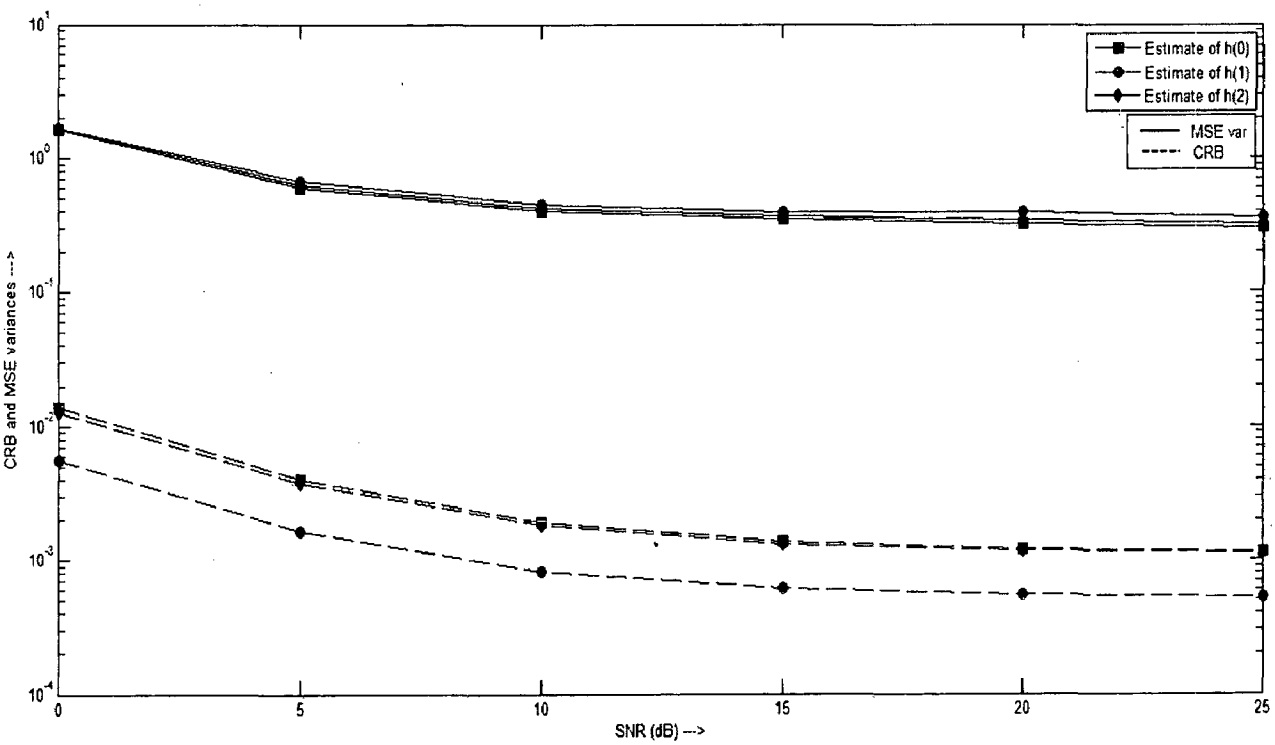

Figure 4.3: CRB and MSE variance versus varying SNR (dB) values for blind precoding-based algorithm with precoding constant (p) = 0.1 for uniform channel PDP

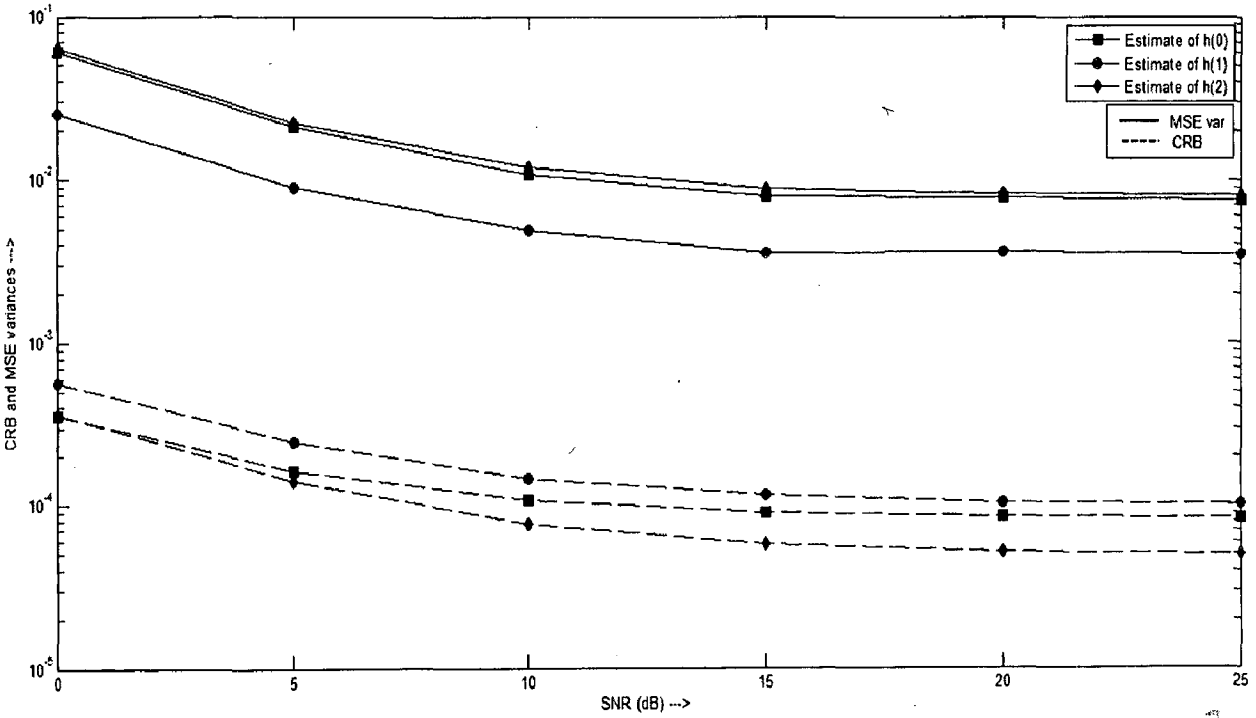

Figure 4.4: CRB and MSE variance versus varying SNR (dB) values for blind precoding-based algorithm with precoding constant (p) = 0.5 for exponential channel PDP

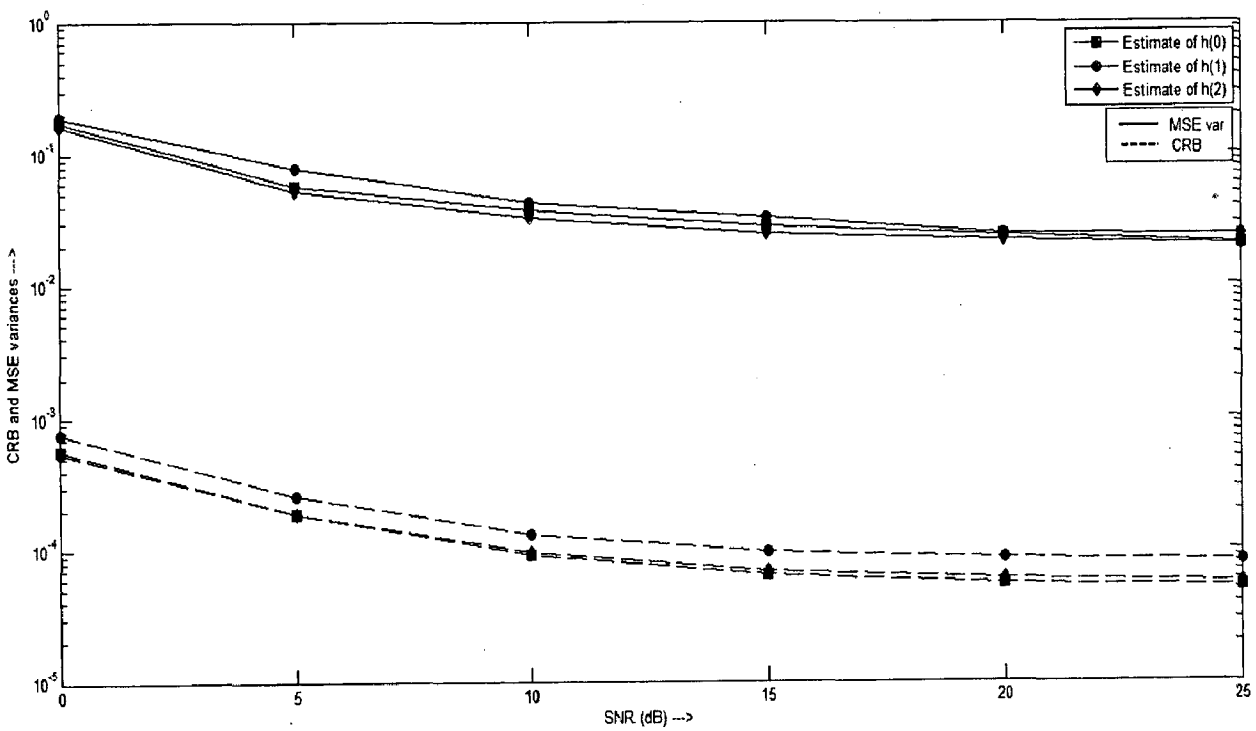

Figure 4.5: CRB and MSE variance versus varying SNR (dB) values for blind precoding-based algorithm with precoding constant (p) = 0.5 for uniform channel PDP

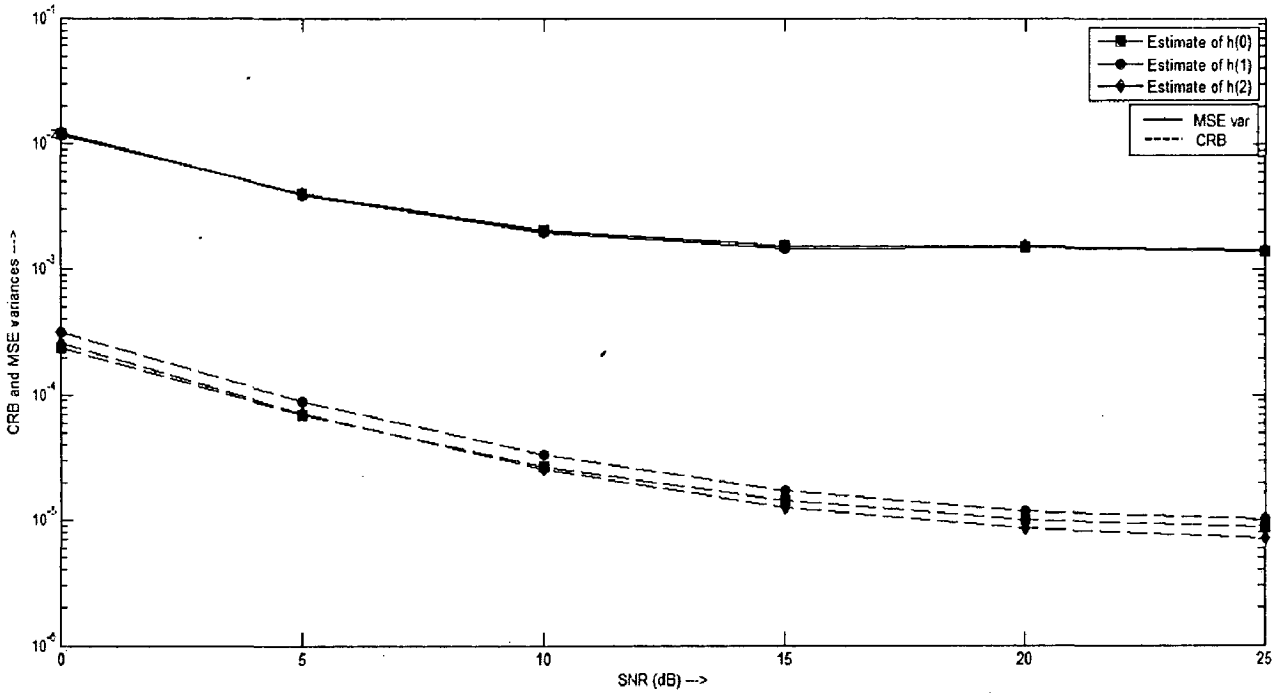

Figure 4.6: CRB and MSE variance versus varying SNR (dB) values for blind precoding-based algorithm with precoding constant (p) = 0.9 for exponential channel PDP

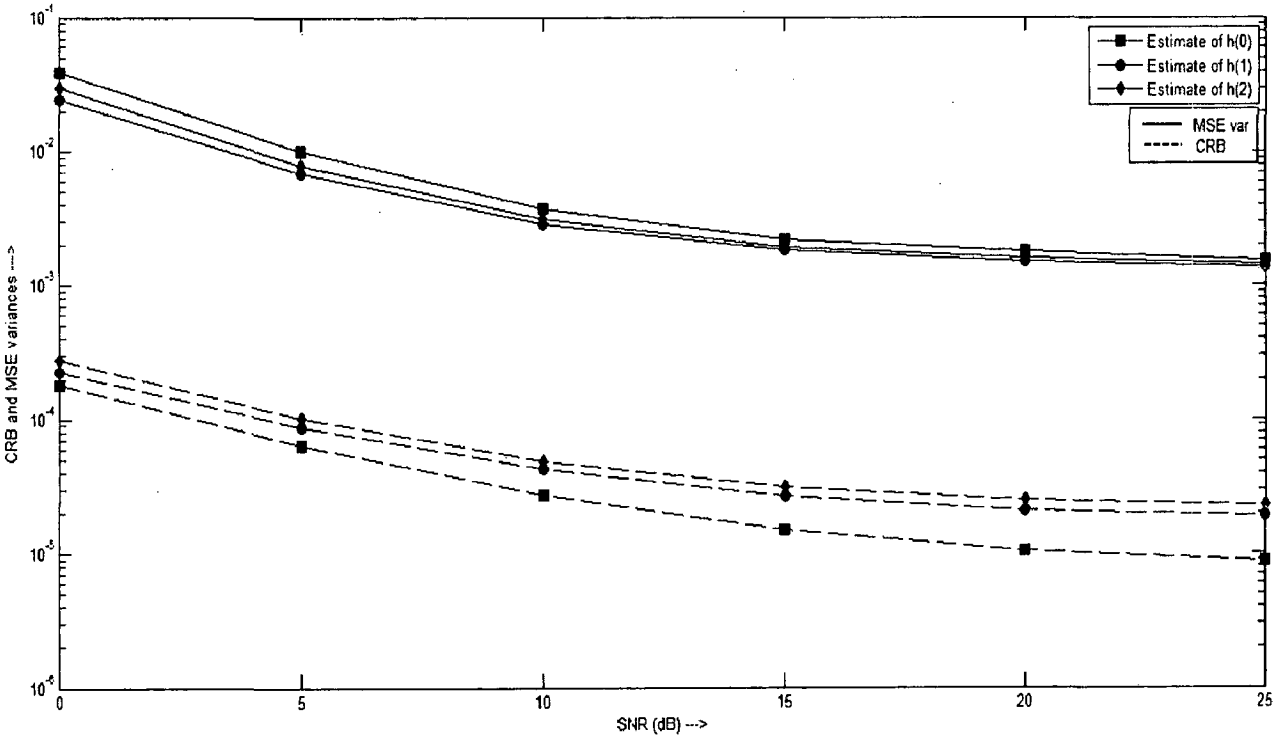

Figure 4.7: The plot of CRB and MSE variance versus varying SNR (dB) values for blind precoding-based algorithm with precoding constant (p) = 0.9 for uniform channel PDP

The following observations can be made from *fig. 4.2 – fig. 4.7*:

Note: The phrase 'on an average' refers to average over three time-domain channel coefficients $\{h_0 \equiv h(0), h_1 \equiv h(1)$ and $h_2 \equiv h(2)\}$.

- For a given channel PDP and the value of p, the MSE variance achieved is, on an average, at least *100* times more than the CRB.
- As the SNR is varied over the range, both CRB and MSE variance achieved by the estimator improves by a factor *10* dB on an average irrespective of channel PDP and the value of p.
- From *fig. 4.2 – fig. 4.7*, it can be observed that when SNR is increased beyond *15* dB, the performance saturates and no further improvement in either CRB or MSE variance achieved by the estimator can be observed.
- As p is increased, both the CRB and the MSE variance achieved by the estimator decreases irrespective of the channel PDP. At *0* dB SNR, from *fig. 4.2 - fig. 4.5*, i.e., when p is increased from *0.1* to *0.5*, an improvement of around *5* dB and *10* dB on an average for exponential and uniform channel PDPs respectively, can be observed in both CRB and MSE variance. At *25* dB SNR, an improvement of *10* dB in MSE variance can be observed irrespective of channel PDP. Further, an improvement of *2* dB and *10* dB can be observed in CRB for exponential and uniform channel PDP. Similar observations can be made, from *fig. 4.4 - fig. 4.7*, i.e., when p is increased from *0.5* to *0.9*.
- For a given value of p, the estimator achieves the lowest MSE variance when the channel PDP is exponential. At *0* dB, from *fig. 4.2* and *fig. 4.3*, a difference of *13* dB in MSE variance on an average can be observed between the cases when the channel PDP is exponential and uniform. Similar observations can be made at *0* dB SNR from *fig. 4.4* and *fig.4.5* (a difference of *7* dB) and *fig. 4.6* and *fig. 4.7* (a difference of *5* dB) for MSE variances. Similarly, at higher SNR values, for instance at *25* dB, from *fig. 4.2 - fig. 4.7* differences of *6* dB, *4* dB and *0* dB in MSE variances respectively can be observed between the cases when the channel PDP is exponential and uniform.

4.1.2. COMPARISON OF SUBSPACE AND PRECODING-BASED TECHNIQUES

This sub-section presents a comparison of subspace-based and precoding-based blind channel estimation techniques in terms of MSE performance over varying length of OFDM blocks and varying SNR (dB) values for 4-PAM, 8-PSK and 16-QAM over two different channel PDP as given in the specifications. The linear non-redundant precoding matrix mentioned in previous sub-section with precoding constant (p) = *0.5* is used along with the procedure given in flowchart of *fig. 4.1* to obtain the channel estimate using precoding-based technique. The procedure given by the flowchart shown in *fig. 4.8* is used to obtain the channel estimate using subspace-based technique. It is assumed that two consecutive OFDM blocks are combined (J = *2*) to form a composite OFDM block for subspace technique.

The MSE performance of two blind techniques versus length of OFDM blocks used at *30* dB SNR with exponential and uniform channel PDP are shown in *fig. 4.9* and *fig. 4.10* respectively. Similarly, the MSE performance of the same versus SNR (dB) values assuming that the length of OFDM blocks used is *1000* with exponential and uniform channel PDP are shown in *fig. 4.11* and *fig. 4.12* respectively.

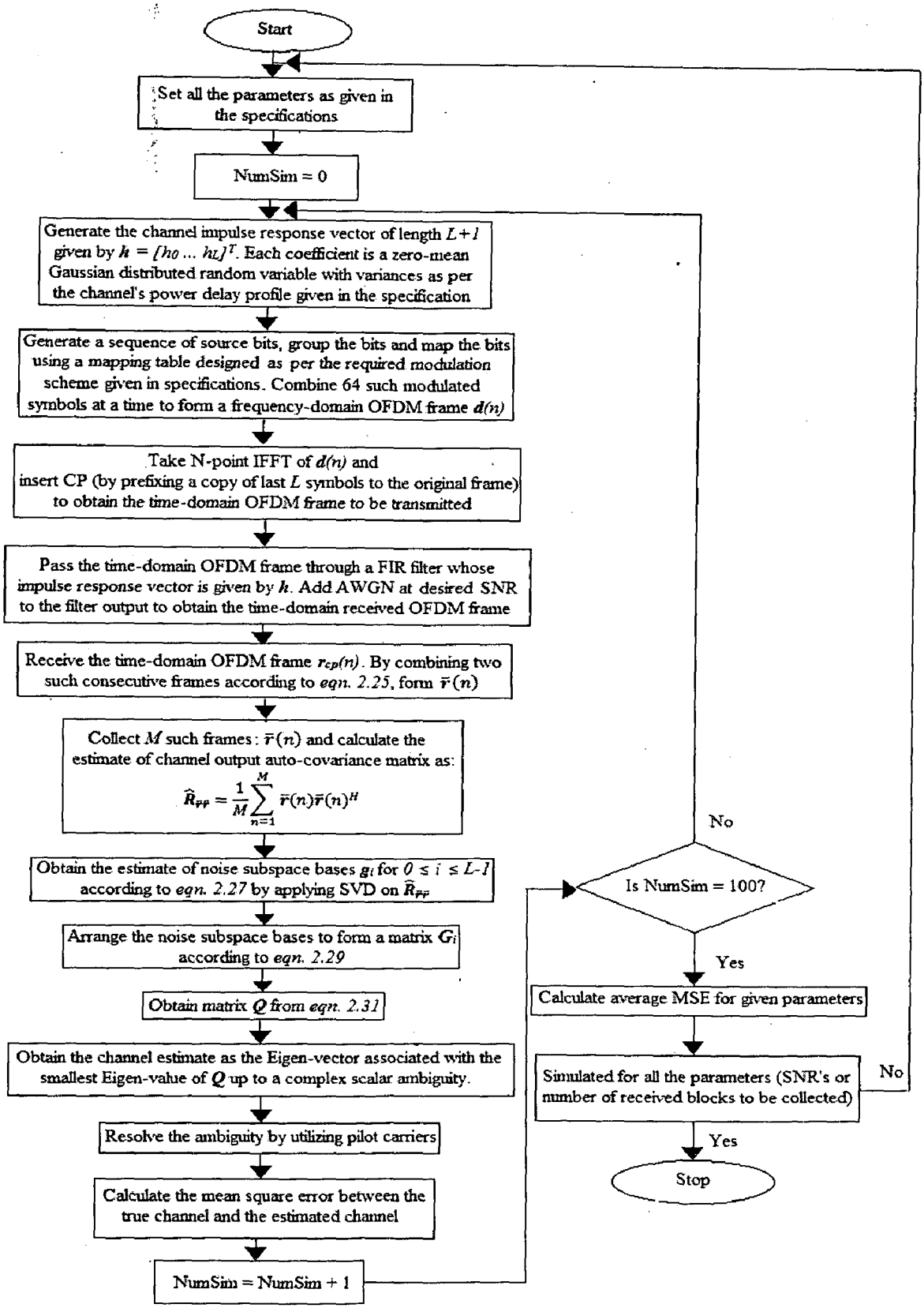

Figure 4.8: Blind channel estimation using generalized subspace-based technique for SISO-OFDM systems

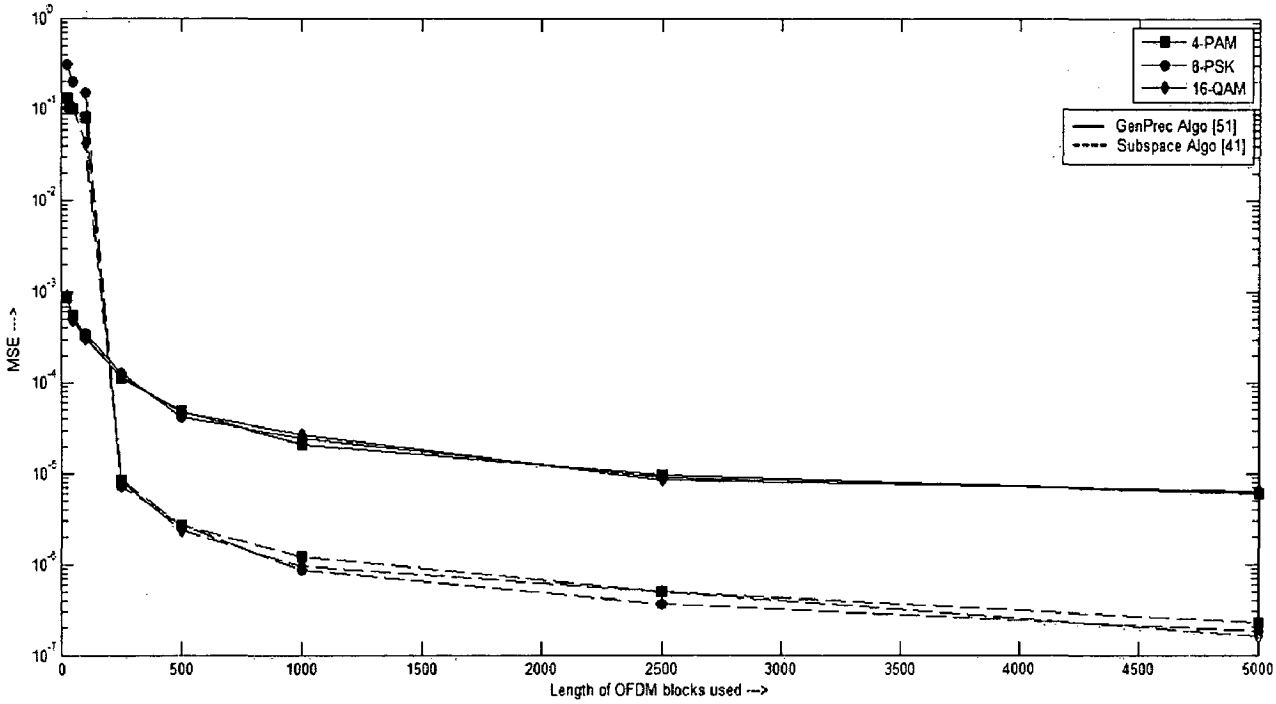

Figure 4.9: MSE versus length of OFDM blocks used at SNR = 30 dB for exponential channel PDP

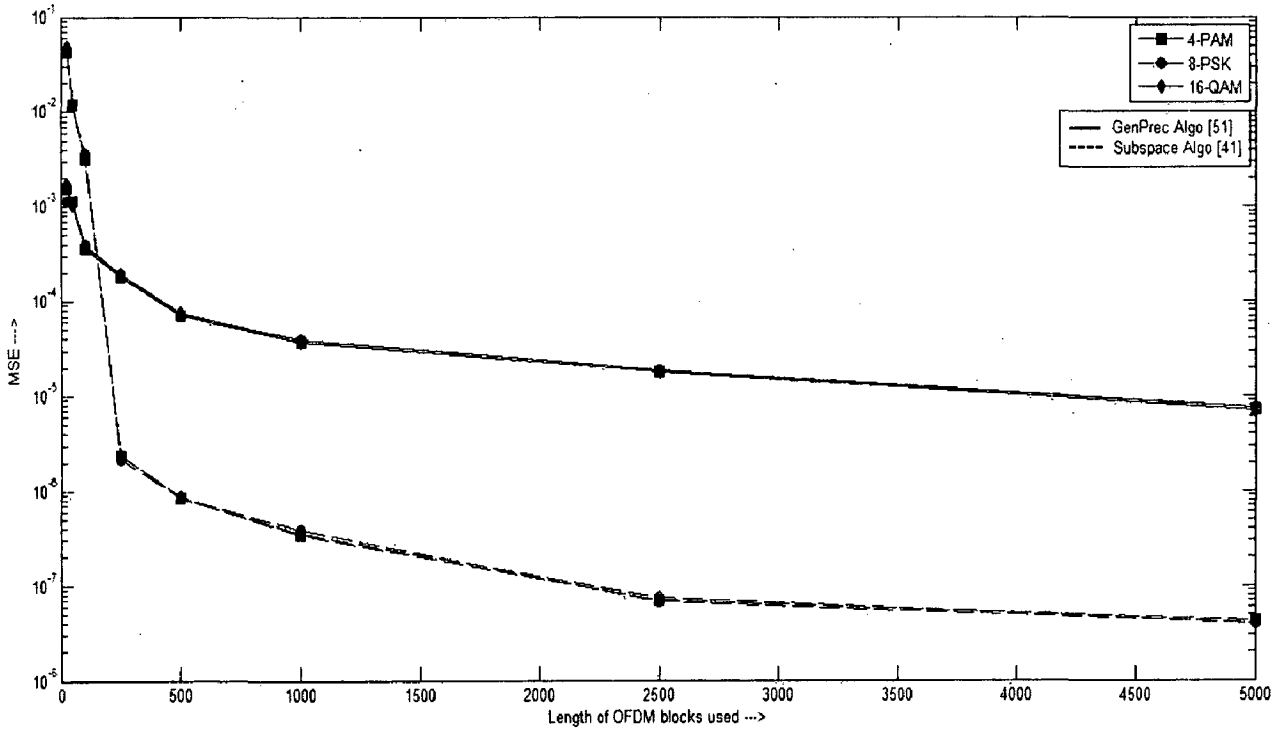

Figure 4.10: MSE versus length of OFDM blocks used at SNR = 30 dB for uniform channel PDP

Following observations can be made from *fig. 4.9* and *fig. 4.10*:

- The performance is independent of the modulation/ mapping scheme used for both the estimation techniques irrespective of channel PDP.
- As stated by p. o. e. assumption, since $J = 2$ and $N = 64$, the minimum length of OFDM frames required for proper formation of subspaces and hence the reliable channel estimates is *128*. From the *fig. 4.9* and *fig. 4.10*, significant difference in performance of subspace algorithm can be observed around this point ($N = 128$).
- Unlike subspace-based method, the precoding-based technique provides a good estimate of the channel even when the length of OFDM frames is small. From *fig. 4.9* and *fig. 4.10*, it can be seen that MSE value of order of 10^{-3} is achieved even when the length of OFDM blocks is as low as *25*.
- The performance of both the techniques improves as the length of the OFDM blocks used is increased. The performance improvement is exponential (gradual) for precoding-based method and is step-like for subspace method. The step-like characteristics is due to p. o. e. assumption (restriction). On the right side of the threshold, the performance shows an exponential behaviour.
- The performance of precoding-based technique is worse than that for subspace-based method when the length of OFDM blocks used exceeds the minimum threshold put forth by p. o. e. assumption. When the length of OFDM blocks is *1000*, the difference in the MSE performances of the two approaches is around *14* dB for exponential channel PDP case and *20* dB for uniform channel PDP case.
- The asymptotic performance of precoding-based method is similar irrespective of channel PDP under consideration. When the length of OFDM blocks is *5000*, the MSE value for exponential PDP case is 6.41×10^{-6} and for uniform PDP case, is 7.467×10^{-6} (a difference of *1* dB). In contrast to the former, the subspace method shows an improvement of around *7* dB when uniform PDP is considered, compared to exponential PDP.
- Comparing *fig. 3.4* and *fig. 4.9*, it can be seen that the generalized precoding-based method is at least *10* times better than simple-precoding based method at lower lengths of OFDM blocks and is almost *20* times better asymptotically. This is because, unlike simple-precoding, the generalized-precoding induces correlation among all the subcarriers and all the columns of output auto-covariance matrix are utilized for channel estimation. This makes the latter more robust to AWGN and distortion due to non-availability of infinite blocks for time-averaging and hence leads to better channel estimate.

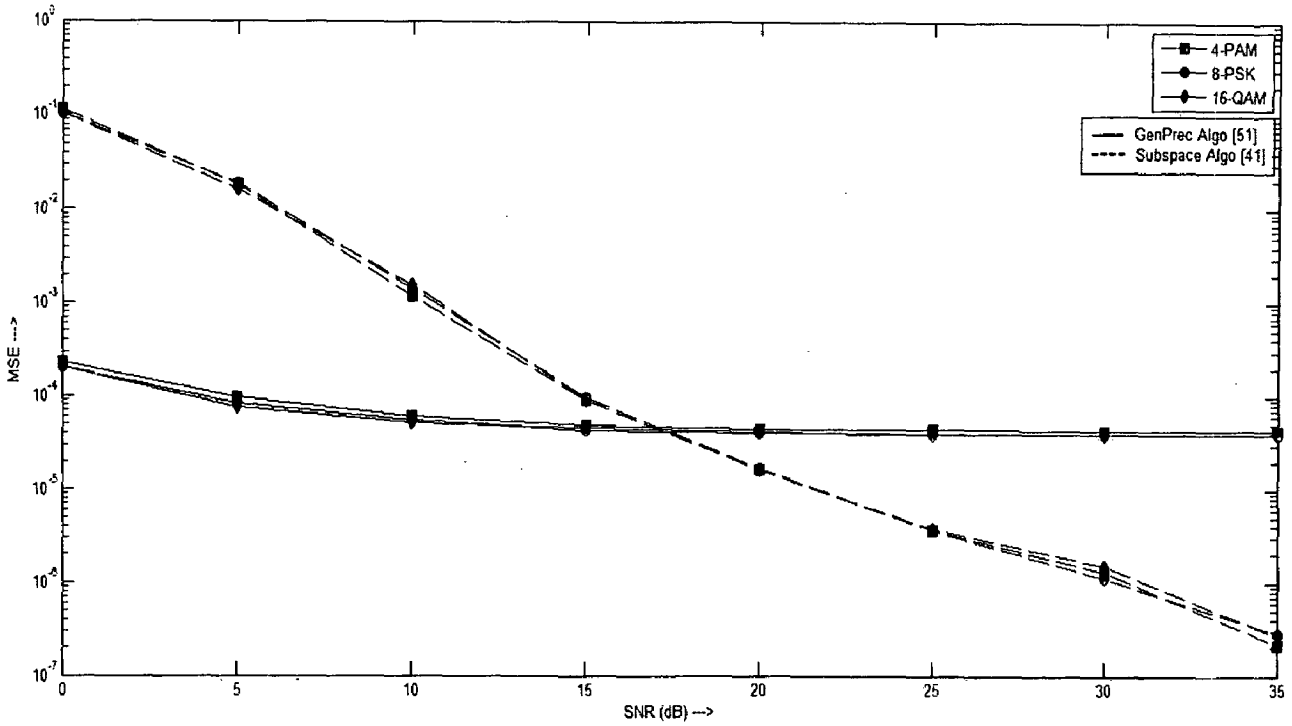

Figure 4.11: MSE versus SNR (dB) with length of OFDM blocks equal to 1000 for exponential channel PDP

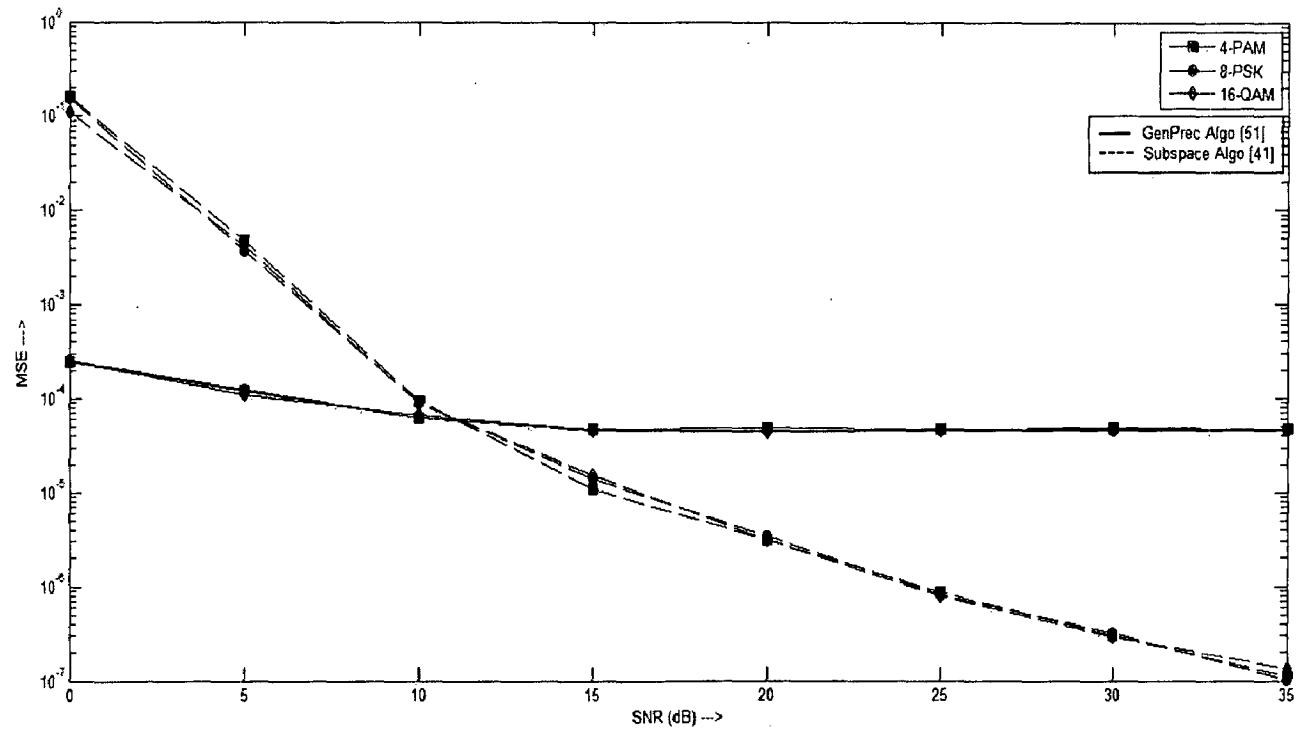

Figure 4.12: MSE versus SNR (dB) with length of OFDM blocks equal to 1000 for uniform channel PDP

Following observations can be made from *fig. 4.11* and *fig. 4.12*:

- The performance is independent of the modulation/ mapping scheme used for both the estimation techniques irrespective of channel PDP.
- Analogous to single-carrier case (*fig. 2.5*), the performance of subspace-based method is almost linear with varying SNR (dB) values. Similarly, precoding-based technique shows an exponential improvement in the performance with increasing SNR values.
- The asymptotic performance of precoding-based technique is similar irrespective of channel PDP under consideration. At *35* dB SNR, the MSE is 3.89×10^{-5} for exponential PDP and MSE is 4.2×10^{-5} for uniform PDP case. For subspace method, the asymptotic performance when exponential PDP is used is slightly better (by *4* dB) than when uniform PDP is used.
- Over the range the SNR values from *0* dB to *35* dB, the performance improvement for the case of precoding-based method is *7* dB irrespective of channel PDP under consideration. In contrast to this, the subspace-based method shows an improvement of around *60* dB.
- For lower SNR values, the precoding-based technique performs better than the subspace-based method. At *0* dB, precoding technique achieves an MSE of *0.000203* (*fig. 4.11*) and *0.000257* (*fig. 4.12*) on an average whereas the subspace method achieves an MSE of *0.1053* (*fig 4.11*) and *0.115* (*fig 4.12*) on an average. At higher SNR values, the precoding method performance is comparably worse than that for the subspace technique. At *35* dB, precoding technique achieves MSE of 3.89×10^{-5} (*fig 4.11*) and MSE of 4.2×10^{-5} (*fig. 4.12*); whereas subspace approach achieves MSE of 2.36×10^{-7} (*fig. 4.11*) and MSE of 1.004×10^{-7} (*fig. 4.12*).
- The saturation observed in the performance of precoding-based technique is due to the fact that the channel estimates in this case are more sensitive to distortion due to non-availability of infinite OFDM blocks for time-averaging (as mentioned earlier) than distortion due to SNR.
- In the case of precoding-based technique, at lower SNR (say *0* dB), the MSE performance is of the order of 10^{-3}, which is at least *100* times better than that observed for subspace method. This is because, since the length of OFDM blocks used is *1000* and joint-correlation-averaging (all the columns of auto-covariance matrix) is used for channel estimation, the effect of AWGN is nullified.
- The 'cross-over' in the performance occurs at around *17* dB for exponential channel PDP case and at around *12* dB for uniform channel PDP case.

4.2. COMPARISON OF SUBSPACE- AND PRECODING-BASED METHODS IN MIMO-OFDM SYSTEMS

This sub-section presents a comparison of subspace-based and precoding-based blind channel estimation techniques with 16-QAM mapping in terms of MSE performance over varying length of OFDM blocks and over varying SNR (dB) values in MIMO-OFDM system for two different channel PDPs as given in the specifications. The procedure given in the flowchart shown in *fig. 4.13* is used to obtain the channel estimate using subspace-based technique. As mentioned earlier, it is assumed that $J = 2$ for subspace technique. The linear non-redundant block-time-variant precoding matrix is given by: $\boldsymbol{W}_{ij} = \boldsymbol{P}_{ij}$ where,

$$[\boldsymbol{P}_{ij}]_{mq} = \begin{cases} 1.2 & m = q = 1, \cdots, \frac{N}{2} \\ 0.8 & m = q = \frac{N}{2} + 1, \cdots, N \\ \frac{2}{3} & otherwise \end{cases} \qquad for\ i = j \qquad (4.2a)$$

$$[\boldsymbol{P}_{ij}]_{mq} = \begin{cases} 0.8 & m = q = 1, \cdots, \frac{N}{2} \\ 1.2 & m = q = \frac{N}{2} + 1, \cdots, N \\ \frac{1}{3} & otherwise \end{cases} \qquad for\ i \neq j \qquad (4.2b)$$

is used along with the procedure given in flowchart of *fig. 4.14* to obtain the channel estimate using precoding-based technique. The range of values the variable indices, i and j in *eqn. 4.2* can assume depends upon the number of transmitting antenna:

Case 1: $M_t = 2$

$i = j = \{1, 2\}$

Case 2: $M_t = 4$

$i = j = \{1, 2, 3, 4\}$

The comparison of MSE performance for the two methods over varying length of OFDM frames at *30* dB SNR for two different channel PDPs in *2×2*, *2×4*, *4×4* and *2×1* (with oversampling rate: $q = 2$) MIMO-OFDM systems are shown in *fig. 4.15 – fig. 4.18* respectively. Similar comparison of MSE performance over varying SNR (dB) values assuming that the length of OFDM blocks is *1000* are shown in *fig. 4.19 – fig. 4.22* respectively.

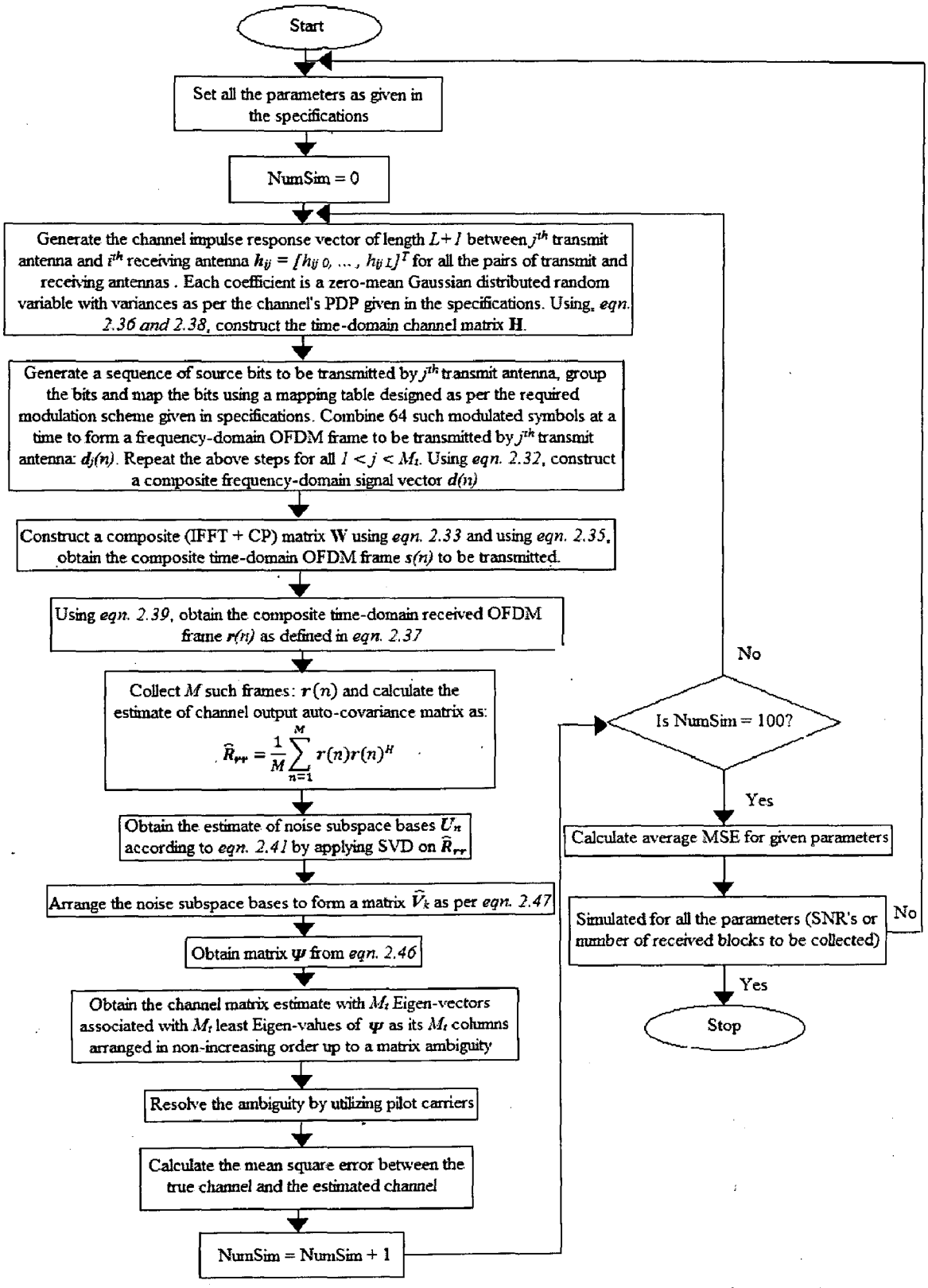

Figure 4.13: Blind channel estimation using subspace-based technique for MIMO-OFDM systems

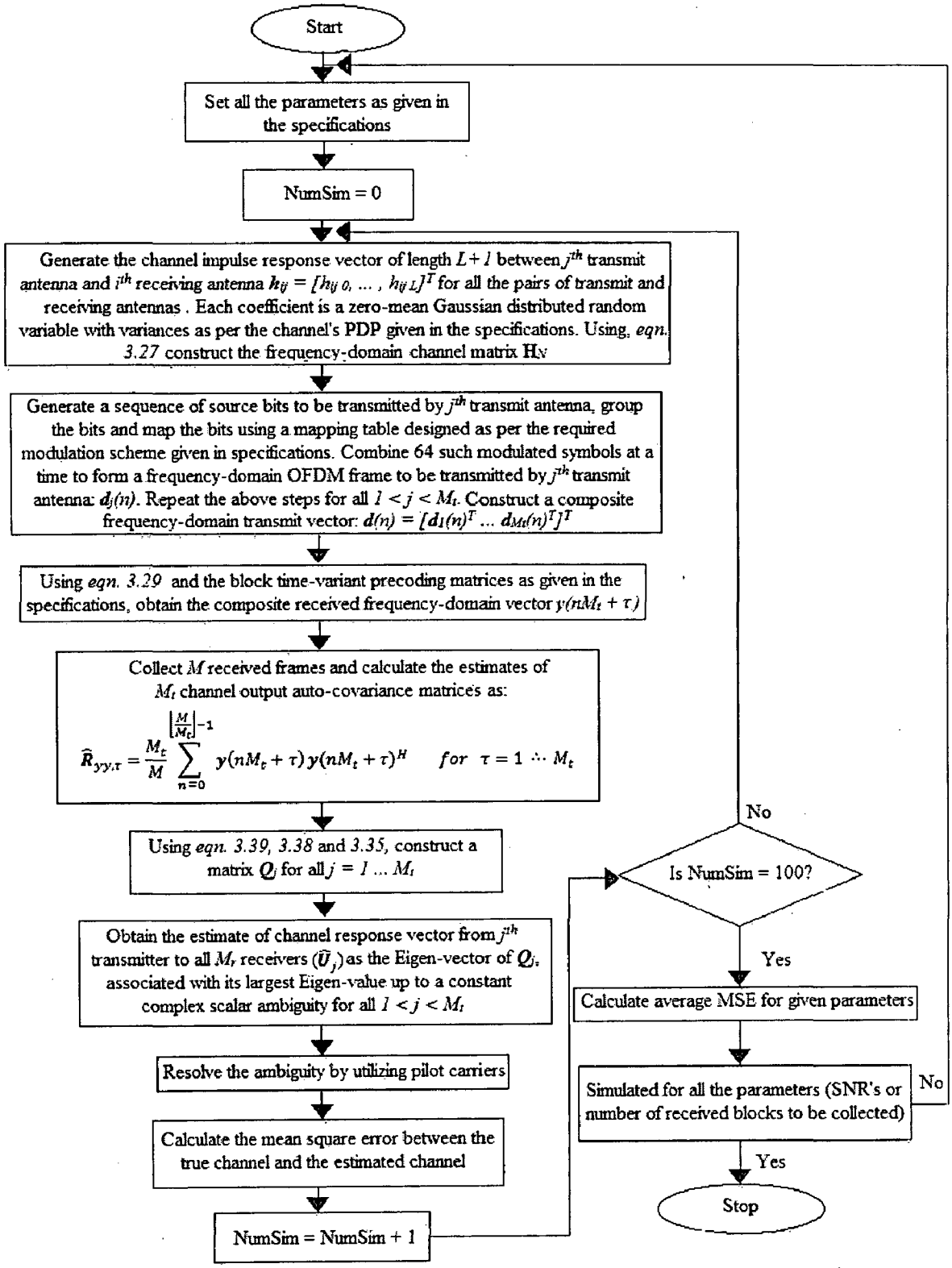

Figure 4.14: Blind channel estimation using block-time-variant precoding-based technique for MIMO-OFDM systems

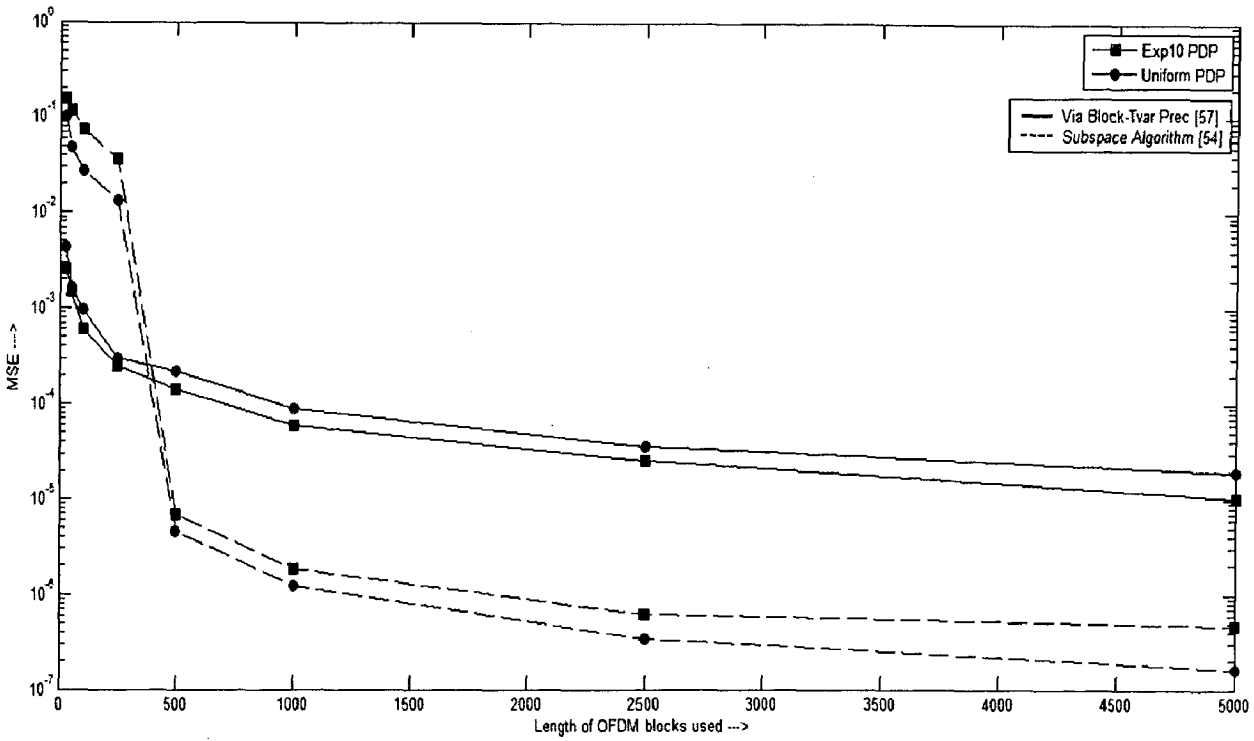

Figure 4.15: MSE versus length of OFDM blocks at 30 dB SNR for 2×2 MIMO-OFDM system for 16-QAM

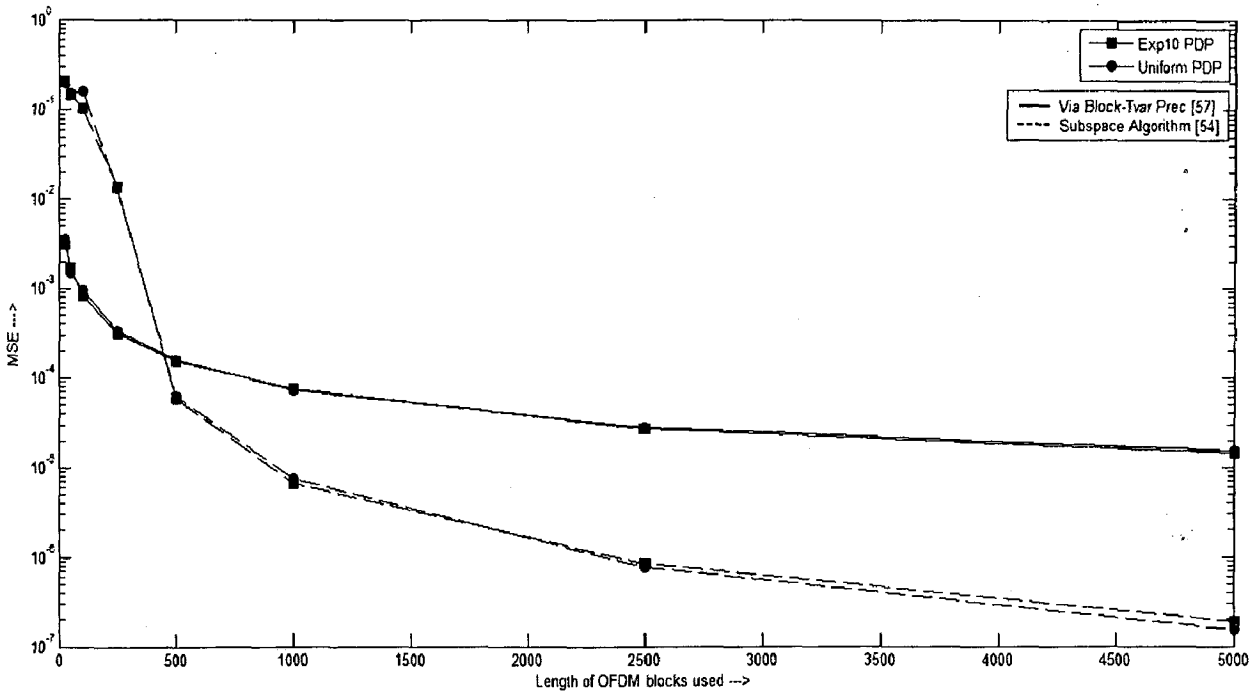

Figure 4.16: MSE versus length of OFDM blocks at 30 dB SNR for 2×4 MIMO-OFDM system for 16-QAM

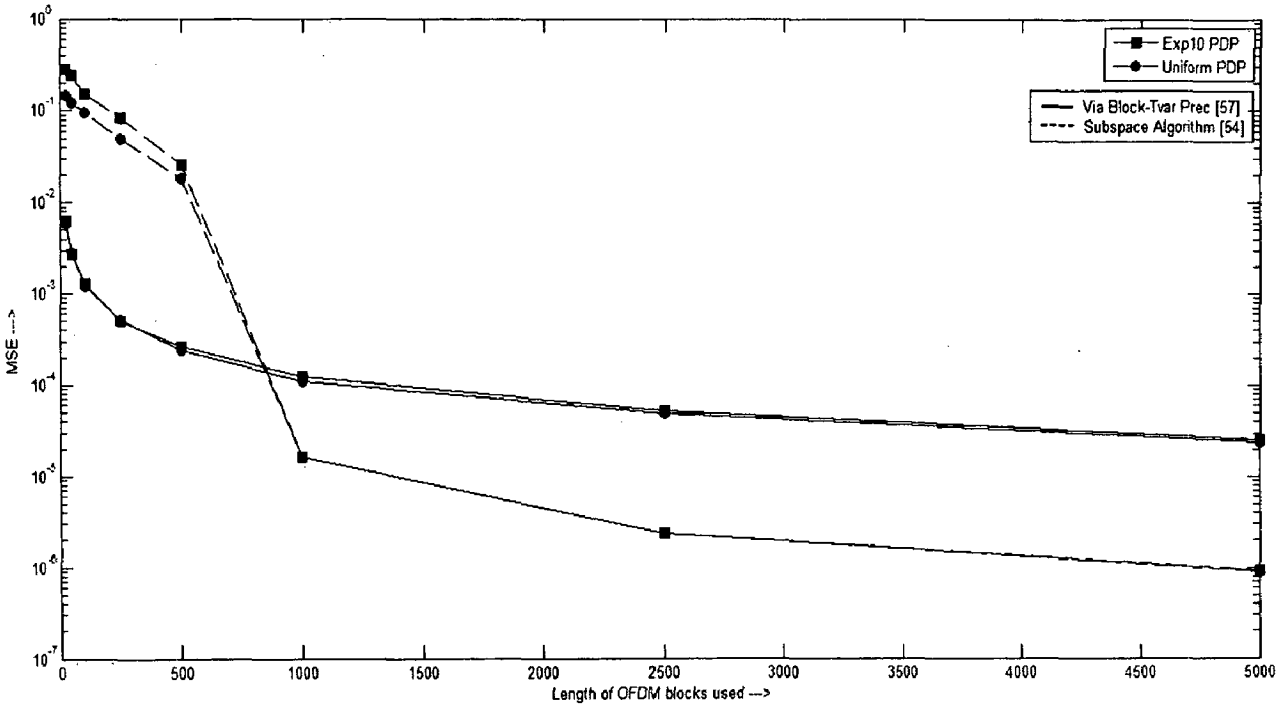

Figure 4.17: MSE versus length of OFDM blocks at 30 dB SNR for 4×4 MIMO-OFDM system for 16-QAM

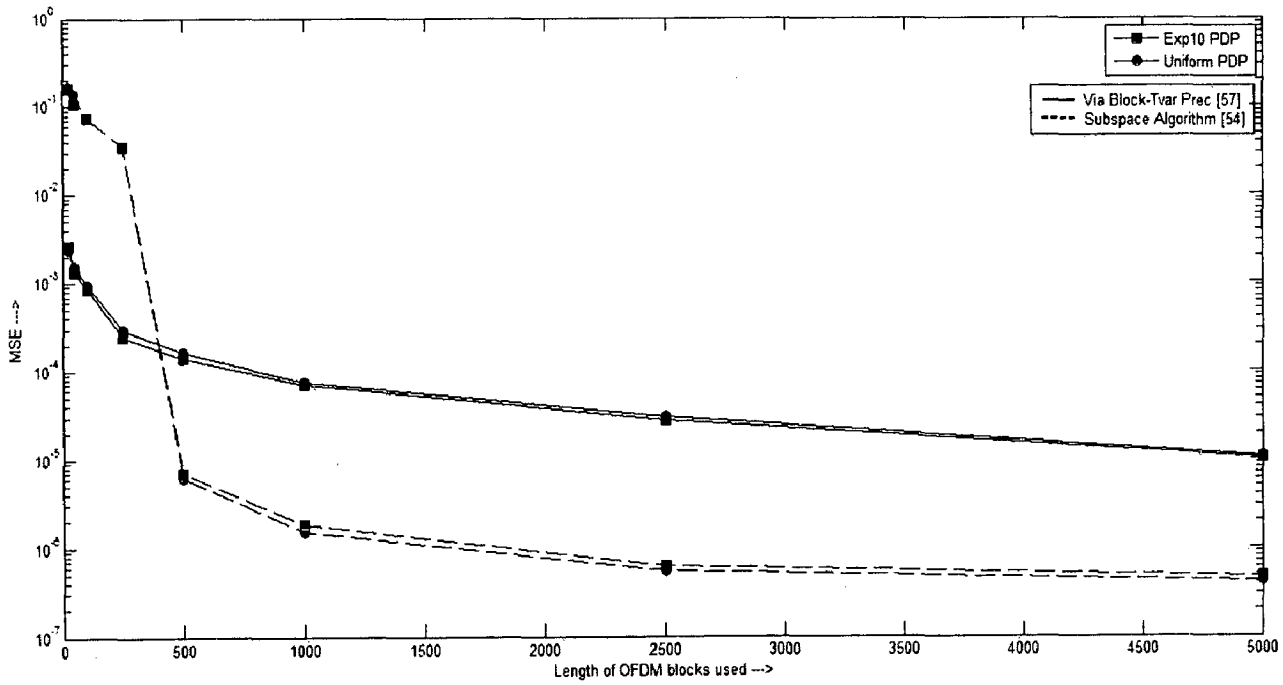

Figure 4.18: MSE versus length of OFDM blocks at 30 dB SNR for 2×1 MIMO-OFDM system for 16-QAM with an oversampling rate (q) of 2

Following observations can be made from *fig. 4.15 - fig. 4.18*:

- The performance is independent of the channel PDP under consideration for all the combinations of M_t and M_r shown.
- As stated earlier using p. o. e. assumption, since $J = 2$ and $N = 64$, the minimum length of OFDM frames required for proper formation of subspaces and hence the reliable channel estimates is $128M_t$. For $M_t = 2$ (i.e., 2×2, 2×4 and 2×1 MIMO), the threshold is hence *256* and for $M_t = 4$ (4×4 MIMO), the threshold is *512*. From the *fig. 4.15 - fig. 4.18*, significant difference in performance of subspace algorithm can be observed around this point ($M = 256$ for $M_t = 2$ and $M = 512$ for $M_t = 4$).
- Unlike subspace-based method, the precoding-based technique is not restricted by p. o. e. assumption. The algorithm provides a good estimate of the channel even when the length of OFDM frames is small. From *fig. 4.15* and *fig. 4.16*, it can be seen that irrespective of channel PDP, MSE value of around 3.5×10^{-3} is achieved in 2×2 MIMO and 2×4 MIMO systems on an average even when the length of OFDM blocks is as low as *25*. Further, from *fig. 4.17*, MSE value of 7×10^{-3} (degradation in performance by a factor of *2* compared to MIMO systems with $M_t = 2$) is achieved when the length of OFDM blocks is *25*.
- Analogous to SISO-OFDM case, the performance of both the techniques improves as the length of the OFDM blocks used is increased. As mentioned earlier, the performance improvement is exponential (gradual) for precoding-based method and is step-like for subspace method. On the right side of the threshold, the performance shows an exponential behaviour.
- The performance of precoding-based technique is worse than that for subspace-based method when the length of OFDM blocks used exceeds the minimum threshold of p. o. e. assumption. When the length of OFDM blocks is *1000* (a value above the threshold), the difference in the MSE performances of the two approaches is around *15* dB on an average for 2×2 MIMO case (*fig. 4.15*), *10* dB for 2×4 MIMO case (*fig. 4.16*) and *8.3* dB for 4×4 MIMO case (*fig. 4.17*).
- Comparing the performance curves of *fig. 4.15 - fig. 4.17*, it can be seen that the precoding-based technique does not show significant change in its performance over the complete range of OFDM block-length. The performance of precoding-based method degrades by just *1* dB when M_t is increased from *2* to *4* on an average. But, increase in M_r does not alter the performance of precoding based method. In contrast

to this, when the length of OFDM blocks is lower than the threshold, the performance of subspace-based approach is almost constant for *2×2* MIMO case and is linear with a negative slope (converging faster) for *2×4* MIMO case. Towards the right of the threshold point, the subspace approach shows an improvement of around *1* dB in average asymptotic MSE performance (i.e., when length of blocks is *5000*) when M_r is increased from *2* to *4* keeping $M_t = 2$ (between *2×2* and *2×4* MIMO systems) and by around *8* dB when M_t is increased from *2* to *4* keeping M_r constant at *4* (between *2×4* and *4×4* MIMO systems).

- In continuation with the previous point, the convergence properties are not altered when M_t and M_r are varied for precoding-based method. In contrast to this, the convergence property of subspace method is significantly altered with varying M_t and M_r. As M_r is increased, slower convergence rate can be observed, but asymptotically, similar performance level is achieved (*1* dB difference in MSE performance as seen in the last point). As M_t is increased, owing to p. o. e. assumption, the threshold is increased and hence the convergence is affected.
- From *fig. 4.15* and *fig. 4.16*, the asymptotic performance of subspace approach is better than that of precoding-based method by around *18* dB for both *2×2* and *2×4* MIMO case. From *fig. 4.17* (*4×4* MIMO), performance difference is *12* dB.
- Comparing with SISO-OFDM systems (*fig. 4.9* and *fig. 4.10*), the precoding-based method performance has degraded by *5* dB for $M_t = 2$ (*2×2* or *2×4* MIMO) and by *7* dB for $M_t = 4$ (*4×4* MIMO). Whereas for subspace method, the asymptotic performance degradation of around *1* dB for *2×2* and *2×4* MIMO-OFDM case and degradation of around *9* dB when $M_t = M_r = 4$ can be observed compared to SISO-OFDM systems. The convergence, as mentioned earlier, becomes slower when compared to SISO-OFDM system owing to p. o. e. assumption.

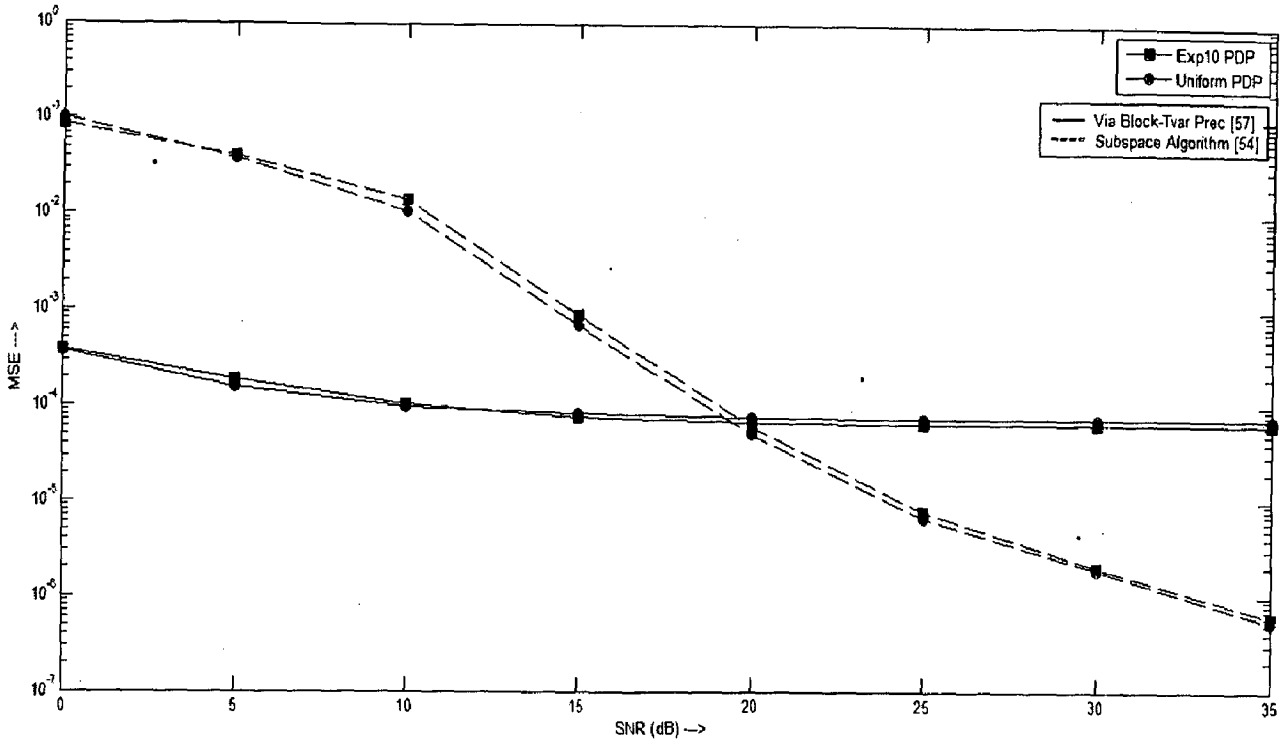

Figure 4.19: MSE versus SNR (dB) with length of OFDM blocks equal to 1000 for 2×2 MIMO-OFDM system for 16-QAM

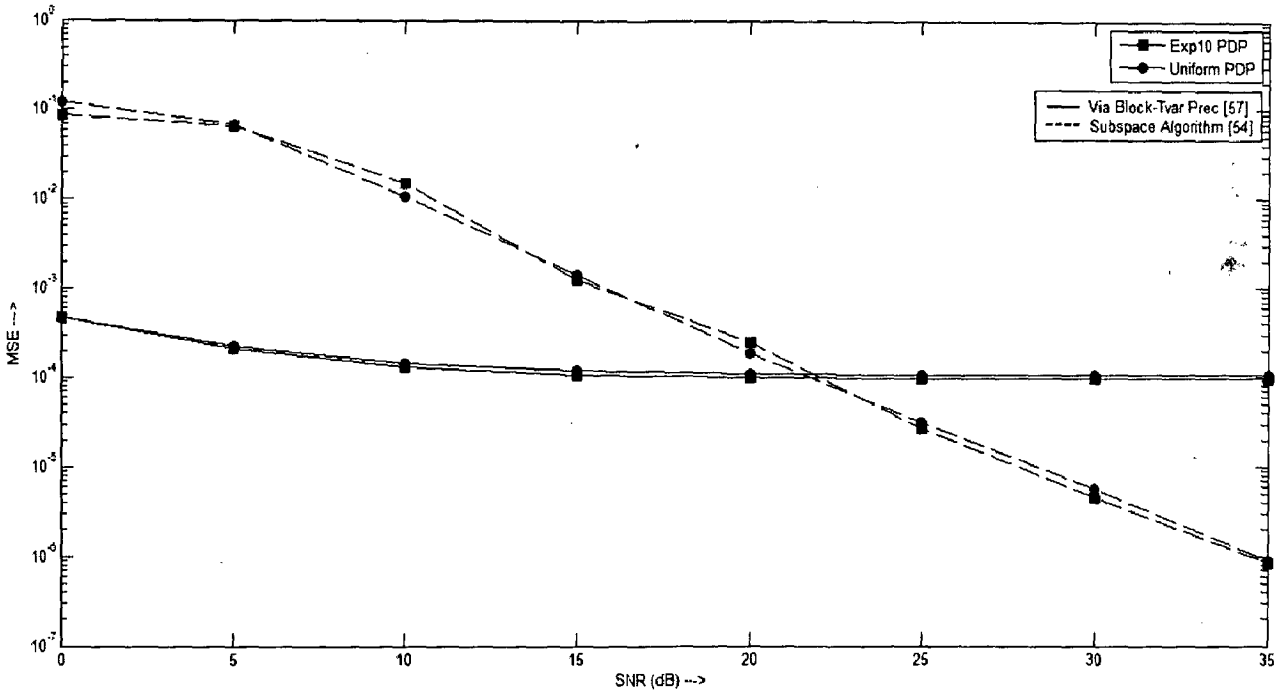

Figure 4.20: MSE versus SNR (dB) with length of OFDM blocks equal to 1000 for 2×4 MIMO-OFDM system for 16-QAM

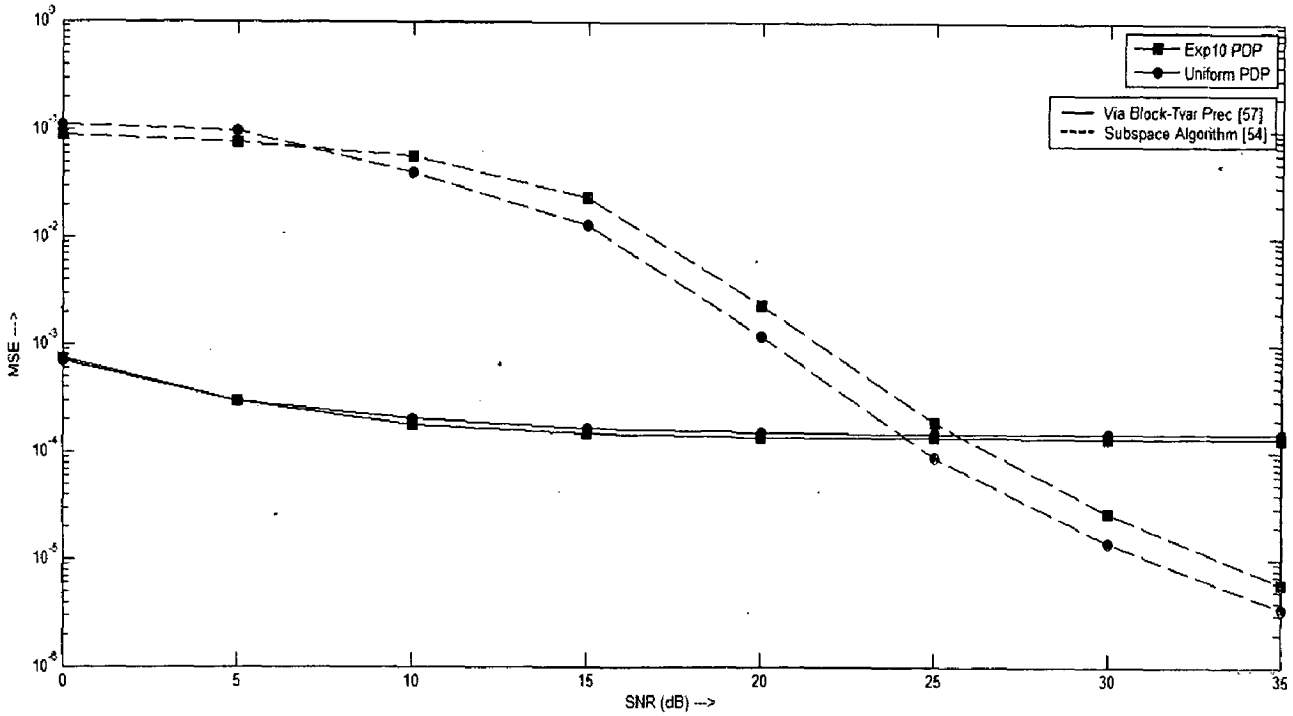

Figure 4.21: MSE versus SNR (dB) with length of OFDM blocks equal to 1000 for 4×4 MIMO-OFDM system for 16-QAM

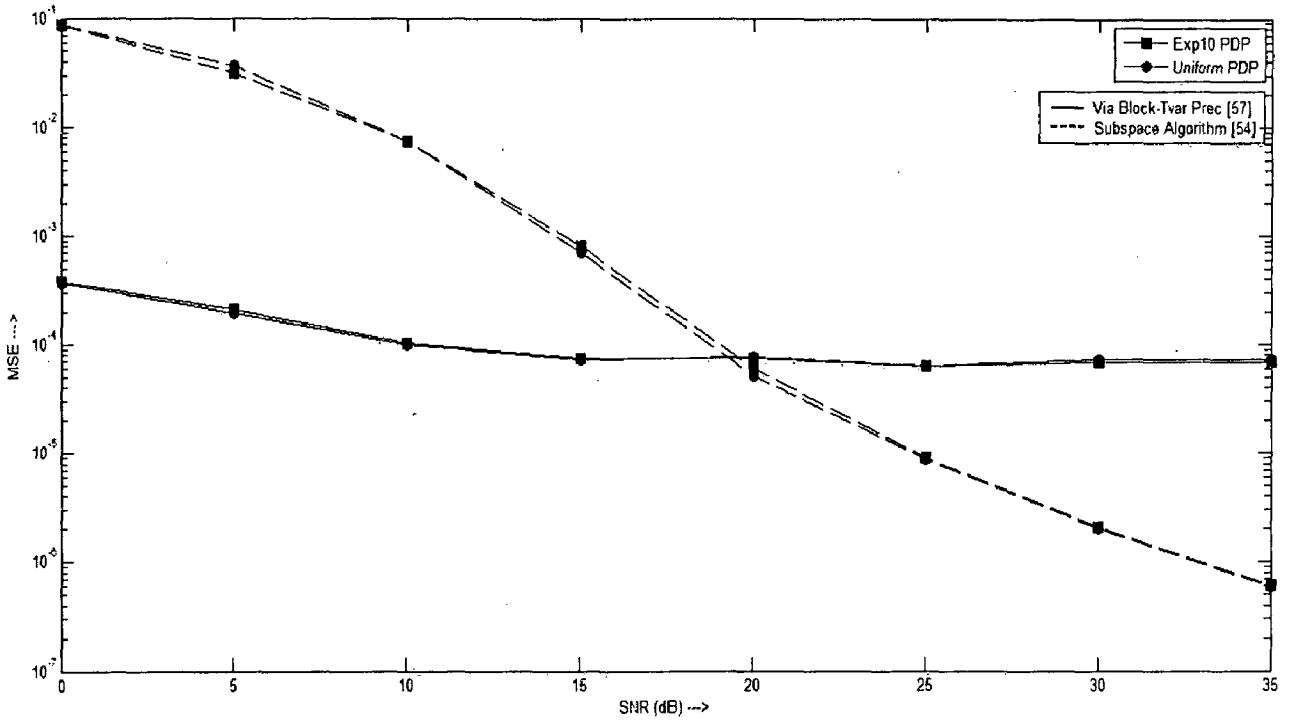

Figure 4.22: MSE versus SNR (dB) with length of OFDM blocks equal to 1000 for 2×1 MIMO-OFDM system for 16-QAM with an oversampling rate (q) of 2

Following observations can be made from *fig. 4.19 - fig. 4.22*:

- The performance is independent of the channel PDP under consideration.
- Analogous to SISO-OFDM case (*fig. 4.11* and *fig. 4.12*), precoding-based technique shows an exponential improvement in the performance with increasing SNR values. For *2×2* and *2×4* MIMO systems, the performance is similar to that in SISO-OFDM case. For *4×4* MIMO, the MSE performance degrades by around *4* dB over the complete range of SNR values on an average compared to SISO-OFDM and MIMO-OFDM with $M_t = 2$.
- Unlike SISO-OFDM case, the subspace method performance for *2×2* MIMO-OFDM system resembles a reflected tan-sigmoid function {A function of the form $f(x) = c + \tanh(-x)$, where c is a constant} with $c = 5\times10^{-4}$. Similar to SISO case, MSE value of around 10^{-1} can be observed when $M_t = 2$. As SNR value is increased the performance improvement is comparably slower than that in SISO-OFDM case. As a result, at *35* dB, the MSE value is *5* dB higher as compared to SISO case. For *2×4* MIMO-OFDM system, the performance curve is almost constant at lower SNR values (*0-5* dB) and thereafter shows linear characteristics. The MSE value of 10^{-6} is achieved at *35* dB SNR. Similarly, for *4×4* MIMO, the convergence is much slower. The MSE curve remains almost constant for SNR values ranging from *0-10* dB and thereafter linear characteristics can be seen. At *35* dB SNR, the MSE value is 4×10^{-6}.
- Over the range the SNR values, between *0* dB and *35* dB, the performance improvement for the case of precoding-based method is *6* dB, *3* dB and *5* dB for *2×2*, *2×4* and *4×4* MIMO-OFFDM systems respectively. In contrast to this, the subspace-based method shows an improvement of around *52* dB for *2×2* and *2×4* MIMO systems and an improvement of *45* dB for *4×4* MIMO system.
- For lower SNR values, the precoding-based technique performs better than the subspace-based method. At *0* dB, precoding technique achieves an MSE of *0.0004* (*fig. 4.19* and *fig. 4.20*) and *0.000847* (*fig. 4.21*) on an average whereas the subspace method achieves an MSE of around *0.1* on an average. At higher SNR values, the precoding method performance is comparably worse than that for the subspace technique. At *35* dB, on an average, precoding technique shows an MSE of 7.19×10^{-5} (*fig 4.19*), 1.0×10^{-4} (*fig. 4.20*) and 1.54×10^{-4} (*fig. 4.21*) whereas subspace approach achieves much better MSE of 5.87×10^{-7}, 9.492×10^{-7} and 4.672×10^{-6} respectively.
- As mentioned in SISO-OFDM case, the saturation observed in the performance of precoding-based technique is due to higher sensitivity of the estimate to time-averaging

distortion than distortion due to AWGN. Since the length of OFDM blocks used is *1000* and joint-correlation-averaging (all the columns of auto-covariance matrix) is used for channel estimation, the effect of AWGN is nullified.

- The 'cross-over' in the performance occurs at around *20* dB for *2×2* MIMO-, at *22* dB for *2×4* MIMO- and at *25* dB for *4×4* MIMO-OFDM system.

Note: As mentioned earlier, since $N > 1$, the precoding-based correlation-averaging algorithm is applicable for any number of transmit and receiving antenna. In contrast to this, for MIMO-OFDM systems with $M_t > M_r$, the full-rank criterion of the matrix (**A**) of *eqn. 2.39* is not satisfied for subspace-based method to be applicable. Hence, the redundancy introduced due to oversampling at the receiver is utilized along with that of CP for channel estimation (*Chapter 2*). For present discussion, the performance of a *2×1* MIMO-OFDM system with an oversampling factor (q) of *2* is considered.

Due to oversampling, the effective number of receiving antenna turns out to be *2*, which is equal to the number of transmitting antenna. Thus, there are four pairs of paths for signal propagation. Even though the physical mechanism employed is different, this leads to channel model structure similar to that of *2×2* MIMO-OFDM system. Since, for simulation purpose, the input is assumed to be stochastic, the statistical performance of the modified algorithm is similar as that for *2×2* MIMO-OFDM case as it can be observed by comparing *fig. 4.15* with *fig. 4.18* and *fig. 4.19* with *fig. 4.22*. Thus the discussion and conclusions made for *2×2* MIMO-OFDM systems is valid for *2×1* MIMO-OFDM system with an oversampling factor of *2* at the receiver.

Chapter 5

COMPLETELY BLIND CHANNEL ESTIMATION TECHNIQUES FOR OFDM

As mentioned in the previous chapters, the channel estimate obtained by utilizing only SOS of the channel output suffers from an ambiguity. This ambiguity is inherent to the problem. As far as SISO-OFDM systems are concerned, the channel estimate obtained by using subspace-based method (*Chapter 2*) suffers from a complex scalar ambiguity. The amplitude ambiguity can be resolved by precoding at the transmitter as mentioned in *Chapter 3*. Thus, the channel estimate obtained by precoding-based techniques suffers only from a constant phase ambiguity. The phase ambiguity can be resolved either by using pilots (*Chapter 4*) or by utilizing the information regarding the characteristics of the source in blind manner [37, 62-64]. The former approach of using pilot carriers has been widely researched on owing to its practical simplicity. But by using pilots, the charm of blind approaches is lost. A brief survey of different blind schemes to resolve the phase ambiguity for SISO-OFDM systems is presented in this chapter, followed by design and performance analysis of a completely blind channel estimation technique using constellation-splitting technique for PAM systems [65]. A generalization of the same for applicability over different modulation schemes by using hybrid time-frequency algorithm is also presented along with the performance analysis.

5.1. ON BLIND TECHNIQUES TO RESOLVE PHASE AMBIGUITY

A brief survey of blind techniques to resolve the phase ambiguity in SISO-OFDM systems is presented. The thumb rule is that, more the information about the source known at the receiver, better the estimation accuracy is. As per the author's knowledge, not much work has been done as far as completely/ totally blind approaches are concerned. A very few handful of references are available in the literature. As far as SISO-OFDM systems are concerned, some characteristics like channel coding [37], finite alphabet property of the source [62], utilizing asymmetric constellation [63], mixed-order modulation [64] and source statistics information are employed. In some methods, it is assumed that the source symbols are taken from a finite alphabet set [62]. For example, consider a system in which Mary-PSK modulation is used. This scheme has constant modules property, with the symbol phase

chosen from a finite known set. These source properties can be used to resolve the phase ambiguity. Some of known algorithms [62] are minimum-distance (MD), phase-directed (PD) and decision-directed (DD) approaches. MD aims to minimize the Euclidian distance measure and involves searching over all possible values of channel vectors; PD is an iterative process in which ambiguity is resolved by searching over phase values and DD consists of equalizing k^{th} subcarrier and projecting it on to a valid symbol from the set. This equalized symbol is then used to estimate the channel co-efficient. Since M-PSK modulation which has constant modulus property is used, this method is not applicable for any other mapping schemes like M-PAM and M-QAM. Some approaches wherein, in the source constellation, one or more symbol point is skewed so as to get an asymmetrical arrangement [63] have been proposed. The phase relationship information due to this variation is utilized for phase correction.

In [63], a posteriori probability (APP) estimator is used for first stage estimation. Further, this algorithm is applicable to any modulation schemes. The disadvantage is that, since asymmetry is induced in the source constellation, the dc level in an OFDM data frame is non-zero in statistical sense. This may cause significant dc power dissipation and hence not feasible for power-limited systems like handheld and mobile transceiver devices. As far as PSK is concerned, mixed-order modulation among alternate subcarriers can be employed as proposed by Necker [64]. This type of mapping induces a unique phase relationship among alternate subcarriers that can be employed in phase-correction.

For instance, a 3-PSK and 4-PSK can be combined and assigned among alternate subcarriers in a given OFDM frame. Since, the symbol phases are non-overlapping, phase correction is possible. But, Mary-PSK mapping with $M \neq 2^n$ ($n \in Z^+$) means non-binary coding. For example, 3-PSK can be generated by mapping a ternary symbol set $S = \{0, 1, 2\}$ on to three phase values. This means quantizer design has to be altered which leads to encoding/ decoding design issues. Further, the approach proposed in [64] is applicable for PSK mapping which has constant modulus property. Further, this approach uses ML-type estimator to obtain first approximation of the channel. ML estimator demands high implementation complexity and hence is not practically feasible.

5.2. SYSTEM MODEL

Consider the block diagram of the proposed baseband equivalent model of completely blind channel-estimator for SISO-OFDM systems shown in *fig. 5.1.*

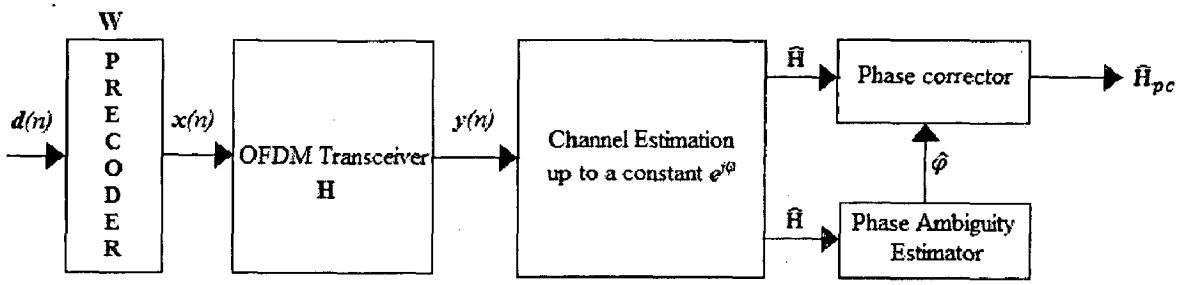

Figure 5.1: Baseband equivalent model of blind phase-correct channel-estimator for SISO-OFDM systems

As mentioned earlier, the precoder block multiplies the incoming frequency-domain OFDM frame: $\boldsymbol{d}(n) = [d(n, 0), \ldots, d(n, N-1)]^T$ by a precoding matrix **W** of dimension $N \times N$ to yield $\boldsymbol{x}(n)$. The function of OFDM transceiver block (see *fig. 3.2*) can be mathematically described by *eqn. 3.3* and *eqn. 3.4*. Combining the function of precoder and the OFDM transceiver, the frequency-domain channel model can hence be mathematically described as given by *eqn. 3.6.* The channel estimator block estimates the channel up to a constant phase-ambiguity factor using any of the standard methods of *Chapter 2* and/ or *Chapter 3*. The phase-ambiguity-estimator estimates the ambiguity using the side information provided by the source mapping techniques and thus the output of phase-corrector block is a phase-correct channel estimate in frequency-domain.

5.3. PHASE-AMBIGUITY CORRECTION FOR PAM SYSTEMS

The problems of dc-level, synchronization, non-uniform quantization/ coding and non-applicability to non-constant modulus mapping have been overcome by an algorithm proposed by Sameera Bharadwaja H. and D. K. Mehra [65] for SISO-OFDM systems with Mary-PAM mapping. The channel is estimated in frequency-domain up to a constant phase ambiguity factor by precoding-based technique (*Chapter 3*). The channel estimate obtained is thus of the form (*Chapter 3*):

$$\hat{\mathbf{H}} = \mathbf{H}e^{j\varphi} \tag{5.1}$$

where, **H** is the true frequency-domain channel vector and φ is the unknown phase ambiguity factor.

5.3.1. CONSTELLATION-SPLITTING

This technique provides the required side-information to the phase-ambiguity-estimator-corrector unit for blind phase-correct channel estimation [65]. Consider an OFDM frame *d(n)*, with each of the alternate subcarrier symbol chosen from an (M/2)-ary PAM constellation instead of M-ary constellation. For even numbered subcarriers, the constellation points are shifted to right by (*M/2*) such that the symbols have zero phases and for odd numbered subcarriers, they are shifted to left by (*M/2*) such that they have a phase of 180^0 each. This is analogous to splitting the M-ary constellation along the axis of symmetry into two subsets; assigning the right subset to even numbered subcarriers and the left subset to odd numbered subcarriers. This is known as 'Constellation-splitting' [65]. The concept is illustrated in *fig. 5.2* for 8-PAM system.

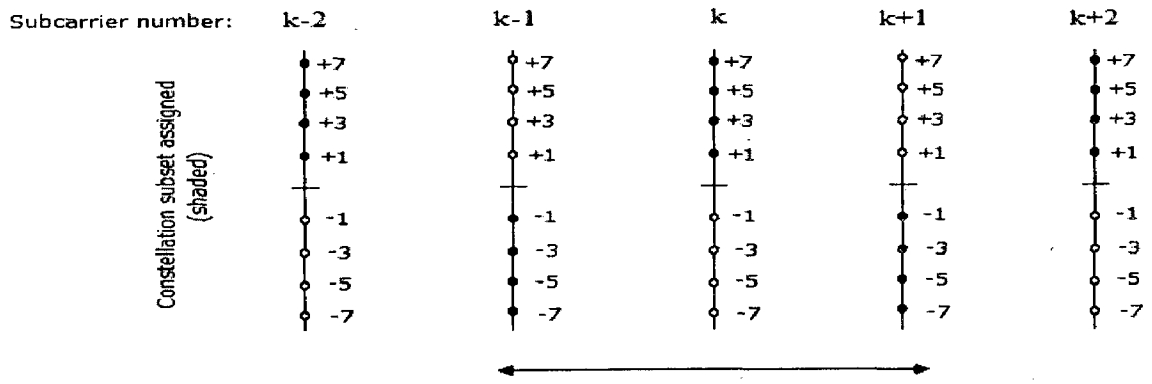

Figure 5.2: Illustration of constellation subset assignment scheme among alternate subcarriers in an OFDM frame for 8-PAM mapping

Single OFDM frame thus consists of symbols chosen from M-ary constellation and have zero dc in statistical sense. Also, a unique phase relationship is introduced among the alternate subcarriers. This information can be used at the receiver for phase-ambiguity estimation and correction.

5.3.2. PHASE-AMBIGUITY ESTIMATION AND CORRECTION ALGORITHM

Assuming that each subcarrier symbol of the frequency-domain OFDM frame $\boldsymbol{d(n)}$ is constructed as per the rules of constellation-splitting technique, we can write:

$$\boldsymbol{d}(n) = [|d(n,0)|e^{j0} \quad |d(n,1)|e^{j\pi} \quad \cdots \quad |d(n,N-1)|e^{j\pi}]^T \tag{5.2}$$

where,

$$d(n,k) \in \begin{cases} Right\ signal\ subset, & k\ even \\ Left\ signal\ subset, & k\ odd \end{cases} \qquad for\ 0 \leq k \leq N-1$$

The precoder matrix W is chosen such that the phase relationship among the subcarriers is retained. Thus,

$$\boldsymbol{s}(n) = \boldsymbol{W}\boldsymbol{d}(n) = [|s(n,0)|e^{j\theta} \quad \cdots \quad |s(n,N-1)|e^{j(\theta+\pi)}]^T \tag{5.3}$$

Assuming sufficient CP and noiseless situation, from *eqn. 3.6*, the received signal vector can be written as:

$$\boldsymbol{y}(n) = \begin{bmatrix} |s(n,0)||H_0|e^{j(\theta+\theta_1)} \\ \vdots \\ |s(n,N-1)||H_{N-1}|e^{j(\theta+\pi+\theta_{N-1})} \end{bmatrix} \tag{5.4}$$

where, **H** is the frequency-domain channel vector (*eqn. 3.2*):

$$\mathbf{H} = [|H_0|e^{j\theta_1} \quad \cdots \quad |H_{N-1}|e^{j\theta_{N-1}}]^T$$

The first-order estimate of **H** given by *eqn. 5.1* can be expanded as,

$$\hat{\mathbf{H}} = \left[|\hat{H}_0|e^{j(\hat{\theta}_1+\varphi)} \quad \cdots \quad |\hat{H}_{N-1}|e^{j(\hat{\theta}_{(N-1)}+\varphi)}\right]^T \tag{5.5}$$

where, $|\hat{H}_k|$ is the estimate of $|H_k|$; $\hat{\theta}_k$ is the estimate of θ_k and φ is the phase ambiguity. From *eqn. 5.4* and *eqn. 5.5*, it is clear that the phase ambiguity per subcarrier can be obtained as (with $\theta = 0$),

$$\hat{\varphi}_k = Angle\{\hat{\mathbf{H}}\} - Angle\{\boldsymbol{y}(k)\} + \boldsymbol{B} \quad for\ k = 0 \rightarrow N-1 \tag{5.6}$$

where, $\boldsymbol{B} = [0,\ 180^0,\ 0,\ \ldots,\ 180^0]^T$ is the bias vector. The bias vector represents the possible phase values the source symbols can take for a given subcarrier. For present discussion, owing to constellation splitting, the source values are fixed at 0^0 for even subcarriers and at 180^0 for odd subcarriers. For noisy-channel, the value of $\hat{\varphi}_k$ is averaged over sufficient number of OFDM frames and over the subcarriers to combat the ill-effects of AWGN. The final estimate of ambiguity term: $\hat{\varphi}$ is given by,

$$\hat{\varphi} = Mean\{E[\hat{\varphi}_k]\} \tag{5.7}$$

Using the result of *eqn. 5.7* in *eqn. 5.5*, the phase error in $\hat{\mathbf{H}}$ can be corrected to obtain the phase-correct channel estimate, $\hat{\mathbf{H}}_{pc}$ as:

$$Angle\{\hat{\mathbf{H}}_{pc}(k)\} = Angle\{\hat{\mathbf{H}}(k)\} - \hat{\varphi} \quad for\ k = 0 \rightarrow N-1 \tag{5.8}$$

Since no pilots/ reference symbols are used, this method is completely blind. The disadvantage is that, since (M/2)-ary constellation points are allotted per subcarrier instead of

M-ary constellation points, the communication link suffers from a rate loss of one bit/subcarrier-symbol. This can be made insignificant for all practical purposes if the constellation size chosen is sufficiently large.

5.3.3. PERFORMANCE ANAYLSIS OF COMPLETELY BLIND ESTIMATOR FOR PAM

A. Simulation Parameters

- Complex discrete baseband equivalent FIR channel is assumed to be of length (L) = *2*.
- Each channel coefficient is a zero-mean Gaussian random variable with variances given according to either of the two channel PDP (*Chapter 4*).
- Number of sub-carriers/ OFDM frame (N) = *64*
- Number of OFDM frames collected for estimation purpose = *1000*
- SNR (unless otherwise mentioned) = *30* dB.
- The 'phase-retaining' precoder matrix W used is given by:

$$W = \begin{bmatrix} 1 & -p & p & \cdots & -p \\ -p & 1 & -p & \cdots & p \\ \vdots & \vdots & \vdots & \ddots & \vdots \\ -p & p & -p & \cdots & 1 \end{bmatrix}_{N \times N}$$

  where, $0 < p < 1$. The results are shown for $p = 0.5$.
- The results are averaged over 500 Monte-Carlo simulation runs.

The frequency-domain OFDM frame $d(n)$ of size $N \times 1$ is constructed according to the rules of constellation-spitting technique for a given value of M (Mary-PAM). The channel estimate up to a constant phase ambiguity is obtained using the procedure illustrated by the flowchart of *fig. 4.1*. The phase ambiguity is estimated and corrected by utilizing the side-information provided by source mapping using *eqn. 5.6 – eqn. 5.8*. For present discussion, the simulation results are shown for 4- and 8-PAM. The timing and frequency synchronization are assumed.

B. Simulation results and conclusion

The MSE performance of the completely blind technique versus the length of OFDM blocks used at *30* dB SNR with exponential and uniform channel PDP is shown in *fig. 5.3*. Similarly, the MSE performance of the same versus SNR (dB) values assuming that the length of OFDM blocks used is *1000* for both the channel PDP is shown in *fig. 5.4*.

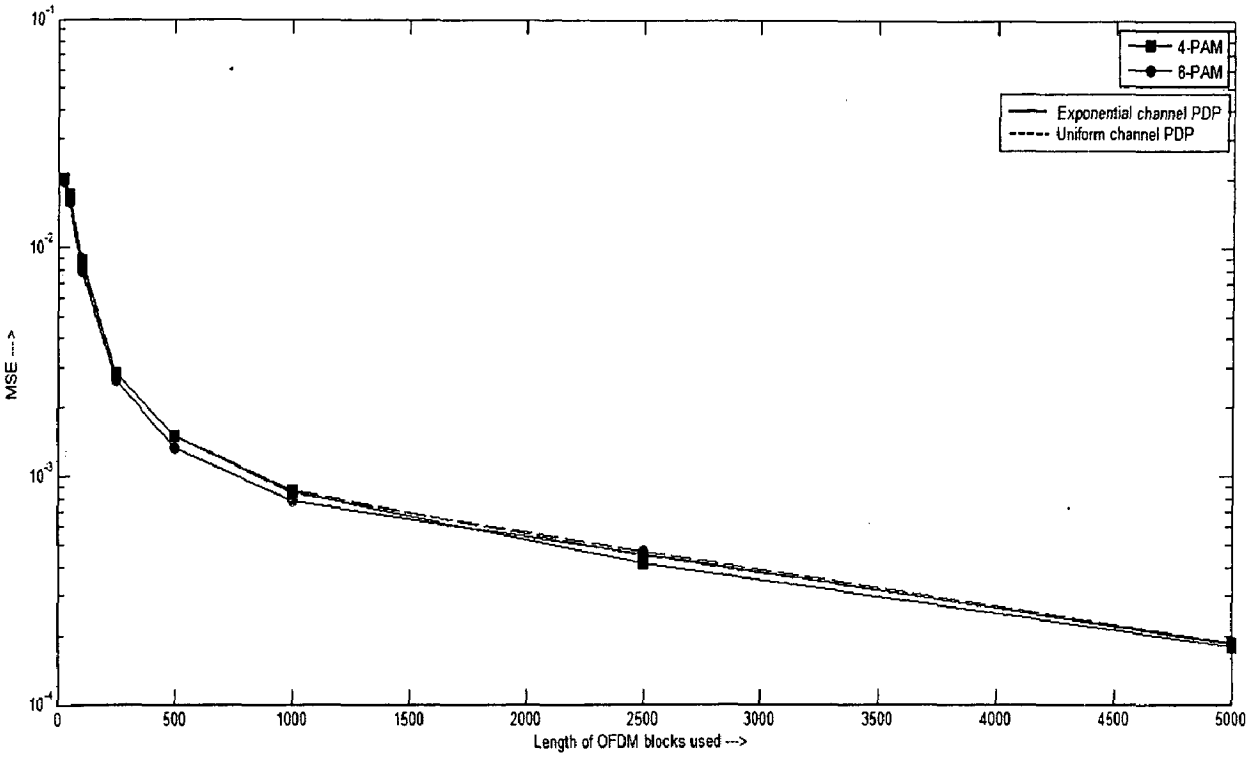

Figure 5.3: MSE versus length of OFDM blocks at 30 dB SNR of completely blind estimator for SISO-OFDM system for PAM mapping

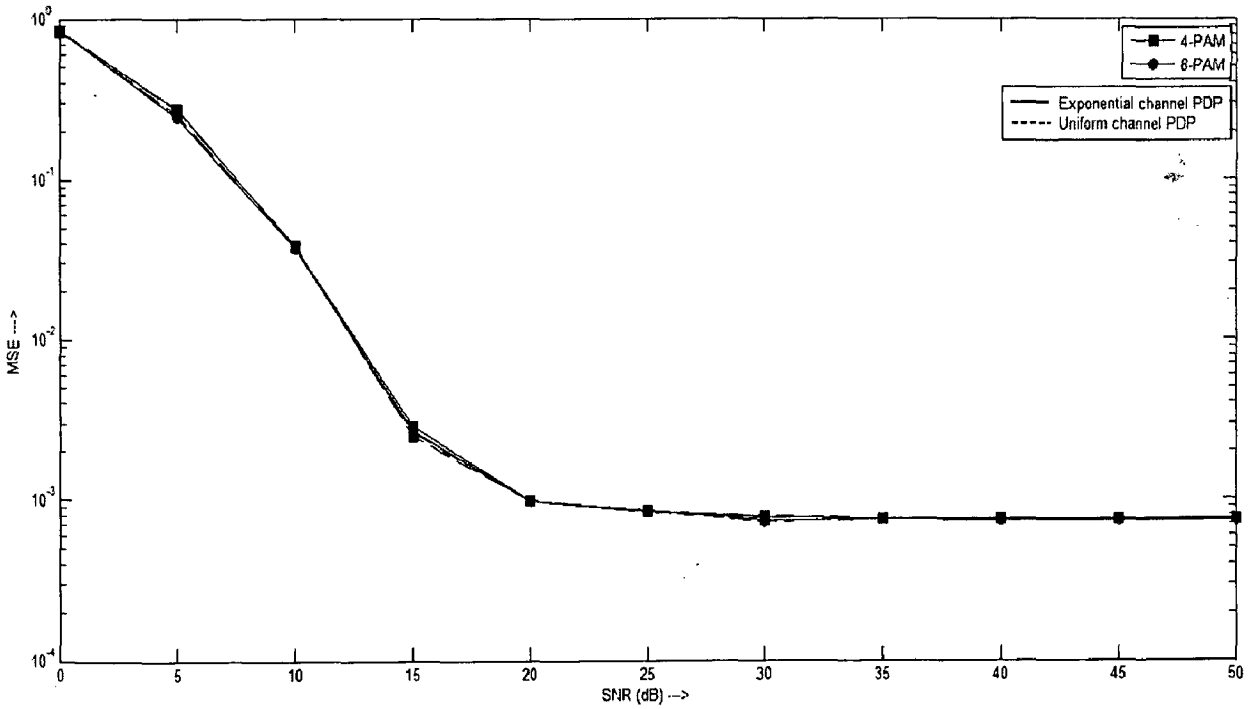

Figure 5.4: MSE versus SNR (dB) with length of OFDM blocks equal to 1000 of completely blind estimator for SISO-OFDM system for PAM mapping

The following observations can be made from *fig. 5.3* and *fig. 5.4*:

- The performance is independent of the modulation scheme and the channel PDP used.
- From *fig. 5.3,* it can be observed that the MSE performance improves exponentially as the length of OFDM blocks is increased. The value of MSE is around 2×10^{-2} when the length of OFDM blocks is *25* and around 1.8×10^{-4} when the length is *5000* blocks (an improvement of around *20* dB).
- From *fig. 5.4,* it can be observed that the MSE performance decreases from *0.94* at *0* dB to around 8.8×10^{-4} at *20* dB in nearly linear manner. When the SNR is increased beyond *20* dB, no further improvement in performance can be observed.
- Compared to its semi-blind counterpart, the performance of the completely blind estimator is worst by at least *10* dB. For example, comparing *fig. 4.9* and *fig. 4.10* with *fig. 5.3*, the performance of completely blind estimator is worst by around *11* dB when the length of OFDM blocks is 25 and around *14* dB when the length of the OFDM blocks is *5000*. Similarly, comparing, *fig. 4.11* and *fig. 4.12* with *fig. 5.4,* the performance is worst by *38* dB at *0* dB SNR and by around *14* dB at *50* dB SNR.

5.4. GENERALIZED PHASE-AMBIGUITY CORRECTION ALGORITHM

A generalization of constellation-splitting based method applicable for Mary-PAM, Mary-QAM and Mary-PSK mapping schemes is described followed by a generalized phase-estimator-corrector algorithm based on time-frequency hybrid estimation technique.

5.4.1. GENERALIZED CONSTELLATION-SPLITTING TECHNIQUE

The constellation splitting scheme for Mary-QAM is described. This can be used without much alteration for Mary-PAM (one-dimensional version of QAM) and also for Mary-PSK (degenerative case of QAM). The constellation-splitting can be done in any of the three ways:

a) The constellation is split into two halves, along x-axis (horizontal/ in-phase axis).
b) The constellation is split into two halves, along y-axis (vertical/ quadrature-phase axis).
c) The constellation is split into four halves, along both x-axis and y-axis.

Note: Types a) and c) are not applicable for Mary-PAM mapping.

We consider 16-QAM and illustrate the third case. The other two are straightforward simplified versions of this scenario. The concept of constellation-splitting and signal point assignment to subcarriers of OFDM frame for 16-QAM mapping is shown in *fig. 5.5*. Each

group of four subcarriers has any of the 3 unique phase points associated with them. It is reasonable to assume that the blind algorithm at the receiver has the knowledge of these phase values.

Assignment table

Quadrant number	Assigned to subcarriers $k \rightarrow 0-N-1$ if
1	k mod $4 = 0$
2	$(k-1)$ mod $4 = 0$
3	$(k-2)$ mod $4 = 0$
4	$(k-3)$ mod $4 = 0$

Constellation diagram: 16-QAM

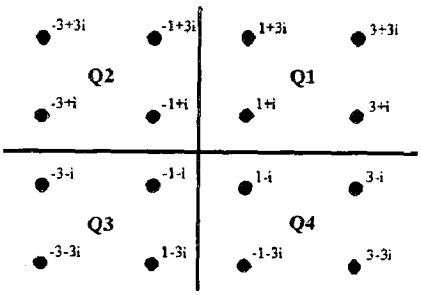

Figure 5.5: Illustration of constellation-splitting concept (Type c) for 16-QAM mapping

5.4.2. PHASE-AMBIGUITY ESTIMATION AND CORRECTION ALGORITHM

We propose a generalized phase-estimator-corrector algorithm is this section. The n^{th} OFDM frame to be transmitted: $d(n)$ is constructed according to the rules of generalized constellation-splitting technique described above. The QAM signal points even though are from a finite alphabet set for a given quadrant, can be random within that quadrant (For example, four possible values of signal points exists per quadrant for 16-QAM). Hence, designing the precoder with phase-retaining property is not feasible. Thus, the phase estimates obtained via precoding-based technique (*Chapter 3*) cannot be used as an input for phase-ambiguity-estimator block.

Assuming that the channel response remains more or less static for T_0 time units (spanning over M OFDM frames), during the first T_1 ($T_1 < T_0$) units of time (spanning over M_1 OFDM frames) the transmitted OFDM frames are not precoded. During this time, the precoding matrix W is assumed to be an identity matrix of size $N \times N$. The first approximation of the channel phase in time-domain is obtained at the receiver during this time by subspace method in time-domain using the redundancy induced by CP at the transmitter (*Chapter 2*). By taking N-point DFT of this estimate, the frequency-domain phase estimate of the channel which is used as an input for phase-correction algorithm can be obtained. The time duration T_1 is chosen such that subspace decomposition is feasible (see p. o. e. assumption, *Chapter 2*). The channel amplitude estimates obtained using the subspace method is useless since they

suffer from an ambiguity. During last T_0-T_1 units, the OFDM frames are precoded using the precoding matrix given by *eqn. 4.1* with $p = 0.5$. The precoding-based algorithm (*Chapter 3*) is used to obtain channel's magnitude estimate in frequency-domain by tracing over different starting points (q) in *eqn. 3.13* to *eqn. 3.15*. The amplitude and phase estimates thus obtained are combined to obtain the channel estimate which is of the form given by *eqn. 5.5*. Thus, a hybrid time-frequency algorithm is used to obtain the first estimate of the channel.

The phase-ambiguity estimate cannot be obtained directly by using *eqn. 5.6* since the source-phase values are random from a given known set and hence the bias vector $\boldsymbol{B}$ is not fixed, unlike for the Mary-PAM case. Finding the bias vector involves a search over different phase values from the given valid-phase-value set. It can be concluded that, since the ambiguity term is theoretically same for all the subcarriers (zero variance), for a given test vector, the ambiguity-estimate vector: $\hat{\boldsymbol{\varphi}} = [\hat{\varphi}_0 \quad \cdots \quad \hat{\varphi}_{N-1}]^T$ has the least variance over the subcarriers if the phase values of test vector are same as that of the original source vector. This criterion is used as the search parameter. Further, since the ambiguity term is a constant over all the subcarriers; a subset of OFDM frame can be used for testing purpose. This reduces the number of test vector combinations that must be traced. For the present discussion, it is assumed that the test vector combinations are traced over first *4* subcarriers ($N_{trc} = 4$). For 16-QAM, the set of first-quadrant-phase-values is given by: $\boldsymbol{\varphi}_I = [18.4349^0 \; 45^0 \; 71.5651^0]$. Since the constellation is symmetric, the phase-value set for II, III and IV quadrant can be thus written as: $\boldsymbol{\varphi}_{II} = \boldsymbol{\varphi}_I + \pi/2$; $\boldsymbol{\varphi}_{III} = \boldsymbol{\varphi}_I + \pi$ and $\boldsymbol{\varphi}_{IV} = \boldsymbol{\varphi}_I + 3\pi/2$ respectively.

As mentioned earlier, for noisy-channel, the value of $\hat{\varphi}_k$ should be averaged over sufficient number of OFDM frames and over the subcarriers to combat the ill-effects of AWGN. For present discussion, the average is done over M_I OFDM frames. Assuming that all the angles are in radians, the pseudo-code to obtain the phase-ambiguity estimate is given on *Page 91*. The proposed procedure is known as modified phase-directed (MPD) algorithm. This algorithm is similar to PD, but owing to constellation splitting which reduces the number of phase-values over which the search is to be performed and since phase-ambiguity is constant over all the subcarriers which facilitates the search over partial frame, MPD is computationally efficient compared to PD approach. The disadvantage is that, as mentioned earlier, splitting the constellation into two halves leads to a rate loss of one bit/subcarrier-symbol. Similarly, splitting the constellation into four halves leads to rate a loss of two bits/ subcarrier-symbol. This can be made insignificant for all practical purposes if large constellation size is used.

```
AmbiguityEstimate = [0 0 ... 0]^T                    % Initialization (Dim: M_I×1)
for Iter = 1 → M_I                                   % Bold-case denotes vectors
  Check = 1;
  for S_1 = 1 → length(φ_I)                          % Search over all source vectors
    for S_2 = 1 → length(φ_II)
      for S_3 = 1 → length(φ_III)
        for S_4 = 1 → length(φ_IV)
          BiasVector = [φ_I(S_1) φ_II(S_2) φ_II(S_3) φ_II(S_4)]^T
% Estimate of ambiguity-vector to be analysed for least-variance
          for k = 1 → 4
            ToAnalyse(k) = Ĥ(k)-y(k)+ BiasVector(k)
          end
% Choose that source-phase vector as BiasVector which yields the lowest-variance-
% Ambiguity-Estimate vector
          if (Check == 1)
            AmbiguityEstimate (Iter) = mean (ToAnalyse)
            DecisionParameter = variance (ToAnalyse)
            Check = 0
          else
            if ((variance(ToAnalyse)) < DecisionParameter)
              AmbiguityEstimate (Iter) = mean (ToAnalyse)
              DecisionParameter = variance (ToAnalyse)
            end
          end
        end
      end
    end
  end
end
AmbiguityEstimate = mean (AmbiguityEstimate)      % Average over M_I OFDM frames
```

Note: For a symmetric signal constellation, the error in the decision occurs when two or more source-phase vectors theoretically (noiseless case) yields zero-variance-ambiguity-vector estimate, or analogously in noisy channel case, the decision on the correct source-phase vector cannot be made with enough confidence. This condition occurs if and only if $Angle(\hat{s}_1(n)) = Angle(\hat{s}_2(n)) + K$, where $\hat{s}_1(n)$ and $\hat{s}_2(n)$ are two possible estimates of the source-phase vectors that yield zero-variance-ambiguity-vector estimate and K is a constant angular-shift. The probability of occurrence of this situation is very low in practice. Further, this problem can be overcome if the average is taken over number of OFDM frames.

5.4.3. PERFORMANCE ANAYLSIS OF COMPLETELY BLIND ESTIMATOR FOR 16-QAM

A. Simulation Parameters

- Complex discrete baseband equivalent FIR channel is assumed to be of length (L) = *2*.
- Each channel coefficient is a zero-mean Gaussian random variable with variances given according to either of the two channel PDP (*Chapter 4*).
- Baseband modulation: 16-QAM
- Number of sub-carriers/ OFDM frame (N) = *64*
- Total length of OFDM frames used unless otherwise mentioned (M)= *1000*
- The length of OFDM frames assumed to be received during time duration T_I (M_I) = $2 \times N$
- SNR (unless otherwise mentioned) = *30* dB.
- The precoder matrix W of *eqn. 4.1* is used with the value $p = 0.5$.
- The results are averaged over 250 Monte-Carlo simulation runs.

The frequency-domain OFDM frame $d(n)$ of size $N \times 1$ is constructed according to the rules of generalized constellation-spitting technique for 16-QAM. The channel magnitude estimate, as mentioned earlier, is obtained via precoding-based method using the procedure given in the flowchart of *fig. 4.1* and *eqn. 3.13* to *eqn. 3.15* by tracing over all the values of $q = \{1, \ldots, N\}$ and the channel phase estimate is obtained by using subspace-based method as given by the procedure shown in flowchart of *fig. 4.8*. The phase ambiguity is estimated and corrected by utilizing the side-information provided by source mapping using the generalized MPD algorithm as given by the pseudo-code (*Page 93*).

B. Simulation results and conclusion

The MSE performance of the generalized completely blind technique versus the length of OFDM blocks used at *30* dB SNR with exponential and uniform channel PDP for 16-QAM mapping is shown in *fig. 5.6*. Similarly, the MSE performance of the same versus SNR (dB) values assuming that the length of OFDM blocks used is *1000* for both the channel PDP with 16-QAM mapping is shown in *fig. 5.7*.

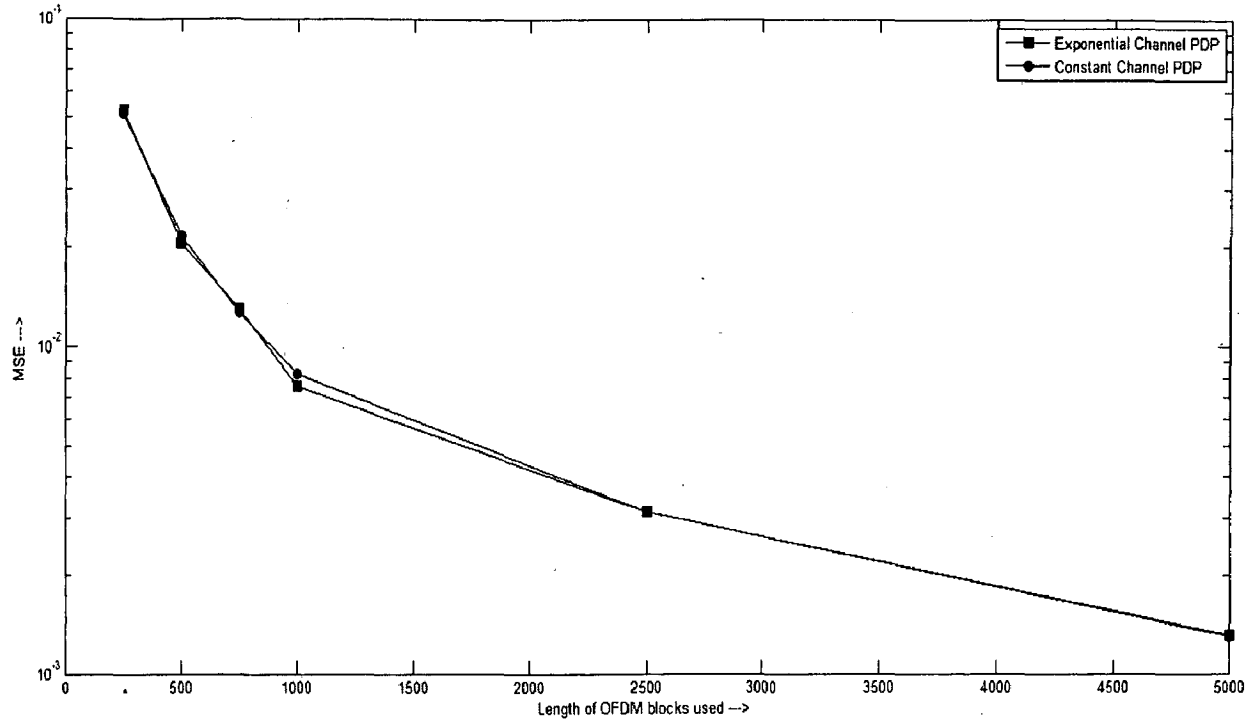

Figure 5.6: MSE versus length of OFDM blocks at 30 dB SNR of generalized completely blind estimator for SISO-OFDM system for 16-QAM

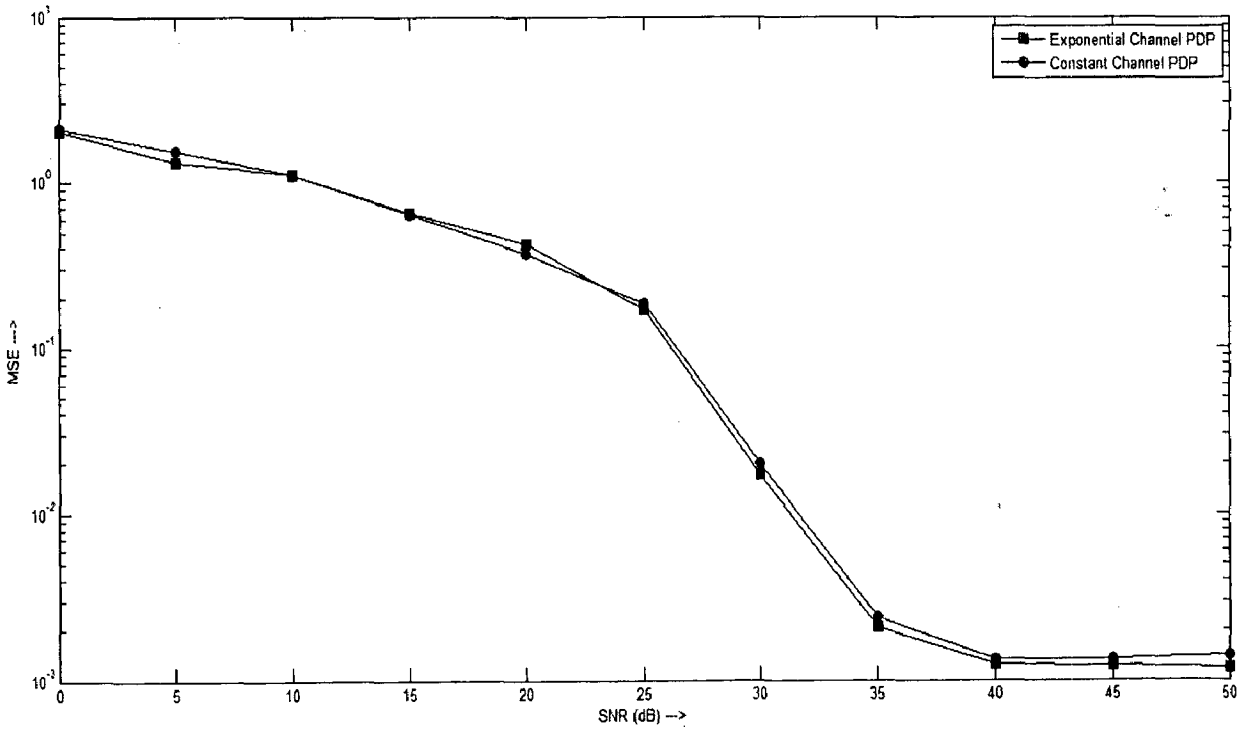

Figure 5.7: MSE versus SNR (dB) with length of OFDM blocks equal to 1000 of generalized completely blind estimator for SISO-OFDM system for 16-QAM

The following observations can be made from *fig. 5.6* and *fig. 5.7*:

- The performance is independent of the channel PDP used.
- Since hybrid algorithm is used to obtain the first approximation of the channel, as per p. o. e. assumption, the minimum number length of OFDM blocks required to obtain reliable phase-estimate using subspace method is *128*. This restricts the practical applicability of the estimator for fast-varying channels.
- From *fig. 5.6*, it can be observed that the MSE performance improves exponentially as the length of OFDM blocks is increased. The value of MSE is around 5.3×10^{-2} when the length of OFDM blocks is *250* and around 1.2×10^{-3} when the length is *5000* blocks (an improvement of just *16* dB for *20* times increase in the length of OFDM blocks used).
- From *fig. 5.7*, it can be observed that the MSE performance decreases from *2.053* at *0* dB to around *0.172* at *25* dB in nearly linear manner. Similarly, a linear improvement with a slightly higher falling rate can be observed between *25* dB and *35* dB SNR values. When the SNR is increased beyond *40* dB, no further improvement in performance can be observed. At *50* dB SNR, the MSE value is around 1.3×10^{-3} on an average.
- The performance of completely blind hybrid estimator is worst than either of the two of its semi-blind counterparts: the precoding-based method and the subspace-based method. Comparing *fig. 4.9* and *fig. 4.10* with *fig. 5.6*, the performance difference between precoding-based method and the hybrid method is around *27* dB and the difference between subspace-based method and the hybrid method is around *39* dB when the length of OFDM blocks is *250*. Similarly, when the length of the OFDM blocks is *5000*, the differences are *24* dB and *55* dB.
- Similarly, comparing *fig. 4.11* and *fig. 4.12* with *fig. 5.7*, the performance difference, at *0* dB SNR, between precoding-based method and the hybrid method is around *40* dB and the difference between subspace-based method and the hybrid method is around *12* dB. The performance of the estimator is very poor at lower and middle-order values of SNR compared to its two semi-blind counterparts. At *35* dB SNR, the differences in MSE performances are respectively, *6* dB and around *40* dB compared to two semi-blind methods.

CONCLUSION

Among the various blind channel estimation techniques, moment-based techniques have been researched owing to their wide range of applicability including burst-type/ asynchronous communication links. In particular, SOS-based techniques are preferred owing to their structural simplicity and faster convergence compared to HOS-based methods. These techniques rely on the channel structure for estimation purpose.

In this work, we describe TXK algorithm which essentially exploits the SOCS of the received signal to identify the FIR channels using SIMO model. A Subspace decomposition technique in single-carrier systems for which TXK algorithm forms a basis is described. This algorithm is based on the SIMO channel structure and the orthogonality property of the signal and the noise subspaces which makes it structurally simpler and fast converging. Owing to SIMO structure of the channel, a linear parameterization of the noise subspace in terms of the channel parameters is possible. This yields a cost function that can be minimized to obtain the channel estimate. Further, the performance analysis of subspace-based method for three-tap exponential PDP channel is presented using MATLAB simulations. From the simulation results, it can be concluded that reasonable MSE performance (of order of 10^{-3}) is achieved at *30* dB SNR when the length of data samples exceeds *250* and for SNR > *15* dB when the length of data samples is *1000*.

Recently, OFDM and MIMO-OFDM have been adopted in most of the wireless standards owing to higher-data rates that can be achieved with reasonably good QoS. The classical approaches have been extended and generalized so as to be compatible with the technological advances. In literature, subspace-based techniques have been proposed owing to their structural simplicity. As far as OFDM systems are concerned, subspace-based techniques rely on the redundancy introduced either due to cyclic prefix, virtual carriers or oversampling (at the receiver). The latter two techniques can function even in the in-sufficient CP situation. For the present discussion, the CP-induced-redundancy-based technique is considered.

A generalized subspace-based technique applicable for any number of subcarriers and channel length for SISO-OFDM is presented in *Chapter 2*. This algorithm can estimate the channel in time-domain up to a complex constant scalar estimation ambiguity. The simulation results are shown in *Chapter 4*. The improvement in MSE performance resembles a falling-step as length of OFDM blocks is increased at a given SNR. This is due to p. o. e.

assumption. Similarly, improvement in MSE performance is linear with varying SNR (dB) values. The generalization of the subspace-based method for MIMO-OFDM systems is presented in *Chapter 2*. The channel is estimated in time-domain up to a complex constant matrix ambiguity. For the MIMO-OFDM systems with number of transmitting antennas greater than the number of receiving antennas, CP along with oversampling (at the receiver) is utilized to aid in channel estimation. The simulation results are shown in *Chapter 4*. Analogous to SISO-OFDM systems, the improvement in MSE performance resembles a falling-step as length of OFDM blocks is increased. As the size of MIMO is increased, the convergence rate of subspace technique becomes slower. The improvement in MSE performance is linear with varying SNR (dB) values at higher SNR values (SNR > *15* dB). For lower SNR values, the performance is exponentially decaying for *2×2* MIMO and approaches a constant level as size of MIMO is increased (e.g. *4×4* MIMO). An MSE value of the order of 10^{-3} is achieved when the length of OFDM blocks is more than that demanded by p. o. e. assumption or when SNR > *15* dB.

The amplitude ambiguity can be resolved by using a transmitter-end technique known as precoding as mentioned in *Chapter 3*. Precoding induces certain correlation among the subcarriers in a given OFDM frame which can be utilized at the receiver for channel estimation in frequency-domain by simple correlation-averaging. This fact makes the technique computationally simpler than Eigen-value based subspace methods. For the present discussion, two linear non-redundant frequency-domain precoding based methods for SISO-OFDM systems have been presented.

A simple-precoding based approach in which the correlation is induced on a single-subcarrier is presented in *Chapter 3* along with performance analysis using MATLAB simulations. This approach estimates the channel in frequency-domain up to a constant complex ambiguity. From the simulation results, an exponential improvement in MSE performance can be seen when the length of OFDM blocks is increased. Similarly, improvement in MSE performance is exponential as SNR is increased. MSE converges to a lower limit of around 10^{-3} and no further improvement can be observed as SNR is increased beyond *20* dB. A generalized algorithm which uses joint (row-column) correlation-averaging algorithm and hence is more robust to presence of channel nulls and noise can be used as described in *Chapter 3* for channel estimation up to a constant phase-ambiguity in frequency-domain. The simulation results are shown in *Chapter 4*. The performance similar in nature to that of simple-precoding based method can be observed. The performance is better at lower

SNR values than that of simple-precoding based technique. A comparison of the statistical CRB and MSE variance of blind precoding-based estimator is presented in *Chapter 4* for various channel PDP and precoding-constant values. It can be concluded that the MSE performance of the estimator is at least 100 times worst than the CRB. Further, as the precoding constant is increase from *0* to *1*, the estimator performance improves.

The generalization of generalized precoding based technique has been described for MIMO-OFDM systems in *Chapter 3*. Unlike subspace-based technique, this algorithm is applicable to MIMO systems with any number of transmitting and receiving antennas without any modifications. Further, a block-time-variant precoder is used which makes the channel estimation possible up to a complex constant scalar ambiguity per transmitting antenna as against matrix ambiguity. The simulation results are shown in *Chapter 4*. The performance characteristics similar to that of SISO-OFDM case can be observed. The convergence rate is not affected by the size of the MIMO system.

The performance comparison of subspace- and precoding-based channel estimation techniques for SISO- and MIMO-OFDM systems have been presented in *Chapter 4* using MATLAB simulations. The MSE variations over varying length of OFDM frames and varying SNR (dB) values are also presented. From the results, it can be concluded that, at lower lengths of OFDM blocks and lower SNR values, precoding-based approach performs better than the subspace based technique. This makes the former a suitable candidate for low power and high-mobility applications. Further, at higher SNRs and lengths of OFDM blocks, the performance of subspace technique surpasses that of the precoding-based technique. The performance improvement observed in precoding-based technique is very low compared to subspace-based technique as the length of OFDM frames and SNR values are increased.

The blind techniques, as mentioned earlier, suffer from an estimation ambiguity. Using precoding, the amplitude ambiguity has been resolved. In practice, the phase-ambiguity has been resolved by employing pilot carriers. We have proposed a completely blind channel estimation technique for SISO-OFDM with PAM mapping using constellation splitting in *Chapter 5*. This algorithm has an advantage over its predecessors: the OFDM frame has zero-dc, the algorithm is structurally simpler and computationally efficient with an efficient encoding/ decoding logic. The performance analysis over different PAM constellation sizes and channel PDP are presented using MATLAB simulations. Further, a generalization of constellation splitting technique applicable for any modulation schemes and a modified phase

directed technique for phase-ambiguity estimation and correction is proposed in *Chapter 5*. The performance analysis using MATLAB simulations have been presented for 16-QAM mapping over different channel PDP. It can be seen from the simulation results that the completely blind techniques perform slightly worse than their semi-blind blind counterparts but yet can estimate the channel within acceptable MSE tolerance for all practical purposes.

SCOPE FOR FUTURE WORKS:

From the previous discussions, it can be concluded that the precoding-based approach for blind channel estimation proves to be a promising candidate for low-power and high-mobility communication systems. Future works should aim at development of fast computationally efficient completely blind algorithms which may involve proper signal design technique for MIMO-OFDM system.

Further, most of the blind techniques ignore the channel coding and assume that the source covariance matrix is diagonal with known variance. This restricts the practically applicability of most of the blind approaches [37]. Thus design of blind algorithms for practical standards and/ or modification of existing techniques to be applicable in practical standards can be considered as one of the research topics. Further, it is assumed that the channel length is known. Precoding based approaches are highly sensitive to channel order estimation errors due to de-noising step involved in channel estimation. This can be resolved by estimation of channel order using Eigen-value based techniques [19 and 20] in time-domain. This calls for hybrid time-frequency channel estimation algorithms (*Chapter 5*).

BIBLIOGRAPHY

[1] John Proakis, "Digital Communications," 4th edition, McGraw-Hill, 2000.

[2] S. Haykin, "Adaptive filter theory," 4th edition, Prentice Hall, 2002.

[3] H. Liu, G. Xu, L. Tong and T. Kailath, "Recent developments in blind channel equalization: from cyclostationarity to subspaces," Elsevier, Signal Processing (SP) - 50 (1996), pp. 85–99, 1996.

[4] Lang Tong, Perreau S., "Multichannel blind identification: from subspace to maximum likelihood methods," Proceedings of the IEEE, vol. 86, no. 10, pp. 1951-1968, Oct 1998.

[5] S. Haykin (Editor), "Blind Deconvolution," PTR Prentice Hall, 1994.

[6] Godard D., "Self-Recovering Equalization and Carrier Tracking in Two-Dimensional Data Communication Systems," IEEE Transactions on Communications, vol. 28, no. 11, pp. 1867- 1875, Nov 1980.

[7] Sato Y., "A Method of Self-Recovering Equalization for Multilevel Amplitude-Modulation Systems," IEEE Transactions on Communications, vol. 23, no. 6, pp. 679-682, Jun 1975.

[8] Bellini S., "Bussgang Techniques for Blind equalization," IEEE Global Telecommunication Conference (GLOBECOM' 86), Houston, TX, pp. 1634-1640, 1986.

[9] J. A. R. Fonollosa and J. Vidal, "System Identification using a Linear Combination of Cumulant Slices," IEEE Trans. on Signal Processing, SP-41 (7): 2405–2412, July 1993.

[10] D. Boss, B. Jelonnek, and K. Kammeyer, "Eigenvector Algorithm for Blind MA System Identification," Elsevier, Signal Processing, SP-66 (1): 1–26, April 1998.

[11] J. K. Tugnait, "Identification of linear stochastic system via second and fourth-order cumulant matching," IEEE Transactions on Information Theory, vol. 1T-33, May 1987.

[12] Jing Liang, Zhi Ding, "Blind MIMO system identification based on cumulant subspace decomposition," IEEE Trans. on Signal Proc., vol. 51, no. 6, pp. 1457- 1468, June 2003.

[13] Lang Tong, Guanghan Xu, Kailath T., "Blind identification and equalization based on second-order statistics: a time domain approach," IEEE Transactions on Information Theory, vol. 40, no. 2, pp. 340-349, Mar 1994.

[14] Serpedin E., Giannakis G. B., "Blind channel identification and equalization with modulation-induced cyclostationarity," IEEE Transactions on Signal Processing, vol. 46, no. 7, pp. 1930-1944, Jul 1998.

[15] M. Tsatsanis and G. B. Giannakis, "Transmitter induced cyclostationarity for blind channel equalization," IEEE Trans. on Signal Processing, vol. 45, pp.1785 - 1794, 1997.

[16] Ching An Lin, Jwo Yuh Wu, "Blind identification with periodic-modulation: a time-domain approach," IEEE Transactions on Signal Processing, vol. 50, no. 11, pp. 2875-2888, Nov 2002.

[17] Hui Liu, Guanghan Xu, Lang Tong, "A deterministic approach to blind identification of multi-channel FIR systems," IEEE International Conference on Acoustics, Speech, and Signal Processing (ICASSP), Adelaide, SA, Australia, vol. 4, pp. IV/581-584, Apr 1994.

[18] Moulines E., Duhamel P., Cardoso J.-F., Mayrargue S., "Subspace methods for the blind identification of multichannel FIR filters," IEEE Transactions on Signal Processing, vol. 43, no. 2, pp. 516-525, Feb. 1995.

[19] Perros-Meilhac L., Moulines E., Abed-Meraim K., Chevalier P., Duhamel P., "Blind identification of multipath channels: a parametric subspace approach," IEEE Transactions on Signal Processing , vol.49, no.7, pp.1468-1480, Jul 2001

[20] Hoteit L., "Extending the subspace method for blind identification," Fourth International conference on Signal Processing Proceedings (ICSP-1998), Beijing, China, vol. 1, pp. 347-350, 1998.

[21] Lambotharan S., Chambers J. A., "A new blind equalization structure for deep-null communication channels," IEEE Transactions on Circuits and Systems II: Analog and Digital Signal Processing, vol. 45, no. 1, pp. 108-114, Jan 1998.

[22] Panci G., Scarano G., Jacovitti G., "Blind identification and order estimation of FIR communications channels using cyclic statistics," IEEE International Conference on Acoustics, Speech and Signal Processing 1998, Seattle, Washington, USA, vol. 4, pp. 2389-92, 12-15 May 1998.

[23] Lisheng Fan, Feifei Gao, Yunkai Feng, Xianfu Lei, Yongquan Jiang, "On the use of signal subspace information in blind FIR channel estimation," 3rd International Symposium on Systems and Control in Aeronautics and Astronautics (ISSCAA), Harbin, China, pp.1174-1177, 8-10 June 2010.

[24] Ayadi J., Slock D. T. M., "On linear channel-based noise subspace parameterizations for blind multichannel identification," IEEE Third Workshop on Signal Processing Advances in Wireless Commn. (SPAWC – 2001), Taoyuan, Taiwan, pp. 78-81, 2001.

[25] Kristensson M., Ottersten B., "A statistical approach to subspace based blind Identification," IEEE Transactions on Signal Processing, vol. 46, no. 6, pp. 1612-1623, Jun 1998.

[26] Abed Meraim K. et al, "Prediction error methods for time-domain blind identification of multichannel FIR filters," International conf. on Acoustics, Speech, and Signal Processing, 1995. ICASSP-95, Detroit, MI, USA, vol. 3, no., pp. 1968-1971, May 1995.

[27] Yifeng Zhou, Henry Leung, Patrick Yip, "Blind identification of multichannel FIR systems based on linear prediction," IEEE Transactions on Signal Processing, vol. 48, no. 9, pp. 2674-2678, Sep 2000.

[28] Zhi Ding and Ye Li, "Blind Equalization and Identification," Marcel Dekker, 2001

[29] Zhi Ding, "Matrix outer-product decomposition method for blind multiple channel identification," IEEE Transactions on Signal Processing, vol. 45, no. 12, pp. 3053-3061, Dec 1997.

[30] Lang Tong and Qing Zhao, "Joint order detection and blind channel estimation by least squares smoothing," IEEE Transactions on Signal Processing, vol. 47, no. 9, pp. 2345-55, Sep 1999.

[31] Qing Zhao, Tong L., "Adaptive blind channel estimation by least squares smoothing," IEEE Transaction on Signal Processing, vol. 47, no. 11, pp. 3000-3012, Nov 1999.

[32] Gardner W.A., "A new method of channel identification," IEEE Transactions on Communications, vol. 39, no. 6, pp. 813-817, Jun 1991.

[33] Lang Tong, Guanghan Xu, Hassibi B., Kailath T., "Blind channel identification based on second-order statistics: a frequency-domain approach," IEEE Transaction on Information Theory, vol. 41, no. 1, pp. 329-334, Jan 1995.

[34] Bordin C. J., Bruno M. G. S., "Particle Filters for Joint Blind Equalization and Decoding in Frequency-Selective Channels," IEEE Transactions on Signal Processing, vol. 56, no. 6, pp. 2395-2405, June 2008.

[35] Insung Kang, Fitz M. P., Gelfand S. B., "Blind estimation of multipath channel parameters: a modal analysis approach," IEEE Transactions on Communications, vol. 47, no. 8, pp. 1140-1150, Aug 1999.

[36] Lopes R. R., Barry J. R., "Exploiting error-control coding in blind channel estimation," Global Telecommunication conference (GLOBECOM), San Antonio, Texas, vol. 2, pp. 1317-1321, 2001.

[37] Scherb A., Kuhn V., Kammeyer K. D., "On phase correct blind de-convolution of flat MIMO channels exploiting channel encoding," IEEE International Conference on Acoustics, Speech, and Signal Processing (ICASSP), Philadelphia, Pennsylvania, USA, vol. 3, pp. iii/1045- iii/1048, 18-23 March 2005.

[38] Yeredor A., "Blind channel estimation using first and second derivatives of the characteristic function," IEEE Signal Proc. Letters, vol. 9, no. 3, pp. 100-103, Mar 2002.

[39] C-C Jay Kuo, Michele Morelli and Man-On Pun, "Communication and Signal Processing vol. 3: Multi-Carrier Techniques for Broadband Wireless Communications- A signal processing perspective," Imperial College Press, 2007.

[40] Yonghong Zeng, Tung Sang Ng, "A proof of the identifiability of a subspace-based blind channel estimation for OFDM systems," IEEE Signal Processing Letters, vol. 11, no. 9, pp. 756- 759, Sept. 2004.

[41] B. Muquet, M. de Courville, and P. Duhamel, "Subspace-based blind and semi-blind channel estimation for OFDM systems," IEEE Transactions on Signal Processing, vol. 50, no. 7, pp. 1699–1712, Jul. 2002.

[42] Chengyang Li, Roy S., "Subspace-based blind channel estimation for OFDM by exploiting virtual carriers," IEEE Transactions on Wireless Communications, vol. 2, no. 1, pp. 141- 150, Jan. 2003.

[43] Heath R. W. Jr., Giannakis G. B., "Exploiting input cyclostationarity for blind channel identification in OFDM systems," IEEE Transactions on Signal Processing, vol. 47, no. 3, pp. 848-856, Mar 1999.

[44] Roy S. Chengyang Li, "A subspace blind channel estimation method for OFDM systems without cyclic prefix," IEEE Transactions on Wireless Communications, vol. 1, no. 4, pp. 572- 579, Oct 2002.

[45] Ruifeng Zhang, "Blind OFDM channel estimation through linear precoding: a subspace approach," Thirty-Sixth Asilomar Conference on Signals, Systems and Computers, Pacific Grove, California, vol. 1, pp. 631- 633, 3-6 Nov. 2002.

[46] Petropulu A., Ruifeng Zhang, Lin R., "Blind OFDM channel estimation through simple linear precoding," IEEE Transactions on Wireless Communications, vol. 3, no. 2, pp. 647- 655, March 2004.

[47] Yi Ma, Yi Huang, Na Yi, "Exploiting subcarrier correlation for blind channel estimation in block precoded OFDM systems," The Joint Conference of the 10th Asia-Pacific Conference on Communications and the 5th International Symposium on Multi-Dimensional Mobile Communications, vol. 1, pp. 338- 342, 29-Aug. to 1-Sept. 2004.

[48] Liang Y., Luo H. Huang J., "Redundant Precoding Assisted Blind Channel Estimation for OFDM Systems," 8th International Conference on Signal Processing, Guilin, China, vol.3, 16-20 2006.

[49] Lin R., Petropulu A. P., "Linear precoding assisted blind channel estimation for OFDM systems," IEEE Trans. on Vehicular Technology, vol. 54, no. 3, pp. 983- 995, May 2005.

[50] Taejoon Kim, Iksoo Eo, "Blind Channel Estimation and Equalization in OFDM System With Circular Precoding," IEEE International Conference on Acoustics, Speech and Signal Processing (ICASSP), Toulouse, France, vol. 4, pp. IV, 14-19 May 2006.

[51] Gao F., Nallanathan A.,. "Blind Channel Estimation for OFDM Systems via a Generalized Precoding," IEEE Transactions on Vehicular Technology, vol. 56, no. 3, pp. 1155-1164, May 2007.

[52] A.J. Paulraj, D.A. Gore, R.U. Nabar, H. Bölcskei, "An overview of MIMO communications - A key to gigabit wireless," Proceedings of the IEEE, Vol. 92 , Issue: 2, pgs: 198 – 218, Feb. 2004.

[53] Helmut Bölcskei, "MIMO-OFDM Wireless Systems: Basics, Perspectives, and Challenges," Communication Technology Laboratory, ETH Zürich, 2007

[54] Shin C., Heath R.W., Powers, E.J., "Blind Channel Estimation for MIMO-OFDM Systems," IEEE Trans. on Vehicular Technology, vol.56, no.2, pp.670-685, March 2007

[55] Feifei Gao, Yonghong Zeng, Nallanathan A., Tung-Sang Ng, "Robust subspace blind channel estimation for cyclic prefixed MIMO ODFM systems: algorithm, identifiability and performance analysis," IEEE Journal on Selected Areas in Communications, vol. 26, no. 2, pp. 378-388, February 2008.

[56] Chao-Cheng Tu, Champagne B., "Subspace-Based Blind Channel Estimation for MIMO-OFDM Systems With Reduced Time Averaging," IEEE Transactions on Vehicular Technology, vol. 59, no. 3, pp. 1539-1544, March 2010.

[57] Feifei Gao, A. Nallanathan, "Blind Channel Estimation for MIMO OFDM Systems via Nonredundant Linear Precoding," IEEE Transactions on Signal Processing, vol. 55, no. 2, pp. 784-789, Jan. 2007.

[58] Vudata Swarupa Gandhi, "Blind channel estimation for OFDM systems", M. Tech. Dissertation, Indian Institute of Technology Roorkee, Roorkee, June 2008.

[59] G. B. Giannakis, Y. Hua, P. Stoica and L. Tong (Editors), "Signal Processing Advances in Wireless and Mobile Communications – Trends in Channel Equalization and Equalization," Vol. 1, PTR Prentice Hall, 2001.

[60] P. Stoica, E. G. Larsson, and A. B. Gershman, "The stochastic CRB for array processing: A textbook derivation," IEEE Signal Processing Letter, vol. 8, no. 5, pp. 148–150, May 2001.

[61] R. van Nee and R. Prasad, "OFDM for Wireless Multimedia Communications," Boston, MA: Artech House, 2000.

[62] Shengli Zhou, Giannakis G. B., "Finite-alphabet based channel estimation for OFDM and related multicarrier systems," IEEE Transactions on Communications, vol. 49, no. 8, pp. 1402-1414, Aug 2001.

[63] Sanzi F., Necker M. C., "Totally blind APP channel estimation for mobile OFDM systems," IEEE Communications Letters, vol. 7, no. 11, pp. 517- 519, Nov. 2003.

[64] Necker M. C., Stuber G. L., "Totally blind channel estimation for OFDM on fast varying mobile radio channels," IEEE Transactions on Wireless Communications, vol. 3, no. 5, pp. 1514- 1525, Sept. 2004.

[65] Sameera Bharadwaja H and D. K. Mehra, "A completely blind channel estimation technique for OFDM using constellation-splitting," Proceedings of ICEIT national conference in Wireless Cellular Telecommunications: Technologies and Services, New Delhi, pp: 74-79, 14-15 Apr. 2011.

APPENDIX A

DERIVATION OF DUAL CONDITION FOR ANY N AND L (N ≥ 2L)

The derivation of the dual equation for the orthogonality condition given in *eqn. 2.28* for the generalized subspace-based blind channel estimation technique in SISO-OFDM system (*Chapter 2*) by mathematical induction is illustrated.

Case I: $N = 4, L = 1$

From *eqn. 2.24b*, we get:

$$C_0 = h(0) = h_0 \text{ and } C_1 = h_1$$

$$C_0' = \begin{bmatrix} h_0 & 0 & 0 \\ h_1 & h_0 & 0 \\ 0 & h_1 & h_0 \end{bmatrix}; \quad C_1' = \begin{bmatrix} h_1 \\ 0 \\ 0 \end{bmatrix} \quad and \quad C_1'' = [0 \quad 0 \quad h_1]$$

Hence, from *eqn. 2.25*, the channel matrix can be written as:

$$\mathbf{H}(h) = \left[\begin{array}{ccc:c:ccc:c} h_0 & 0 & 0 & h_1 & 0 & 0 & 0 & 0 \\ h_1 & h_0 & 0 & 0 & 0 & 0 & 0 & 0 \\ 0 & h_1 & h_0 & 0 & 0 & 0 & 0 & 0 \\ \hdashline 0 & 0 & h_1 & h_0 & 0 & 0 & 0 & 0 \\ \hdashline 0 & 0 & 0 & h_1 & 0 & 0 & 0 & h_0 \\ \hdashline 0 & 0 & 0 & 0 & h_0 & 0 & 0 & h_1 \\ 0 & 0 & 0 & 0 & h_1 & h_0 & 0 & 0 \\ 0 & 0 & 0 & 0 & 0 & h_1 & h_0 & 0 \\ \hdashline 0 & 0 & 0 & 0 & 0 & 0 & h_1 & h_0 \end{array}\right]$$

From *eqn. 2.27*, the left null-space vector of size $(2N+L) \times L = 9 \times 1$ can be written as:

$$g = g_i = \left[\begin{array}{c} g_i^1(1) \\ g_i^1(2) \\ g_i^1(3) \\ \hdashline g_i^2(1) \\ \hdashline g_i^3(1) \\ \hdashline g_i^4(1) \\ g_i^4(2) \\ g_i^4(3) \\ \hdashline g_i^5(1) \end{array}\right] \quad for \ 0 \le i \le L-1 \ \rightarrow \quad i = 0$$

Eqn. 2.28 gives the orthogonality condition: $g_i^H \mathbf{H}(h) = 0 \quad for \ i = 0$

Expanding,

$$\left[\begin{array}{c} g_i^1(1)^*h_0 + g_i^1(2)^*h_1 \\ g_i^1(2)^*h_0 + g_i^1(3)^*h_1 \\ \hline g_i^1(3)^*h_0 + g_i^2(1)^*h_1 \\ \hline g_i^2(1)^*h_0 + [g_i^2(1)^* + g_i^3(1)^*]h_1 \\ \hline g_i^4(1)^*h_0 + g_i^4(2)^*h_1 \\ g_i^4(2)^*h_0 + g_i^4(3)^*h_1 \\ \hline g_i^4(3)^*h_0 + g_i^5(1)^*h_1 \\ \hline [g_i^3(1)^* + g_i^5(1)^*]h_0 + g_i^4(1)^*h_1 \end{array}\right] = \mathbf{0}$$

Taking Hermitian and splitting the above vector in dual form,

$$[h_0^* \quad h_1^*]\left[\begin{array}{cc|c|c|cc|c|c} g_i^1(1) & g_i^1(2) & g_i^1(3) & g_i^2(1) & g_i^4(1) & g_i^4(2) & g_i^4(3) & g_i^3(1)+g_i^5(1) \\ g_i^1(2) & g_i^1(3) & g_i^2(1) & g_i^1(1)+g_i^3(1) & g_i^4(2) & g_i^4(3) & g_i^5(1) & g_i^4(1) \end{array}\right] = \mathbf{0}$$

... (A.1)

$$\Rightarrow \quad \boldsymbol{h^H G_i = 0} \quad for\ i = 0$$

Case II: $N = 8,\ L = 2$

From *eqn. 2.24b,* we get:

$$\boldsymbol{C_0} = \begin{bmatrix} h_0 & 0 \\ h_1 & h_0 \end{bmatrix} \ and \ \boldsymbol{C_1} = \begin{bmatrix} h_2 & h_1 \\ 0 & h_2 \end{bmatrix}$$

$$\boldsymbol{C_0'} = \begin{bmatrix} h_0 & 0 & 0 & 0 & 0 & 0 \\ h_1 & h_0 & 0 & 0 & 0 & 0 \\ h_2 & h_1 & h_0 & 0 & 0 & 0 \\ 0 & h_2 & h_1 & h_0 & 0 & 0 \\ 0 & 0 & h_2 & h_1 & h_0 & 0 \\ 0 & 0 & 0 & h_2 & h_1 & h_0 \end{bmatrix};\ \boldsymbol{C_1'} = \begin{bmatrix} h_2 & h_1 \\ 0 & h_2 \\ 0 & 0 \\ 0 & 0 \\ 0 & 0 \\ 0 & 0 \end{bmatrix} \ and \ \boldsymbol{C_1''} = \begin{bmatrix} 0 & 0 & 0 & 0 & h_2 & h_1 \\ 0 & 0 & 0 & 0 & 0 & h_2 \end{bmatrix}$$

Hence, from *eqn. 2.25*, the channel matrix can be written as:

$$\mathbf{H}(h) = \left[\begin{array}{cccccc|cc|cccccc|cc}
h_0 & 0 & 0 & 0 & 0 & 0 & h_2 & h_1 & 0 & 0 & 0 & 0 & 0 & 0 & 0 & 0 \\
h_1 & h_0 & 0 & 0 & 0 & 0 & 0 & h_2 & 0 & 0 & 0 & 0 & 0 & 0 & 0 & 0 \\
h_2 & h_1 & h_0 & 0 & 0 & 0 & 0 & 0 & 0 & 0 & 0 & 0 & 0 & 0 & 0 & 0 \\
0 & h_2 & h_1 & h_0 & 0 & 0 & 0 & 0 & 0 & 0 & 0 & 0 & 0 & 0 & 0 & 0 \\
0 & 0 & h_2 & h_1 & h_0 & 0 & 0 & 0 & 0 & 0 & 0 & 0 & 0 & 0 & 0 & 0 \\
0 & 0 & 0 & h_2 & h_1 & h_0 & 0 & 0 & 0 & 0 & 0 & 0 & 0 & 0 & 0 & 0 \\
\hline
0 & 0 & 0 & 0 & h_2 & h_1 & h_0 & 0 & 0 & 0 & 0 & 0 & 0 & 0 & 0 & 0 \\
0 & 0 & 0 & 0 & 0 & h_2 & h_1 & h_0 & 0 & 0 & 0 & 0 & 0 & 0 & 0 & 0 \\
\hline
0 & 0 & 0 & 0 & 0 & 0 & h_2 & h_1 & 0 & 0 & 0 & 0 & 0 & 0 & h_0 & 0 \\
0 & 0 & 0 & 0 & 0 & 0 & 0 & h_2 & 0 & 0 & 0 & 0 & 0 & 0 & h_1 & h_0 \\
\hline
0 & 0 & 0 & 0 & 0 & 0 & 0 & 0 & h_0 & 0 & 0 & 0 & 0 & 0 & h_2 & h_1 \\
0 & 0 & 0 & 0 & 0 & 0 & 0 & 0 & h_1 & h_0 & 0 & 0 & 0 & 0 & 0 & h_2 \\
0 & 0 & 0 & 0 & 0 & 0 & 0 & 0 & h_2 & h_1 & h_0 & 0 & 0 & 0 & 0 & 0 \\
0 & 0 & 0 & 0 & 0 & 0 & 0 & 0 & 0 & h_2 & h_1 & h_0 & 0 & 0 & 0 & 0 \\
0 & 0 & 0 & 0 & 0 & 0 & 0 & 0 & 0 & 0 & h_2 & h_1 & h_0 & 0 & 0 & 0 \\
0 & 0 & 0 & 0 & 0 & 0 & 0 & 0 & 0 & 0 & 0 & h_2 & h_1 & h_0 & 0 & 0 \\
\hline
0 & 0 & 0 & 0 & 0 & 0 & 0 & 0 & 0 & 0 & 0 & 0 & h_2 & h_1 & h_0 & 0 \\
0 & 0 & 0 & 0 & 0 & 0 & 0 & 0 & 0 & 0 & 0 & 0 & 0 & h_2 & h_1 & h_0
\end{array}\right]$$

From *eqn. 2.27,* the left null-space of size *(2N+L)* × *L* = *18×2* can be written as: $\boldsymbol{g} = [\boldsymbol{g}_1 \quad \boldsymbol{g}_2]$ where,

$$\boldsymbol{g}_i = \left[\begin{array}{c} g_i^1(1) \\ g_i^1(2) \\ g_i^1(3) \\ g_i^1(4) \\ g_i^1(5) \\ g_i^1(6) \\ \hline g_i^2(1) \\ g_i^2(2) \\ \hline g_i^3(1) \\ g_i^3(2) \\ \hline g_i^4(1) \\ g_i^4(2) \\ g_i^4(3) \\ g_i^4(4) \\ g_i^4(5) \\ g_i^4(6) \\ \hline g_i^5(1) \\ g_i^5(2) \end{array}\right] = \left[\begin{array}{c} \boldsymbol{g}_i^1 \\ \boldsymbol{g}_i^2 \\ \boldsymbol{g}_i^3 \\ \boldsymbol{g}_i^4 \\ \boldsymbol{g}_i^5 \end{array}\right] \qquad for\ 0 \le i \le L-1 \quad \rightarrow \quad i = \{0,1\}$$

Eqn. 2.28 gives the orthgonality condition: $\boldsymbol{g}_i^H \mathbf{H}(h) = 0 \quad for\ i = \{0,1\}$

Expanding,

$$\begin{bmatrix} g_i^1(1)^*h_0 + g_i^1(2)^*h_1 + g_i^1(3)^*h_2 \\ g_i^1(2)^*h_0 + g_i^1(3)^*h_1 + g_i^1(4)^*h_2 \\ g_i^1(3)^*h_0 + g_i^1(4)^*h_1 + g_i^1(5)^*h_2 \\ g_i^1(4)^*h_0 + g_i^1(5)^*h_1 + g_i^1(6)^*h_2 \\ g_i^1(5)^*h_0 + g_i^1(6)^*h_1 + g_i^2(1)^*h_2 \\ g_i^1(6)^*h_0 + g_i^2(1)^*h_1 + g_i^2(2)^*h_2 \\ g_i^2(1)^*h_0 + g_i^2(2)^*h_1 + [g_i^1(1)^* + g_i^3(1)^*]h_2 \\ g_i^2(2)^*h_0 + [g_i^1(1)^* + g_i^3(1)^*]h_1 + [g_i^1(2)^* + g_i^3(2)^*]h_2 \\ g_i^4(1)^*h_0 + g_i^4(2)^*h_1 + g_i^4(3)^*h_2 \\ g_i^4(2)^*h_0 + g_i^4(3)^*h_1 + g_i^4(4)^*h_2 \\ g_i^4(3)^*h_0 + g_i^4(4)^*h_1 + g_i^4(5)^*h_2 \\ g_i^4(4)^*h_0 + g_i^4(5)^*h_1 + g_i^4(6)^*h_2 \\ g_i^4(5)^*h_0 + g_i^4(6)^*h_1 + g_i^5(1)^*h_2 \\ g_i^4(6)^*h_0 + g_i^5(1)^*h_1 + g_i^5(2)^*h_2 \\ [g_i^3(1)^* + g_i^5(1)^*]h_0 + [g_i^3(2)^* + g_i^5(2)^*]h_1 + g_i^4(1)^*h_2 \\ [g_i^3(2)^* + g_i^5(2)^*]h_0 + g_i^4(1)^*h_1 + g_i^4(2)^*h_2 \end{bmatrix} = \mathbf{0}$$

Taking Hermitian and splitting the above vector in dual form,

$$[h_0^* \quad h_1^* \quad h_2^*] \begin{bmatrix} g_i^1(1) & g_i^1(2) & g_i^1(3) & g_i^1(4) & g_i^1(5) & g_i^1(6) & 0 & 0 \\ g_i^1(2) & g_i^1(3) & g_i^1(4) & g_i^1(5) & g_i^1(6) & 0 & 0 & g_i^1(1) \\ g_i^1(3) & g_i^1(4) & g_i^1(5) & g_i^1(6) & 0 & 0 & g_i^1(1) & g_i^1(2) \\ & & & & + & & + & \\ & & & & 0 & 0 & g_i^2(1) & g_i^2(2) \\ & & & & 0 & g_i^2(1) & g_i^2(2) & 0 \\ & & & & g_i^2(1) & g_i^2(2) & 0 & 0 \\ & & & & + & & + & \\ & & & & & & 0 & 0 \\ & & & & & & 0 & g_i^3(1) \\ & & & & & & g_i^3(1) & g_i^1(2) \end{bmatrix} \cdots$$

$$\cdots \begin{bmatrix} g_i^4(1) & g_i^4(2) & g_i^4(3) & g_i^4(4) & g_i^4(5) & g_i^4(6) & 0 & 0 \\ g_i^4(2) & g_i^4(3) & g_i^4(4) & g_i^4(5) & g_i^4(6) & 0 & 0 & g_i^4(1) \\ g_i^4(3) & g_i^4(4) & g_i^4(5) & g_i^4(6) & 0 & 0 & g_i^4(1) & g_i^4(2) \\ & & & & + & & + & \\ & & & & 0 & 0 & g_i^5(1) & g_i^5(2) \\ & & & & 0 & g_i^5(1) & g_i^5(2) & 0 \\ & & & & g_i^5(1) & g_i^5(2) & 0 & 0 \\ & & & & + & & + & \\ & & & & & & g_i^3(1) & g_i^3(2) \\ & & & & & & g_i^3(2) & 0 \\ & & & & & & 0 & 0 \end{bmatrix} = \mathbf{0}$$

... (A.2)

$$\Rightarrow \quad \boldsymbol{h}^H \boldsymbol{G}_i = 0 \quad for\ i = \{0,1\}$$

Observe that *eqn. A.1* and *A.2* has a definite structure that can be generalized by using mathematical induction for any null-space bases matrix of dimension $(2N+L) \times L$ $(N \geq L)$ to obtain the results as given in *eqn. 2.29* and *eqn. 2.30*.